THE UNIVERSITY *of* EDINBURGH

DIVERSE MECHANISMS OF PECTIC POLYSACCHARIDE DEGRADATION DISTINGUISHED IN FRUIT CELL WALLS *IN VIVO*

BABUL AIRIANAH OTHMAN

A THESIS PREPARED IN FULFILMENT OF THE REQUIREMENTS FOR THE DEGREE OF DOCTOR OF PHILOSOPHY (Ph.D.), THE UNIVERSITY OF EDINBURGH

2012

Declaration

This thesis has been composed by myself and the work, of which it is a record, has been carried out by myself. All sources of information have been specifically acknowledged by means of a reference.

Babul Airianah Othman

Acknowledgements

There are a number of people I would like to thank who have made my journey in Edinburgh Cell Wall Group so memorable and who will be cherished all my life. First of all, I would like to thank Prof. Steve Fry for his precious time, patience, help and support which was much needed in completing this study. I also want to thank the members of the Edinburgh Cell Wall Group that I have known throughout the last three years: Janice, for giving guidance and support in all aspects; Sandra, David, Amjad, Lenka and Kyle for helping me when I just started my journey in Edinburgh; Tim who helped me run many HPLC samples; and also Tom, Dimitra, Maria, Christina, Claire, Cam Tu and Becca for being such great friends and helping to make this an enjoyable experience.

My special thank you is to my family in Malaysia for their continuous support and many hours of phone calls. Last but not least, to my wonderful husband for his sacrifices and great patience and for always being great company anytime, anywhere!

This project was funded by the Ministry of Higher Education, Malaysia, together with The National University of Malaysia.

To Abang

Abstract

Cell wall loosening and degradation are important processes in major stages of plant development including fruit ripening. Three main mechanisms have been proposed to contribute towards cell wall polysaccharide degradation *in vivo*: enzymic hydrolysis by endopolygalacturonase (EPG), enzymic elimination by pectate lyase (PL), and non-enzymic scission by hydroxyl radicals ($^{\bullet}OH$). However, little idea as to which of these three mechanisms predominates in homogalacturonan degradation especially during fruit ripening. This study presents an attempt to discover the respective contribution of those three mechanisms of attack. The strategy used to achieve the objective of this study was to identify and measure homogalacturonan molecules that exhibit symptoms of each mechanism of attack.

A method that was developed in this study is a fluorescent labelling method mainly to study the $^{\bullet}OH$ attack on pectic polysaccharides. This labelling method is based on the ability of 2-aminoacridone (2-AMAC) to reductively aminate oxo groups of sugar moieties followed by exhaustive digestion with Driselase. In a model *in-vitro* experiment, the developed novel fluorescent labelling method, when applied to homogalacturonan, that had been attacked by $^{\bullet}OH$ (Fenton reagent), produced at least three fluorescent 'fingerprint' compounds, separable by high-voltage paper electrophoresis (HVPE) based on their charge/mass properties at pH 6.5 and also by high pressure liquid chromatography (HPLC) on a C_{18} column with a fluorescence detector at λ_{em}= 520 nm. These fingerprint compounds include: a monomer, 1A*; a dimer, 2A*; and an unidentified compound, X*. *In-vivo* application with alcohol-insoluble residue (AIR) of seven species of fruit (pear, mango, banana, apple, avocado, strawberry and strawberry tree fruit) at three stages of softening produced at least two fluorescent fingerprint compounds: a monomer, $1A^F$ and a dimer, $2A^F$. X^F, an interesting compound found in a few samples in *in-vivo* experiments, showed electrophoretic mobility similar to X*; however, the retention time of this compound on HPLC did not agree with that of X*. $2A^F$ was suggested to be exclusive evidence for $^{\bullet}OH$ attack *in vivo* while $1A^F$ was suggested to be a useful evidence not only to reveal $^{\bullet}OH$ attack but also to reveal EPG and PL attack on pectic polysaccharides during fruit softening.

HVPE and HPLC results showed an increasing pattern of $2A^F$ in mango, banana, avocado and strawberry tree fruit, which indicated progressive $^{\bullet}OH$ attack on pectic polysaccharides during the softening process. There was no clear evidence of $2A^F$ at any stage of softening in apple and strawberry, which may suggest that fruit softening in apple and strawberry was not associated with $^{\bullet}OH$ attack. On the other hand, HVPE analysis of $1A^F$ showed and increasing pattern in pear, mango, banana, avocado and strawberry tree fruit, which may indicate EPG, PL and/or $^{\bullet}OH$ attack during fruit softening. Production of these fluorescent fingerprint compounds provides good evidence for $^{\bullet}OH$ attack on pectic polysaccharides, and has the potential to give useful information for EPG and PL attack *in vivo*.

Table of contents

List of Figures

List of Tables

Abbreviations

2-AMAC	2-aminoacridone
$^{\bullet}$OH	Hydroxyl radical
ΔUA	Unsaturated uronic acid
AIR	Alcohol-insoluble residue
BAW	Butanol:acetic acid:water
EPG	Endopolygalacturonase
EPW	Ethylacetate:pyridine:water
HPLC	High-pressure liquid chromatography
HVPE	High-voltage paper electrophoresis
kV	Kilovolts
MM	Marker mixture
nm	Nanometre
PAD	Pulse amperometric detector
pAMAC	*Iso*-propyl-AMAC
pAMAC•UA	pAMAC group attached to other than carbon-1 of uronic acid
PL	Pectate lyase
UA-pAMAC	pAMAC group attached to carbon-1 of uronic acid
UA•pAMAC	pAMAC group attached to $^{\bullet}$OH-introduced oxo group at carbon-1 of uronic acid
RG-I/-II	Rhamnogalacturonan I/II
RT	Room temperature
TLC	Thin layer chromatography
UA	Uronic acid
UV	Ultraviolet
Sugar residues:	
Gal	Galactose
GalA	Galacturonic acid
$GalA_2$	Galacturonobiose
$GalA_3$	Galacturonotriose
GalO	Galactonic acid
Glc	Glucose
GlcA	Glucuronic acid
GulA	Guluronic acid
Rha	Rhamnose
TalA	Taluronic acid
1A*, 2A*, X*	Fluorescently labelled compounds from *in-vitro* experiment
$1A^F$, $2A^F$, X^F	Fluorescently labelled compounds from *in-vivo* experiment

1. Introduction

The plant cell wall is a unique metabolically active sub-cellular compartment. It governs many important activities in the living plant including germination (Müller *et al.*, 2006, 2009), growth rate (Cosgrove, 1999, 2005), disease resistance and resistance to microbial digestion (Baydoun & Fry, 1985; Brisson *et al.*, 1994), leaf abscission (Belfield *et al.*, 2005), vitamin C metabolism (Green & Fry, 2005) and fruit ripening (Brummell & Harpster, 2001; Fry *et al.*, 2001). Plant cell wall loosening and degradation that leads to the softness of the fruit during the ripening process is the main interest in this research. Three main mechanisms have been proposed to contribute towards pectic polysaccharide degradation during fruit ripening: enzymic hydrolysis by endopolygalacturonases (Section 1.3.1.1), enzymic elimination by pectate lyases (Section 1.3.1.2) and non-enzymic scission by hydroxyl radicals (Section 1.3.1.3). Both enzymic and non-enzymic degradation are associated with physical and chemical modification of the pectic polysaccharides. Even though at least the enzymic degradation mechanisms have been well described, only little knowledge exists to show which of the three mechanisms predominate(s) in plant cell wall polysaccharide degradation in any specific living plant tissue at any given time. These topics are therefore introduced with reference to fruit ripening and the softening process, including the three proposed mechanisms, followed by the strategy to achieve the aims of this project.

1.1 Fruit ripening

1.1.1 Fruit ripening phenomena

Fruit usually ripens when the seed(s) are completing their development. Fruit ripening is an important physiological process for plants where various chemical changes occur after the fruit has reached its full size and before it reaches its terminal stage of development, in which the mature seeds are released. Ripening has both positive and negative elements for the fruit. In many cases, ripening results in an edible fruit with the pulp becoming softer, a colour change from green to some other colour such as red, orange or yellow, and the fruit becoming sweeter. These changes serve as a temptation to animals including humans, with the evolutionary benefit of dispersing the seeds. But, at the same time, ripening increases fruit susceptibility to pathogen attack and on excessive ripening or after prolonged storage, fruit becomes too soft and gives an undesirable texture to consumers, limiting shelf-life, storage and transport (Prasanna *et al.*, 2007; Payasi & Sanwal, 2010; Bapat *et al.*, 2010).

Ripening influences various quality and nutritional characteristics, including ascorbic acid content, antioxidant activity, levels of several mineral elements (phosphorus, potassium, calcium, magnesium, sodium, iron, manganese, zinc, copper and molybdenum) and phenolic compound content (Rop *et al.*, 2011). Modifications of the biochemistry, physiology and structure of the ripening fruit also influence the appearance, texture, flavour and aroma of the fruit. These modifications include polysaccharide breakdown, organic acid metabolism, alterations in pigment biosynthesis and accumulation, biosynthesis of flavour and aromatic volatiles, changes in the cell wall structure and metabolism, which are thought to result in loss

of firmness of pulp (Goulao & Oliveira, 2008; Fry, 2003). Impact of fruit ripening in this introduction section will focus on a process contributing to fruit texture, viz. fruit softening.

1.1.2 Fruit softening during the ripening process

Fruit texture is one of the important factors for consumers' perception of fruit quality and this factor influences fruit choice. Many commercial fruits, such as banana, mango, pear, avocado and apple, exhibit the climacteric: a sudden increase in ethylene and CO_2 output and O_2 consumption (the climacteric is not discussed in this thesis in detail). This kind of fruit have short shelf-lives after the climacteric while many nonclimacteric fruits such as orange, lemon and melon, ripen slowly and have long shelf-lives (Fry, 2003; Prasanna *et al.*, 2007; Bapat *et al.*, 2010). In the case of climacteric fruits, the rate of softening is a determining factor that controls commercial value as it is influences shelf life, wastage, infection by post-harvest pathogens, and limits for transportation and storage, all of which will lead to commercial losses (Brummell & Harpster, 2001).

Disassembly of the fruit cell wall is responsible for softening during ripening. This is accompanied by solubilisation and depolymerisation of the polysaccharides of the cell wall, and rearrangement of their associations (Redgwell *et al.*, 1997; Hadfield & Bennett, 1998; Rose *et al.*, 1998). Although the relative contribution of each event to fruit ripening and softening is not clear, and probably depends on species, but Fischer and Bennett (1991) and Hadfield and Bennett (1998) reported

that changes in cell wall composition, especially cell wall mechanical strength and cell-to-cell adhesion, have been considered to be the most important factors. All these events result from the combined action of several cell wall-modifying enzymes, responsible for polysaccharide breakdown; these include endoglycanases (e.g. cellulase and endo-polygalacturonase) and exoglycanases (exo-polygalacturonase, β-D-galactosidae, α-L-arabinofuranosidase), pectin methylesterase, xyloglucan endotransglucosylase/hydrolase, pectate lyase and α-expansins (Fischer & Bennet, 1991; Fry, 2003; Payasi *et al.*, 2009). In addition, Fry (1998, 2003) and Fry *et al.* (2001) showed that non-enzymic mechanisms involving the hydroxyl radical, ascorbate and Ca^{2+} may also contribute to polysaccharide degradation. However, the precise roles of particular cell wall-modifying enzymes and non-enzymic agents bringing these about are not known and still open for debate. The regulation mechanisms also probably depend on the species as different species of fruits have different cell wall structure and also patterns of growth and ripening (Goulao & Oliveira, 2008). Thus, those differences in fruit species are expected to influence biochemical modifications of the cell wall and their regulation. Therefore, the roles and effects of the various enzymes and non-enzymic agents on fruit cell wall degradation must be addressed for individual fruits.

Genetic manipulation such as suppression or over-expression of cell wall-modifying enzymes is one of the approaches used to study the *in-vivo* effect of particular enzymes and their role in fruit softening. But there are limitations to this approach especially when they involve an analysis of the function of single gene because most of cell wall-modifying proteins are present as multi-gene families; for example, polygalacturonases are encoded by very large gene families with 78 genes

[The Ar*abidopsis* Information Resource (TAIR) annotation, 2011]. Therefore, if another isoform is present that can complement the function of the suppressed isoform then no phenotype will be observed (Brummell & Harpster, 2001).

On the other hand, the limitations of *in-vitro* enzyme activity assays (i.e. *in-vitro* treatment of a cell wall component such as a solution of homogalacturonan with particular enzymes of interest), also need to be considered when discussing the enzymes' roles. *In-vitro* experiments can be limited by the necessity of other enzyme activities for the action of the applied enzyme of interest. For example, pectin methyl esterase (PME) action may be required to enable the action of PG and PL (Hatfield and Nevins, 1986). Therefore, the limitations and uncertainty to this approach necessitate alternative methods of investigation.

1.2 Plant cell wall structure

The two main types of plant cell wall that exist are classed as primary and secondary. Initially a thin, plastic primary cell wall is laid down whilst the cell undergoes expansion. Once cell expansion has stopped, certain cells begin to form a thick secondary cell wall and at the same time the primary wall no longer needs to be expansible. There are two structural phases associated with primary cell walls: the microfibrillar phase and the matrix phase.

1.2.1 Microfibrillar phase

Microfibrils are bundles of cellulose chains associated parallel to each other through hydrogen bonds and van der Waals forces. Microfibrils are rigid structures and have a skeletal role in the plant cell wall (Gardiner *et al.,* 2003). Microfibril size varies between organisms and can range from ~16 cellulose chains (Guerriero *et al*., 2010) to greater than 200 chains in cellulosic algae (Delmer & Amor, 1995). Cellulose is a highly insoluble unbranched chain of β-(1→4)-linked D-glucose residues and the size of the molecule can vary from 7000 to 14000 sugar moieties in the secondary wall, but can be as low as 500 glucose units in the primary cell wall (Richmond, 1991).

1.2.2 Matrix phase

The matrix phase of primary cell walls consists mainly of pectic and hemicellulosic polysaccharides. Pectic polysaccharides are discussed in detail below. Hemicelluloses consist of several sugar residues including glucose, galactose, mannose, fucose, arabinose, xylose and glucuronic acid. Hemicelluloses often make up 30% of the primary cell wall dry weight. There are several main hemicelluloses including xyloglucans, arabinoxylans, mixed-linkage glucans and glucomannans. Xyloglucans and possibly arabinoxylans and glucomannans have the ability to bind to the surface of microfibrils via hydrogen bonds, possibly helping to hold the wall together (Iiyama, 1994). Figure 1.2.1 shows a diagram of the primary cell wall and the interactions between different components.

Other components in plant cell walls, not described here, include structural proteins, glycoproteins, lignin and phenolic compounds which are tissue-specific and occur in variable quantities.

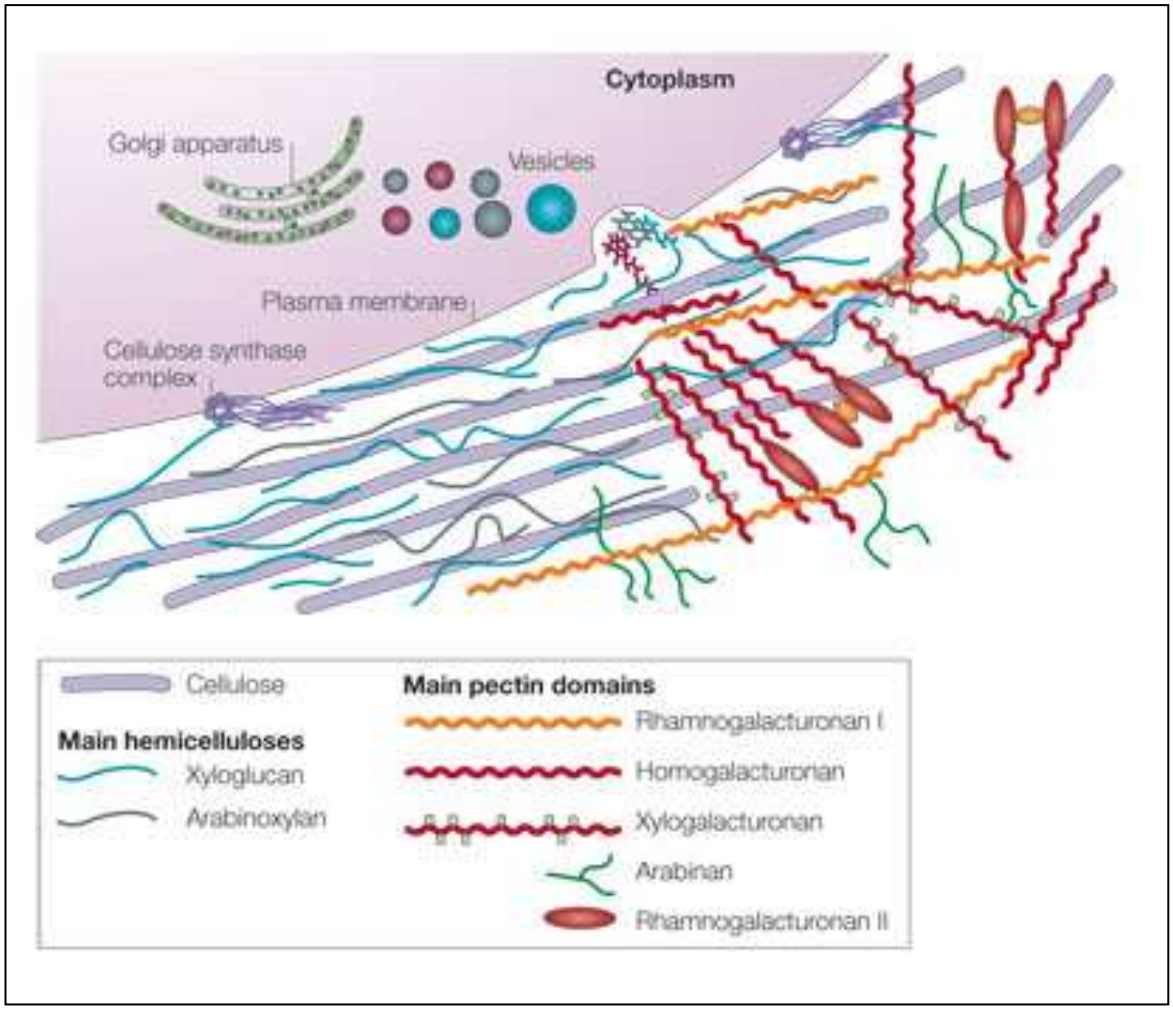

Figure 1.2.1 Schematic representation of plant primary cell wall structure.
Schematic representation of different components of the primary plant cell wall and their interactions. The left part of the figure shows the hemicellulose–cellulose network, without pectins, for clarity. The right part of the figure shows the interaction between pectin domains (Cosgrove, 2005).

1.2.3 Pectic polysaccharides

Pectic polysaccharides are major components of the primary cell wall in higher plants (such as ferns, conifers and flowering plants) and abundant in edible plant parts. Pectic polysaccharides in the plant cell wall may contribute to governing many important activities in the living plant including germination (Müller *et al.*, 2006 & 2009), growth rate (Cosgrove, 1999 & 2005), disease resistance and resistance to microbial digestion (Baydoun & fry, 1985; Brisson *et al.*, 1994), leaf abscission (Belfield *et al.*, 2005) and fruit ripening (Brummell & Harpster, 2001; Fry *et al.*, 2001). All these pectin functions are influenced by the amount and nature of the pectic molecules present in the cell wall. Around 30% of the dry weight of the primary cell wall of dicots (angiosperms with two cotyledons) and many monocots (angiosperms with only one cotyledon) are composed of pectic polysaccharides, while some monocots like grasses and cereals have lower proportions of pectic polysaccharides (McNeil *et al.*, 1984).

There are at least four pectic domains (Figure 1.2.2): homogalacturonan, rhamnogalacturonan I (RG-I), rhamnogalacturonan II (RG-II) and xylogalacturonan (Schols *et al.*, 1995). The simplest pectic domain is homogalacturonan, an unbranched α-(1→4)-linked polymer of D-galacturonic acid residues, which may have higher or lower degrees of methylesterification in different tissues or at different developmental stages (Willats *et al.* 2001). Homogalacturonans also carry acetyl ester groups on position 2 and/or 3, especially in certain plant taxa (Perrone *et al.*, 2002).

RG-I and RG-II are more complex polymers with many side-chains but still contain many GalA residues. RG-I has a backbone made of α-L-rhamnose alternating with α-D-galacturonic acid residues, with long side chains attached to some of the rhamnose residues and comprising either unbranched β-(1→4)-D-galactose or branched α-L-arabinose or type I arabinogalactan. On the other hand, RG-II has a backbone similar to homogalacturonan, but with complex side chains of several types of neutral sugar (Schols & Voragen, 2002). It is a minor cell wall component but RG-II can dimerize as boron di-esters and this may affect the porosity of the wall. Xylogalacturonans are also very similar to homogalacturonan but contain many xylose residues. Other polysaccharides, xyloglucans, may also be covalently bound to pectic polysaccharides (Thompson & Fry, 2000; Popper & Fry, 2005). Figure 1.2.2 shows a schematic representation of pectic polysaccharides structure.

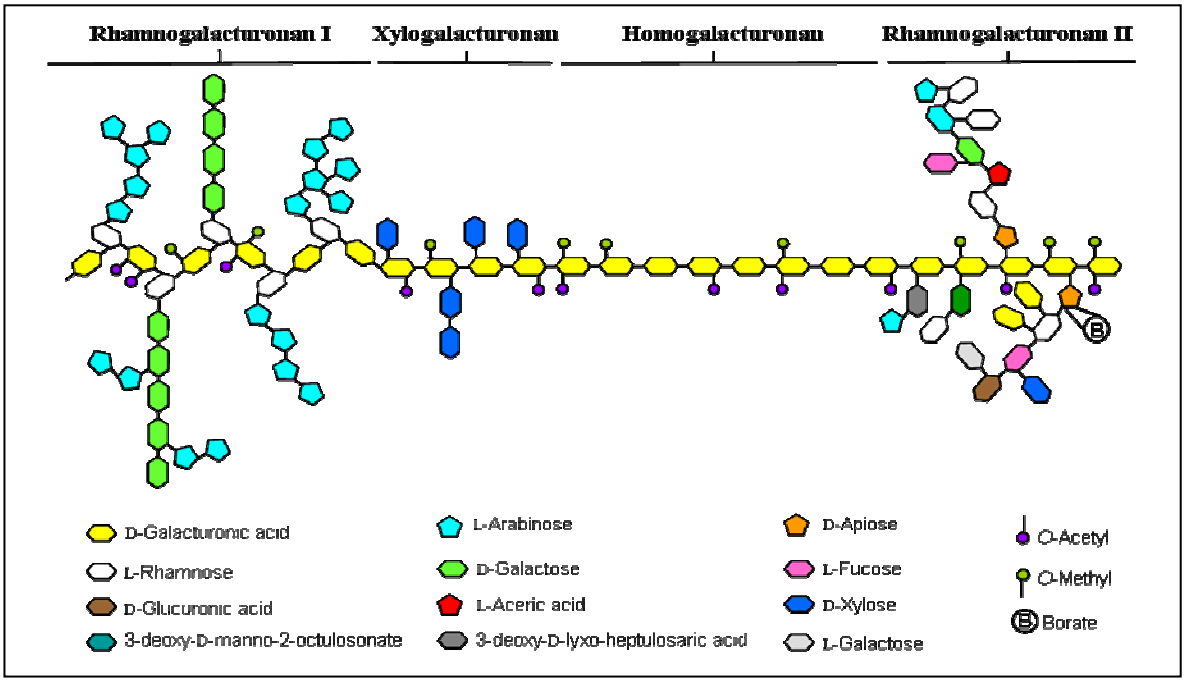

Figure 1.2.2 Schematic representation of pectin structure.
Schematic representation of the four main domains of pectin: rhamnogalacturonan I, xylogalacturonan, homogalacturonan and rhamnogalacturonan II, with different sugars identified by colour (adapted from Schellera *et al.*, 2007).

1.3 Pectic polysaccharide degradation during fruit softening

Cell wall architecture and the polymers of which it is composed are progressively modified during the fruit ripening process (Tucker & Grierson 1987) and the post-synthetic modification of pectic polysaccharides; for instance, pectic degradation and/or solubilisation often accompany and probably cause fruit softening during ripening (Toole *et al.,* 2002). Both in the living plant and post-harvest, cell wall matrix polysaccharides, especially pectic homogalacturonan, which is the focus of this research, undergoes various chemical changes, including partial degradation. In *Arabidopsis* alone, there are about 138 genes encoding putative pectinesterases, about 26 encoding putative pectate lyases (PLs), and about 78 encoding polygalacturonases (both endo and exo) [The Ar*abidopsis* Information Resource (TAIR) annotation, 2011]. The large numbers of these genes in *Arabidopsis* suggest that pectic metabolism has a special significance in plant biochemistry. Knowledge of the mechanism and regulation of pectic degradation is therefore of fundamental and practical importance in understanding and manipulating changes that occur during fruit softening process.

Pericarp (a modified ovary wall that often becomes the edible layer in fleshy fruits) cells have primary walls consisting of pectins (~35% of wall dry weight), hemicelluloses (~25%) and cellulose (~30%). Several changes occur in pectin structure during ripening. Changes in the structure of the cell wall are associated with dissolution of the middle lamella and disruption of the primary cell wall which begin early in the ripening of a soft fruit such as tomato (Crookes & Grierson, 1983) and late in the softening of a crisp fruit such as apple (Ben-Arie *et al.*, 1979). These

changes include not only loss of neutral sugar side-chain residues, and solubilisation and depolymerisation of the polysaccharide backbones, but also rearrangements of their associations (Redgwell *et al.*, 1997; Hadfield & Bennett, 1998; Rose *et al.*, 1998, Brummell & Harpster, 2001; Fry, 2003). As neighbouring cells adhere via the middle lamella (pectin-rich layer), loosening of the primary cell wall and/or middle lamella can cause textural changes in fruit during ripening and the pectic polysaccharides become progressively less firmly wall-bound.

Molecular weight reduction occurs in the pectin fractions during fruit softening such as in postharvest banana fruit (Duan *et al.*, 2008). This is partly due to cleavage of the pectic backbone although it is difficult to determine whether such cleavage is enzymic and/or non-enzymic. Furthermore, pectin depolymerization and the loss of galactose and arabinose side chains of RG-I (Redgwell *et al.*, 1997; Gross and Sams, 1984), increases cell wall porosity. Another change occurring in pectin structure during tomato ripening is methyl-esterified pectin become increasingly de-esterified by a process beginning in the middle lamella at the mature green stage and spreading throughout the wall (Roy *et al.*, 1992; Blumer *et al.*, 2000). Pectins are increasingly de-esterified to generate carboxylate ions, this causes the formation of charged surfaces in the wall, which may be important in modulating pH and ion balance, and may limit the movement of charged proteins through the primary wall from the plasma membrane (Carpita and Gibeaut, 1993). Changes in pH and ionic conditions in the apoplast may also affect the activity of cell wall-localized enzymes (Chun and Huber, 1998; Almeida and Huber, 1999; Takeda and Fry, 2004).

Three principal mechanisms have been proposed (Refer to Figure 1.3.1) that may contribute to homogalacturonan degradation: enzymic hydrolysis by endopolygalacturonase, enzymic elimination by pectate lyase and non-enzymic scission by hydroxyl radicals. However, which of them predominate(s) in homogalacturonan degradation in any particular living plant tissues at any given time is still under debate. Thus, it is of interest to discover their respective contributions to the pectic degradation occurring *in vivo.*

1.3.1 Polygalacturonases

Two types of polygalacturonase (PG), exo and endo, are found in fruit. The exo type (also known as α-D-galacturonidase) releases the non-esterified monosaccharide, GalA, from the non-reducing terminus, whereas the endo type (Figure 1.3.1) attacks low-methylester homogalacturonan domains in mid-chain (Stratilová *et al.*, 1998; Tucker & Seymour, 2002). The fruit ripening-specific enzyme usually considered responsible for PG action is endo-PG (EPG) (Hadfield & Bennett, 1998) and de-esterification of highly-esterified homogalacturonan is essential before it becomes a substrate for EPG (Jarvis, 1984; Carpita and Gibeaut, 1993).

Transcripts of *EPG* genes accumulate in many softening fruits such as tomato (Fray & Grierson, 1993), pear (Fonseca *et al.*, 2004; Hiwasa *et al.*, 2003), apple (Wakasa *et al.*, 2006; Wu *et al.*, 1993), banana (Asif & Nath, 2005) and strawberry (Redondo-Nevado *et al.*, 2001). Fabi *et al.* (2009) also reported that expression of putative EPG (*cpPG* gene) in papaya pulp was strongly induced during the ripening

process in papaya. EPG activity has also been detected in pear (Pressey & Avants, 1976; Hiwasa *et al.*, 2003), and at high level in banana (Ali *et al.*, 2004), avocado (Huber & O'Donoghue, 1993) and tomato (Eriksson *et al.*, 2004). In contrast, some studies reported the lack of EPG activity in strawberry (Huber, 1984) and apple (Bartley, 1978). However, in a more recent study, EPG activity has been detected in strawberry and apple but at levels much lower than in tomato: Nogata *et al.* (1993) detected three different PGs in strawberry, two of which were exo-PG whereas one was EPG, while Wu *et al.* (1993), and Wakasa *et al.* (2006) reported low EPG activity in apple. This might explain previous reports of a lack of EPG activity as the EPG activity may be present in both strawberry and apple but at sometimes undetectable levels. On the other hand, Suntornwat *et al.* (2000) reported a low level of PG activity (both exo and endo-type) in mango at the early stage of ripening (green fruit) but during the ripening process, the exo-PG increase in mango dramatically.

EPG activity has been well studied in fruit cell walls but assays have not always carefully distinguished between EPGs and PLs. Very few studies (e.g. Nagota *et al.*, 1993; García-Romera & Fry, 1995) have investigated the *in-vivo* action of EPGs as distinct from exo-PGs and none has satisfactorily distinguished EPG action from lyase action. Despite that reservation, many workers postulated key roles for EPG in fruit softening by manipulating gene expression and protein level. Transgenic strawberry plants expressing an anti-sense sequence of ripening-related EPG gene (*FaPG1*) significantly reduced fruit softening (Quesada *et al.*, 2009). However, the same approaches also suggested that EPG is neither necessary nor sufficient to promote fruit softening since anti-sense tomato in which EPG activity had been

suppressed to less than 1% of wild type level underwent almost normal pectin solubilisation and depolymerization in fruit (Brummell & Labavitch, 1997). Moreover, in the tomato mutant *rin* (ripening-inhibitor) an experiment where insertion of the chimeric *PG* gene into the *rin* genome only resulted in solubilisation and depolymerisation of homogalacturonan, but not fruit softening (Giovannoni *et al.*, 1989). Therefore, EPG role in fruit softening deserves further investigation to a clearer understanding.

1.3.2 Pectate lyases

Pectate lyases (PLs), like EPGs, attack low-methylester homogalacturonan domains in mid-chain, but do so by an elimination reaction rather than by hydrolysis (Marín-Rodríguez *et al.*, 2002; Tucker & Seymour, 2002) (Figure 1.3.1). Plant *PL* genes are transcribed in certain tissues, but relatively few studies have conclusively demonstrated PL activity in uninfected plant tissues, most studies of PL activity having dealt with the enzymes produced by plant pathogens and saprotrophs.

PL-like genes are widely isolated from many plants with expression mainly towards fruit ripening. In banana, PL mRNA was detected in the early stages of ripening, reached a maximum at the climacteric peak and declined in the over-ripe stage (Dominguez-Puigjaner *et al.*, 1997, Payasi & Sanwal, 2003). Marín-Rodríguez *et al.* (2003) reported the expression of two distinct PL-like genes (*Pel I* and *Pel II*) in ripening banana, and both were expressed only in ripe fruit tissue (both pulp and peel, but not in leaves, roots, corms or green fruit), with *Pel I* predominating. Marín-

Rodríguez *et al.* (2003) reported a Ca^{2+}-dependent PL activity in banana fruit-pulp extracts. Also in banana pulp, Payasi and Sanwal (2003) detected activities of PL and also pectin lyase (pectin lyase catalyses the elimination-degradation of high-methoxy pectin rather than de-esterified homogalacturonan). However, pectin lyase is reported to have no requirement for Ca^{2+} (Pitt, 1988) and later Payasi *et al.* (2006) confirmed the activity of PL in banana pulp (instead of pectin lyase) by omitting Ca^{2+} from the PL assay. The elimination of PL activity in the absence of Ca^{2+} indicates that the purified banana enzyme is pectate lyase rather than pectin lyase.

In mango, Chourasia *et al.* (2006) reported PL-like gene (*MiPel1*) expression, triggered only during the ripening process and fruit specific as no transcript was detected in other tissues or in unripe fruit. In apple, PL activity increased from unripe fruit to ripe fruit but after that remained at similar level throughout the over-ripe stage (Goulao *et al.*, 2007). Strawberry transcribes and translates at least three *PL* genes and all were expressed at higher level in the fruit during the ripening stages (Benitez-Burraco *et al.*, 2003). Expression of an antisense *PL* gene in strawberry was able to decrease post-harvest softening, suggesting a functional role for PL (Jimenez-Bermudez *et al.*, 2002).

EPG has been the focus of studies of pectin degrading enzymes for many years by many researches and the role of PLs has been ignored. One reason for this is probably the difficulties in measuring PL activity in crude extracts. But, as discussed above, *PL* genes are widely transcribed in plants and at least in some tissues, the encoded proteins exhibit PL activity when assayed *in vitro*. However, whether and to what extent PL exhibits action *in vivo* remains to be established with certainty.

1.3.3 Non-enzymic scission by hydroxyl radicals (•OH)

Miller (1986) was the first to report the potential involvement of reactive oxygen species (ROS) in degrading cell wall polysaccharides under physiological conditions. In his experiment, incubation of cellulose, sodium carboxylcellulose, pectin, polygalacturonic acid, xylan and arabinogalactan with hydrogen peroxide exhibited rapid breakdown of the polysaccharides when measured by a reduction of solution viscosity or an increase in reducing groups. Later, •OH was suggested to have important roles in the plant cell wall, particularly in cell growth and cell wall degradation, including during fruit ripening processes. Many reports show that •OH can cause non-enzymic scission of any polysaccharides, including pectin and xyloglucan (Fry, 1998; Schweikert *et al.*, 2002; Uchiyama *et al.*, 1990; Von Sonntag, 1987; Zegota, 2002; Schopfer, 2001). Fry *et al.* (2002) reported a study where membrane-impermeant probes (*N*-[^{3}H]benzoyl-glycylglycylglycine (BzG_3), *N*-[^{3}H]benzoyl-pentalysine methyl ester (BzK_5Me), and *N*-[^{3}H]benzoyl-polyallylamine (Bz-PA)) are used which led to the hypothesis that apoplastic H_2O_2 and polysaccharide-bound Cu^+ could undergo a Fenton reaction as a potential mechanism for •OH formation *in vivo*. In the Fenton reaction, naturally present ascorbic acid is used as antioxidant to reduce Cu^{2+} to Cu^+ (Vreeburg & Fry, 2005; Green & Fry, 2005; Kärkönen & Fry, 2006; Lindsay & Fry, 2007). Others reported that •OH is readily produced under conditions found in the plant apoplast, not only by the Fenton reaction involving reduced transition metal ions plus H_2O_2 (Fry, 1998), but also by a mechanism involving peroxidase-bound iron and the Haber–Weiss cycle (Chen & Schopfer, 1999).

$^{\bullet}$OH attacks polysaccharide chains relatively indiscriminately: if produced directly in the apoplast, it will attack cell wall polysaccharides and lead to their breakage. The proposed mechanism of $^{\bullet}$OH scission is as follows: (a) $^{\bullet}$OH acts on the polysaccharide to abstract a C-bonded H atom, leaving behind a carbon-centred radical, (b) in aerobic solution, the carbon-centred radical reacts with O_2 to form an organic peroxyl radical, (c) a hydroperoxyl radical ($HO_2^{\bullet}$; or its ionized form, $O_2^{\bullet-}$) is eliminated, leaving an oxo group on the polysaccharide (Schuchmann & Von Sonntag, 1977). Figure 1.3.2 shows an illustrated scheme of these proposed reactions at several positions on GalA residues.

Because of the extremely short half-life of $^{\bullet}$OH, detecting its presence and action directly within a cell is very difficult. Studies by Müller *et al.* (2009) only manage to demonstrate and detect the production of $^{\bullet}$OH-precusors and/or products ($O_2^{\bullet-}$and H_2O_2) *in vivo*, in the growing zone of germinating cress seeds and in elongating maize coleoptiles using specific histochemical assays and electron paramagnetic resonance spectroscopy. On the other hand, an indirect way of identifying $^{\bullet}$OH action in the cell wall involves detecting the presence of particular chemical fingerprints, compounds created only after $^{\bullet}$OH attack of cell wall polysaccharides. This approach was reported in Miller & Fry (2001) where acid- and Driselase-digestion of $^{\bullet}$OH-attacked xyloglucan produced several chemical 'fingerprint' compounds diagnostic of $^{\bullet}$OH attack. Fry *et al.* (2001) reported direct evidence for $^{\bullet}$OH attack *in vivo* in pear. In this experiment, AIR isolated from hard, medium and soft pear fruit were treated with NaB^3H_4 and digested with Driselase. The dimer compounds resulting from this digestion were proposed to include α-D-[^{3}H]TalA-(1→4)-D-GalA and/or α-D-[^{3}H]GulA-(1→4)-D-GalA and suggested as

evidence for prior ˙OH attack. Later, Müller *et al.* (2009) used the ^{3}H fingerprinting method to show the production and action of ˙OH in endosperm weakening and radicle elongation. This fingerprint strategy led to the present research, in which I further studied the involvement of ˙OH scission in pectin degradation.

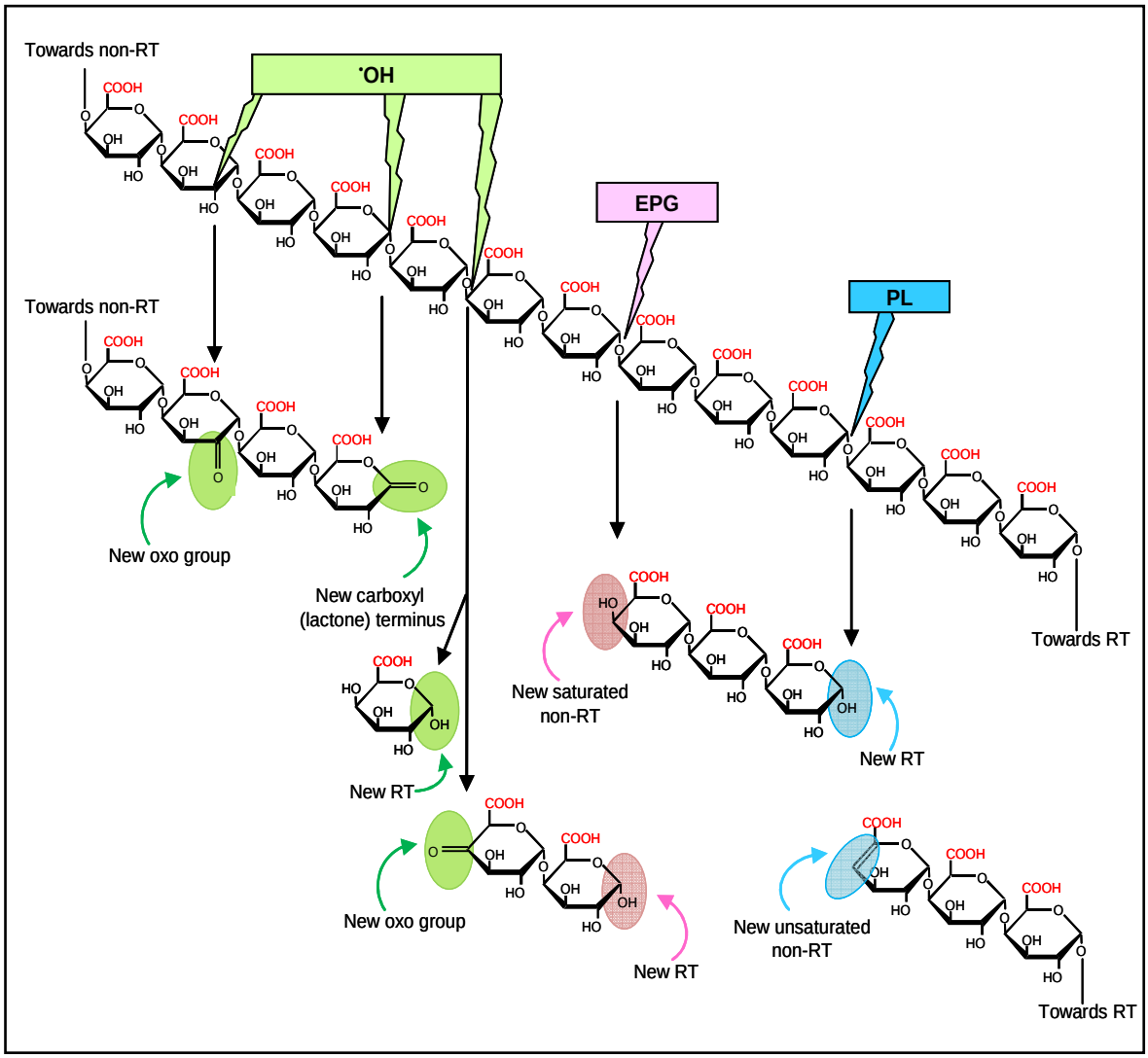

Figure 1.3.1 The three main proposed mechanisms of attack on homogalacturonan domains.
The original homogalacturonan domain represents part of a pectin chain and has been attacked by the three mechanisms resulting in several products that we predict can be recognised as chemical fingerprints after the attack. The three mechanisms of attack are non-enzymic scission by the hydroxyl radical (˙OH) and enzymic scissions by endopolygalacturonase (EPG) and pectate lyase (PL). Each mechanism attacks the mid chain of the homogalacturonan domain and leaves a different chemical fingerprint in the attacked homogalacturonan. EPG generates a reducing and a saturated non-reducing terminus; PL generates a reducing and unsaturated non-reducing terminus; ˙OH generates diverse termini as well as introducing new oxo groups at several positions (adapted from Fry, 2003).

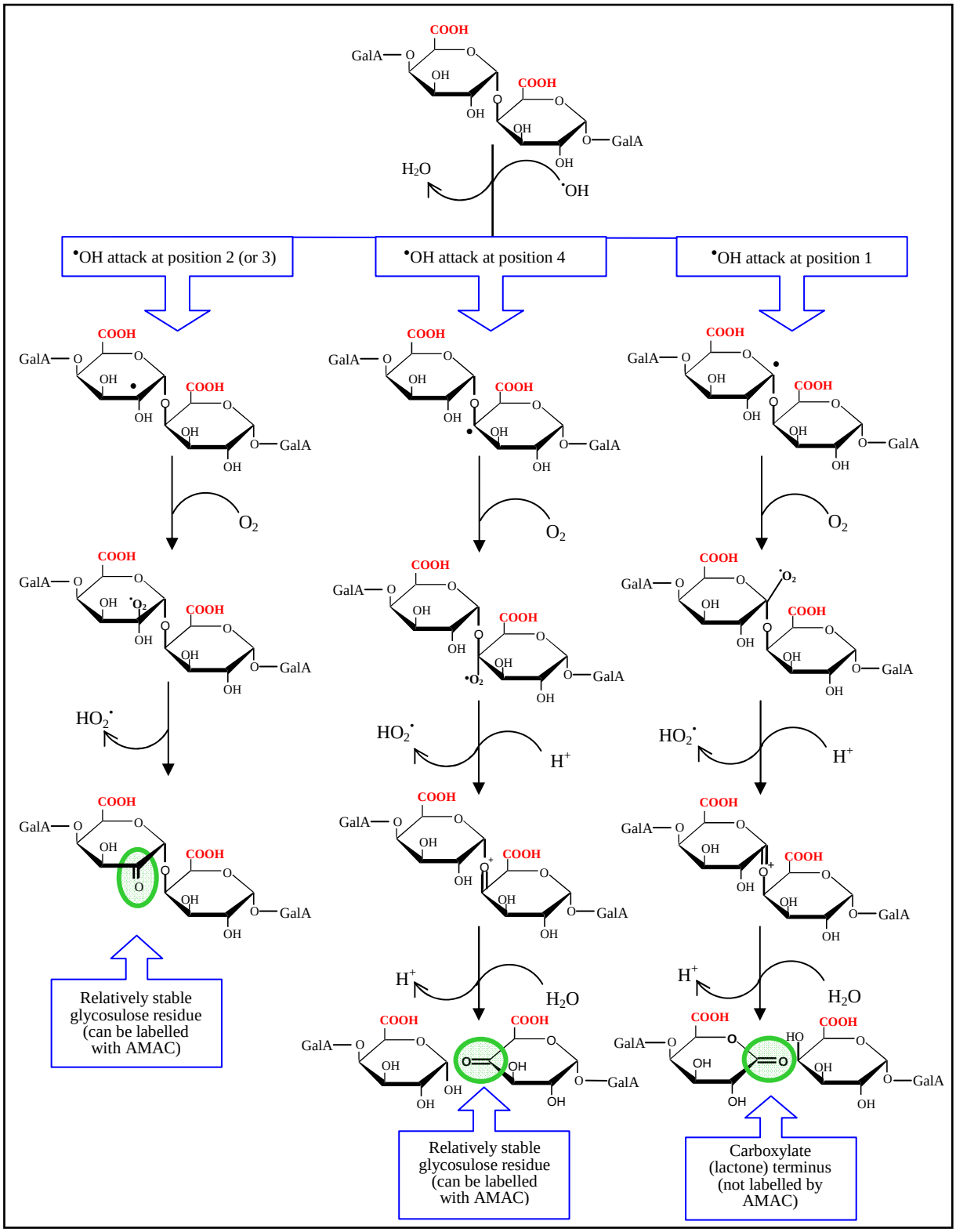

Figure 1.3.2 The proposed reactions of •OH attack at several positions on galacturonic acid (GalA) residues under aerobic conditions.
The GalA residues represent a part of the pectin chain. •OH may attack for example at position 2, position 4 or position 1, in each case abstracting one H atom. If •OH attack involves position 2 (or 3; not shown), an oxo group will be introduced at this position without causing any cleavage of the adjacent glycosidic bond. However, if •OH attack involves position 1 or 4, the reactions will rapidly lead to pectin cleavage (adapted from Lindsay & Fry, 2007)

1.4 Strategy for investigating pectic polysaccharide degradation mechanisms

As discussed above, three main mechanisms have been proposed by which the homogalacturonan chains could be attacked by EPG, PL and ˙OH. The three modes of homogalacturonan degradation mentioned above are functionally equivalent in one sense: 'mid-chain' cleavage, resulting in a decrease in M_r of a pectic polysaccharide. However, their regulation is likely to be quite independent. All three mechanisms could in principle occur simultaneously in the same plant cell; but which of them predominate(s) in given cells at given times is still an important question. Concerning enzymic mechanisms, analysis of transcript accumulation and enzyme activities do not necessarily display their real action *in vivo*. This is because all possible post-transcriptional and post-translation modifications and enzyme activity regulation by the plant cellular environment are not taken into account. In order to overcome those issues, demonstration of *in-planta* action of the enzymes and/or of ˙OH is required.

Thus, this research has taken that challenge. The main strategy involves recognising and measuring homogalacturonan molecules that exhibit symptoms of each of the three mechanisms of attack. Based on recent work by R. A. M. Vreeburg and S. C. Fry (unpublished), each mechanism is believed to leave behind a tell-tale chemical fingerprint in the homogalacturonan molecule that is recognisable by chemical analysis: each EPG action event creates one new reducing terminus and one new saturated non-reducing terminus; each PL action event creates one new reducing terminus and one new unsaturated non-reducing terminus; ˙OH creates a wide

diversity of new termini and also introduces oxo groups at sites of the polysaccharide other than the scission site.

1.4.1 Developing novel methods

This novel method has previously been studied in the Edinburgh Cell Wall Group (R. A. M. Vreeburg & S. C. Fry, unpublished) and mainly to study the $^{\bullet}OH$ attack on pectic polysaccharide. It is a fluorescent labelling method based on the ability of 2-AMAC in the presence of a reactive reducing agent, sodium cyanoborohydride ($NaCNBH_3$), to reductively aminate an oxo group on a sugar residue to form an sugar-amine conjugate. Figure 1.4.1 shows the model experiment *in-vitro* for 2-AMAC labelling: (i) the first step of the labelling method involved a pre-treatment with NaOH and $NaBH_4$ to remove any reducible methyl esters and naturally existing oxo groups including the reducing ends (reaction not shown), thus preventing any 2-AMAC labelling other than of $^{\bullet}OH$-introduced oxo groups, (ii) a treatment with $^{\bullet}OH$ formed from H_2O_2, ascorbate and Cu^{2+} (Fenton reagent) to introduce new oxo group(s) into the pectin chain, (iii) reductive amination of the newly introduced oxo group with the primary amine group of 2-AMAC in the presence of $NaCNBH_3$ to form a secondary amine, (iv) an additional step involving a reaction with acetone (to produce pAMAC) to produce more stable tertiary amine products; a fluorescent sugar derivative (this is based on the ability of secondary amines to react with aldehydes and ketones (e.g. acetone) to produce enamines), (v) followed by enzymic digestion with Driselase to produce several diagnostic compounds that was aimed to give information on the degradation of pectic polysaccharides.

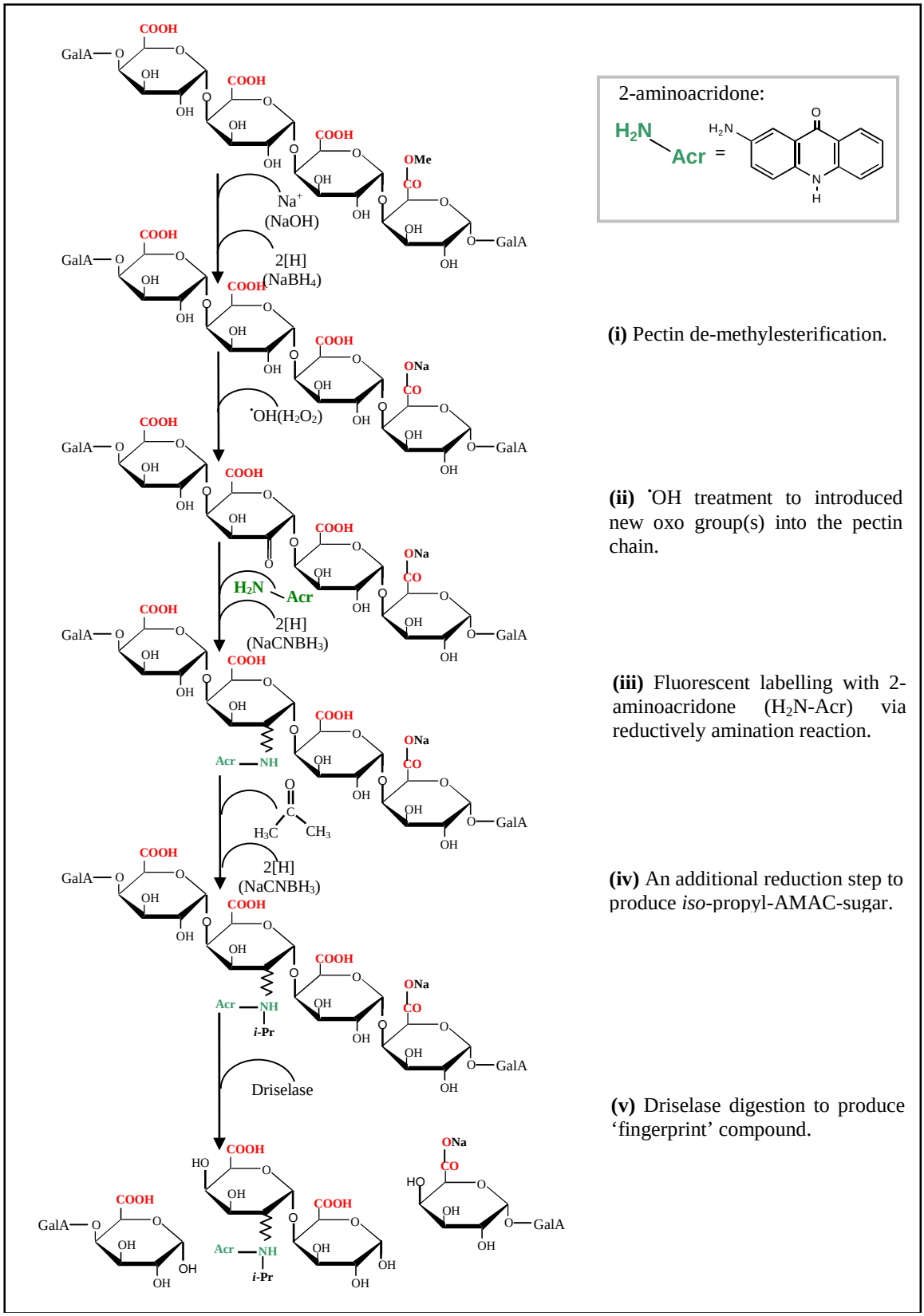

Figure 1.4.1 The proposed reactions on labelling the GalA residues with 2-aminoacridone.
The GalA residues represent a part of pectin chain. (R. A. M. Vreeburg & S. C. Fry, unpublished).

1.4.2 Fluorescent dye: 2-aminoacridone

The strategy for distinguishing the non-enzymic scission by $^{\bullet}OH$ is by exploiting the ability of 2-aminoacridone (2-AMAC) to react with oxo groups in sugar residues. 2-AMAC is a sensitive fluorescent reagent used to modify carbonyl-containing biomolecules (Jackson 1993, 1996). It possesses a primary amine group and in the presence of a reducing agent such as $NaCNBH_3$ can convert a carbonyl group (aldehyde or ketone) to an amine by reductive amination via an intermediate imine.

2-AMAC was originally used for carbohydrate and glycoprotein studies (Jackson 1993, 1996). Since then, it has received a lot of attention and thus this method of analysis is actively developing. It has also been widely used in various analyses including as a reporting group for protease assays (Lazanov *et al.*, 2009), as a fluorescent probe to label oligochitosan (producing 2-AMAC-oligochitosan) in a tobacco cell resistancy study (Zhao *et al.*, 2007), and in pharmacological analyses such as of human blood glucose (Maeda *et al.*, 2007) and human milk carbohydrates (Charlwood *et al.*, 1999).

1.4.3 Key enzyme preparation: Driselase

The methodology to be pursued focuses on novel uses of ‘Driselase’ (available from Sigma Chemical Co.), an extremely versatile fungal enzyme mixture which cleaves almost all glycosidic bonds within homogalacturonan, except at certain rare but informative features such as unsaturated non-reducing termini, to yield the monosaccharide, GalA. In addition, Driselase cleaves RG-I to release

monosaccharides (principally GalA, Rha, Ara and Gal). Driselase also hydrolyses almost all methyl-ester groups from homogalacturonan; the few exceptions are at GalA residues that are also *O*-acetylated (Ishii, 1997; Perrone *et al.*, 2002) which can be readily de-acetylated if necessary.

Driselase was originally used to isolate protoplasts (cells without cell walls) from plant tissues (Zeiger & Hepler, 1976; Shekhawat & Galston, 1983). Later, it has been extensively used to study plant cell wall carbohydrates from many aspects including pectin properties and composition in the plant cell wall. These include the use of Driselase to sequence xyloglucan oligosaccharides by partial digestion (Lorences & Fry, 1993), production of ^{3}H-labelled fingerprint compounds for $^{\bullet}$OH-attack pectin in ripening pear fruit (Fry *et al.*, 2001), and the study of cell wall composition in *Arabidopsis* (Gardner *et al.*, 2002), bryophytes and charophytes (Popper & Fry, 2003).

1.4.4 High-voltage paper electrophoresis (HVPE)

In this research, HVPE is used as one of the main techniques to prepare, identify, purify and analyse the fingerprint compounds resulted from $^{\bullet}$OH attack; it is also used for EPG and PL attack analysis. HVPE provides an analytical method of high resolving power for small molecules and was widely used around the 1950s especially in routine clinical chemistry for blood protein study (Martin & Franglen, 1954; Atfield & Morris, 1961). Since then, the method has been modified and the evolution of the method now enables an advance study of cell-wall building blocks

and their metabolic precursors and is commonly used by Edinburgh Cell Wall group researchers and others. These include the tracking of ascorbate metabolites in its degradation pathway (Green & Fry, 2005), uronic acid studies (Wright & Northcote, 1975; Popper & Fry, 2003) and the study of sugar phosphates involved in cell-wall biosynthesis (Kärkönen & Fry, 2006; Sharples & Fry, 2007).

The HVPE technique used in this research is as described by Fry (2000 & 2011). It is a useful technique for the separation of low-molecular-weight charged molecules, based on differences in their charge:mass ratio, but is also suitable for uncharged molecules that can be given a charge by specific binding to an ion, such as borate or molybdate. It is a rapid separation method, typically taking around 30–60 min and many samples (10–20) can be run simultaneously under identical conditions. The separated compounds can be detected in many ways such as by staining, fluorescence and autoradiography or fluorography if the samples are radiolabelled. Compounds of interest can also be eluted from paper after separation for futher analysis if a non-destructructive detection method is used prior to elution.

1.5 Project aims

The main aim is to develop and optimise novel methods for monitoring the action of EPG, PL, and ˙OH on pectic polysaccharides *in vivo*. The project starts with *in-vitro* ˙OH-attacked model polysaccharides, giving a reference for the fingerprint molecules formed after ˙OH attack. The initial work also includes a preparation and analysis of several authentic markers as reference for fingerprint molecules formed after EPG, PL and ˙OH attack.

The second objective is to apply the developed methodologies to detect homogalacturonan cleavage as result from EPG, PL and ˙OH action in fruit from several contrasting species: pear (*Pyrus communis*), mango (*Mangifera indica* L.), banana (*Musa acuminata* x *Musa balbisiana*), apple (*Malus communis*), avocado (*Persia americana*), strawberry (*Fragaria* x *ananassa*) and strawberry tree fruit (*Arbutus unedo*). All these fruits were chosen based on their variation in several criteria including: (i) botanical origin (tropical and sub-tropical climate species: mango, banana, avocado and strawberry tree fruit; temperate climate species: pear, apple and strawberry), (ii) ripening regulation such as respiration rate regulation (climacteric: pear, mango, banana, apple and avocado; non-climacteric: strawberry and strawberry tree fruit), and also their availability in the market and farm in my local area. This work aimed to determine the action of EPG, PL and ˙OH *in vivo* during the fruit softening process. The unique diagnostic compounds identified as being produced during each mode of attack will be analysed and quantified.

2. Materials and Methods

2.1 Materials

The 2-aminoacridone, Driselase, citrus pectin, galacturonic acid, homogalacturonan, glucose and galactose were from Sigma (Sigma-Aldrich, Sigma Chemical Co., Dorset, United Kingdom) or Fluka (Dorset, United Kingdom). Mini Supelco C_{18} columns were also from Sigma (Sigma-Aldrich, Sigma Chemical Co., Dorset, United Kingdom). The HPLC Luna C_{18} column (250 X 4.6 mm, 5µ C_{18}(2) 100Å) was from Phenomenex (Cheshire, United Kingdom). HPLC CarboPac PA1 and PA100 columns were from Dionex (Surrey, United Kingdom) The HPLC eluants were from VWR (Leicestershire, United Kingdom) or Fisher Scientific (Loughborough, United Kingdom). Other chemicals used throughout were purchased from Sigma-Aldrich (Dorset, United Kingdom) or Fisher Chemicals (Loughborough, United Kingdom). Pear, mango, banana, apple and avocado were bought from Sainsbury's supermarket, Edinburgh. Strawberry was from Belhaven Fruit Farm, Edinburgh and strawberry tree fruit was generously given by Sheffield Botanical Garden, United Kingdom.

2.2 Novel detection method of $^{\bullet}OH$ attack

2.2.1 $^{\bullet}OH$ treatment of commercial citrus pectin

Pectin solution (0.5%, w/v) was demethylesterified with 0.025 M NaOH for 2 h at $0^{\circ}C$ before being pre-treated with 0.062 M $NaBH_4$ (in 0.025 M NaOH) (pH 12.0 to 13.0) at RT overnight to reduce any naturally occurring oxo groups in the pectin

chain. Excess $NaBH_4$ was destroyed with acetic acid until the pH was around 4.0 to 5.0. The sample was dialysed overnight in constantly stirring cool H_2O before being treated with $^{\bullet}OH$ formed from Fenton reagent consisting of 50 mM acetate buffer (pH 4.5), 10 mM H_2O_2, 1 µM $CuSO_4$, and 10 mM ascorbic acid overnight at RT. Controls received no ascorbate, $CuSO_4$ and H_2O_2. Pectin was isolated by precipitation with 75% ethanol, repeatedly washed with 75% ethanol then freeze-dried.

2.2.2 AMAC labelling of $^{\bullet}OH$-treated pectin

Freeze-dried $^{\bullet}OH$-treated pectin (150 µg; ~0.88 µmol GalA residues) was dissolved in a mixture containing 4.5 µl of 0.5% chlorobutanol, 0.5 µl a mixture of acetic acid and pyridine (40% v/v acetic acid and 40% v/v pyridine, final pH 4.0), 8.9 µl of 0.1 M AMAC (= 0.89 µmol) in DMSO and 6.1 µl of fresh 2 M $NaCNBH_3$ (= 12.2 µmol) and vortexed before incubated at RT overnight. After the first incubation, 1 µl acetone (=13.6 µmol) was added and vortexed, immediately followed by 6.1 µl fresh 2 M $NaCNBH_3$ (= 12.2 µmol) and vortexed again before being subjected to another incubation for 1 h at RT. The second incubation with acetone and $NaCNBH_3$ was to convert the secondary amine conjugate from the first incubation to a stable tertiary amine product containing an isopropyl group (pAMAC). Unreacted AMAC was removed by repeated washing with 75% ethanol then the pellet was air-dried. The precipitated, pAMAC-labelled, $^{\bullet}OH$-treated pectin (pAMAC•pectin) was analysed by TLC to determine the success of Fenton treatment and AMAC labelling and also subjected to delactonisation with NaOH followed by Driselase digestion for 14 days.

2.2.3 Preparation of fruit AIR

Unripe fruits were stored in a wooden cupboard at room temperature in the lab, except strawberry tree fruit which was frozen immediately when received from Sheffield Botanical Garden, United Kingdom. At selected days after purchase (when the fruits were hard, medium and soft respectively), individual fruit were peeled and penetrometer reading for each fruit was taken (see Section 2.8). A portion (10 g) of the flesh of the fruit was diced with a razor blade and immediately frozen with liquid N_2 in a mortar and ground to a fine powder with a pestle. Pre-cooled 10 mM $Na_2S_2O_3$ (50 ml; in ethanol/pyridine/ acetic acid/water, 75:2:2:21 by vol.) was added and the mixture was re-ground for another 5 min. Portions of 1 ml were taken from the homogenized suspension into 2-ml Sarstedt tubes and stored at –80°C.

2.2.4 AMAC labelling of fruit AIR

A portion (1 tube containing ~200 mg fresh fruit tissue) of fruit AIR suspension was thawed and centrifuged. The supernatant was removed and the pellet was washed twice with 1 ml ice-cold 75% ethanol, and then air-dried with the aid of filter paper. The pellet was resuspended in a mixture containing 45 µl of 0.5% chlorobutanol, 5 µl a mixture of acetic acid and pyridine (40% v/v acetic acid and 40% v/v pyridine, final pH 4.0), 89 µl of 0.1 M AMAC (= 8.9 µmol) and 61 µl of fresh 2 M $NaCNBH_3$ (= 122 µmol). After the first incubation of the mixture at RT overnight, 10 µl acetone (= 136 µmol) and 61 µl of fresh 2 M $NaCNBH_3$ (= 122 µmol) were added and incubated again, overnight at RT. The AIR was washed with ice-cold 1 ml 96%

ethanol and twice with ice-cold 1 ml 70% ethanol before being air-dried with the aid of filter paper. Cycles of re-suspending and washing the pellet were repeated twice: the pellet was re-suspended in 250 µl pyridine/acetic acid/0.5% chlorobutanol (1:1:98 by vol.) for 10 min at RT before 1 ml ice-cold 96% ethanol was added and centrifuged, and the supernatant was removed. Another 1 ml ice-cold 70% ethanol was added then centrifuged and the supernatant was again removed. The final pellet of pAMAC-labelled fruit AIR (pAMAC•AIR) of this cycle was air-dried and subjected to initial delactonisation followed by Driselase digestion for 14 days.

2.2.5 Delactonisation of undigested pAMAC•pectin or pAMAC•AIR

A pellet of the pAMAC-labelled pectin or fruit AIR was delactonised with 0.5 M NaOH, for 5 h at RT (pH of the solution was checked to be above pH 11.0). Excess NaOH was acidified with acetic acid then the pellet was washed with 1 ml ice-cold 80% ethanol and centrifuged. The pellet was then air-dried and subjected to Driselase digestion.

2.2.6 Driselase digestion of pAMAC•pectin or pAMAC•AIR

The final pellet of pAMAC•pectin or pAMAC•AIR was digested in 1% Driselase (30 µl for pAMAC•pectin or 250 µl for pAMAC•AIR, in pyridine/acetic acid/0.5% chlorobutanol, 1:1:98, by vol.) at RT for up to 42 days. After 7, 14 and/or 42 days, equal volumes of supernatant were taken from the mixture and digestion was stopped

by freezing at –20°C. The supernatant was thawed and subjected to mini Supelco C_{18} purification, delactonisation and analysis by electrophoresis and/or chromatography.

2.2.7 Partial purification of pAMAC-labelled products on a mini Supelco C_{18} column

A C_{18} column (500 mg Supelco column from Sigma-Aldrich) was pre-conditioned with 2 volumes of methanol then 2 volumes of H_2O. The sample (typically 1 – 2 ml) was loaded into a conditioned C_{18} column and washed with 2 × 2 ml H_2O, then the bound solutes were eluted with 2 × 2 ml each of 10%, 20%, 30%, 40%, 50%, 60%, 70%, 80%, 90%, and 100% methanol. Fractions were dried and redissolved in 50 to 200 µl of pyridine/acetic acid/0.5% chlorobutanol (1:1:98, by vol.) then stored at –20°C.

2.2.8 Delactonisation of digested pAMAC•pectin or pAMAC•AIR

A portion (10 – 40 µl) from each C_{18} fraction was dried in a 'SpeedVac' to remove the pyridine/acetic acid/chlorobutanol and/or methanol. The resulting residue of pAMAC•pectin or pAMAC•AIR digestion products was dissolved in 10 µl of 0.5 M NaOH (the pH of the solution was checked with indicator paper to be above pH 11.0). The solution was incubated at RT for 10 min. The excess NaOH was acidified with 0.5 µl of acetic acid to pH 4.0–5.0. These delactonised samples were subjected to electrophoresis and/or chromatography.

2.2.9 Marker preparation— pAMAC-labelling at the reducing terminus of Glc, Gal, GalA, $GalA_2$, and $GalA_3$

Reducing sugar in dry form (0.4 µmol of Glc, Gal, GalA, $GalA_2$, or $GalA_3$) was mixed with 40 µl 0.1 M AMAC (= 4 µmol) in DMSO/acetic acid/pyridine (17:2:1, by vol.) followed immediately by 40 µl of fresh 1 M $NaCNBH_3$ (= 40 µmol). After the first incubation of the mixture at RT overnight, 2 µl acetone (= 27.2 µmol) and 40 µl of fresh 1 M $NaCNBH_3$ (= 40 µmol) were added and incubated for another 1 h at RT. The mixture was diluted with 5 volumes of H_2O and centrifuged (14 000 rpm, 10 min). Next the supernatant was collected and purified on a mini Supelco C_{18} column (refer Section 2.2.7), and the pAMAC-labelled product analysed by electrophoresis and/or chromatography.

2.3 Detection methods of PL and EPG attack

2.3.1 $NaBH_4$ treatment of fruit AIR for PL and EPG analysis

A portion of fruit AIR suspension equal to that used previously for pAMAC labelling was thawed and centrifuged. The supernatant was removed and the pellet was washed twice with 1 ml ice-cold 75% ethanol, and air-dried with the aid of filter paper. The pellet was then treated with 200 µl of 0.05 M $NaBH_4$ (in 0.05 M NaOH) (pH 12.0 to 13.0) at RT overnight to reduce any reducing termini in the pectin chain before being subjected to delactonisation followed by Driselase digestion for 14 days. Sample was boiled for 30 min to stop the digestion then centrifuged. The

supernatant was collected, dried and redissolved in 100 µl of pyridine/acetic acid/0.5% chlorobutanol (1:1:98, by vol.). The digestion products were analysed by HPLC on a PA100 column.

2.3.2 Treatment of non-$NaBH_4$ fruit AIR

Again, an equal portion of fruit AIR suspension that was used previously for pAMAC labelling was thawed and centrifuged. The supernatant was removed and the pellet was washed twice with 1 ml ice-cold 75% ethanol, and air-dried with the aid of filter paper. The pellet was subjected to delactonisation followed by Driselase digestion for 14 days. Sample was boiled for 30 min to stop the digestion then centrifuged. The supernatant was collected, dried and redissolved in 100 µl of pyridine/acetic acid/0.5% chlorobutanol (1:1:98, by vol.). The digestion products were analysed by HPLC on a PA100 column.

2.3.3 Preparation of marker ΔUA-GalA

Homogalacturonan solution (1% w/v in 50 mM CAPS buffer containing 1 mM $CaCl_2$, adjusted to pH 10.0 with NaOH; Brown *et al.,* 2001) was digested with PLase (5 U/ml in the same buffer) for 100 min at RT. Digestion was stopped with 25% formic acid (by vol.) and the products were subjected to paper electrophoresis at pH 6.5. A part of the products on the electrophoretogram was stained with aniline hydrogen-phthalate and another part which was observed to contain the dimer

(ΔGalA-GalA) compound was eluted from the electrophoretogram. A small portion of the eluted dimer was subjected to Driselase digestion for stability confirmation.

2.3.4 Preparation of marker GalA-GalO

A portion (2 mg) of (1→4)-α-galacturonobiose was treated with 2 ml of 0.5 M $NaBH_4$ (in 1 M NH_3) (pH 11.0 to 12.0) at RT for 4 h. Excess $NaBH_4$ was acidified with 300 µl acetic acid to bring the pH to around 4.0 to 5.0. The solution was passed through a 3-ml bed-volume column of Dowex-50 (previously was washed in 1 M HCl followed by plentiful H_2O) in a Pasteur pipette and the products were eluted with 6 ml H_2O. The eluate of non-cationic products was dried in a 'SpeedVac', re-dissolved in 1 ml methanol/acetic acid (10:1 by vol.) and re-dried. This step was repeated for 10 times to remove H_3BO_3. The final pellet was re-dissolved in 2 ml dH_2O and a small portion of the GalA-GalO dimer was subjected to Driselase digestion for stability confirmation.

2.4 Preparation of galacturonobiose/triose from homogalacturonan

A solution (10 ml) of 0.2% homogalacturonan was freshly prepared in 0.5% chlorobutanol. The solution was adjusted to pH 4.0 with ~0.3 ml 10% acetic acid (added dropwise) and digested with 4.2 U EPGase. The digestion mixture was left at RT for 48 h before being subjected to Whatman 3MM descending paper

chromatography (ethyl acetate/acetic acid/water, 10:5:6 by vol.), ethanolic bromophenol blue staining, elution from paper and C_{18} purification.

2.5 Purification of Driselase

The Driselase purification procedure and all chemicals involved were maintained in a cold-room. Driselase (10 g) was stirred for 15 min in 100 ml buffer (50 mM acetic acid, adjust to pH 5.0 with 1.0 M NaOH) and centrifuged for 10 min at 4 000 rpm. The supernatant was collected and solid $(NH_4)_2SO_4$ was added to the supernatant (26 g per 50 ml supernatant) with constant stirring. The solution was left to stand overnight at 4°C then centrifuged for 10 min at 4 000 rpm. The remaining pellet was re-suspended in 100 ml fresh $(NH_4)_2SO_4$ (52 g solid dissolve in 100 ml H_2O) and centrifuged for 10 min at 4 000 rpm. The supernatant was rejected and the pellet was dissolved in 100 ml chilled H_2O. The solution was loaded onto a Sephadex G-25 column (1500-ml bed volume, washed and eluted with 0.5% chlorobutanol). The first colourless eluate was discarded and the following fast-eluting brown material was collected. The eluate was frozen at –70°C, freeze-dried and stored at –20°C.

2.6 Elution of compounds from paper

This method was based on Fry (2000). The zone containing the compound of interest was cut out. The paper was rolled and pressed down into the barrel of a 5-ml disposable syringe. The barrel then hung in 15-ml centrifuge tube. The paper was

wetted with the minimum volume of water then centrifuged at 4 000 rpm, 5 min. The wetting and centrifuging steps were repeated 5 times. The eluate was collected in the centrifuge tube.

2.7 Hydrolysis of non-cellulosic polysaccharides in TFA

The remaining residues after the Driselase digestion in Section 2.2.6, 2.3.1 and 2.3.2 were washed few times with 80% ethanol then air-dried. The air-dried cell walls were re-suspended in 1 ml 2 M trifluoroacetic acid (TFA) in a 2-ml Sarstedt tube. The mixture was heated at 120°C for 1 h in an oven and cooled before being centrifuged. The supernatant was harvested, dried in a 'SpeedVac' then redissolved in H_2O. A portion of 10 – 100 µl of the hydrolysate was subjected to chromatography.

2.8 Firmness test of fruit by penetrometer

The firmness test was performed using a PCE-PTR 200 penetrometer (from PCE Instruments) with Newtons (N) unit measurement. The appropriate penetration probe (6 mm diameter probe in this case) for the type of fruit was chose for the test. Three fruits from each sample were randomly selected at each time point (three time points for three stages of softening in this experiment) for replication. The epicarp of the individual fruit (except strawberry and strawberry tree fruit) was peeled. The fruit and probe were positioned perpendicular to each other. The sensor was pressed down

until it penetrated up to the indicator mark on the sensor and the value shown on the display of the penetrometer was recorded.

2.9 Separation of compounds by electrophoresis and planar chromatography

2.9.1 Paper electrophoresis

Samples were loaded as spots or streaks onto Whatman 1CHR or 3MM paper and dried. The paper was wetted with a buffer pH 6.5 (pyridine/acetic acid/water, 33:1:300 by vol.). The paper was suspended in a large glass tank filled with immiscible coolant (for electrophoresis at pH 6.5, toluene was used). One end of the paper was hung from a trough situated at the top of the tank. This trough contained the specific buffer the paper had been wetted with and also a platinum cathode. The bottom of the tank contained the same buffer to immerse the opposite end of the paper and also a platinum anode. A voltage of 4 kV was then applied through the buffer for a set period of time (30 min–1 h) in order to separate the compounds based on their charge:mass ratios. Fluorescent spots were examined and recorded under a 254-nm UV lamp in the Camlab DocIt system and unlabelled sugars were stained with silver nitrate or aniline hydrogen-phthalate.

2.9.2 Descending paper chromatography

Samples were loaded as spots or streaks onto Whatman 1CHR or 3MM paper and dried. The paper was then placed into a large glass tank and hung from a trough situated at the top of the tank. This trough contained a specific solvent (butanol/acetic acid/water, 12:3:5 by vol. followed by ethyl acetate/pyridine/water, 8:2:1 by vol.). The tank was then sealed with a glass lid and the chromatogram was removed after the appropriate time, normally 16–18 h for each solvent system. Fluorescent spots were examined and recorded under a 254-nm UV lamp in the Camlab DocIt system and unlabelled sugars were stained with silver nitrate or aniline hydrogen-phthalate or eluted from paper.

2.9.3 Thin-layer chromatography

Samples were loaded as spots onto a TLC plate (Merck, non-fluorescent, silica gel 60, 20 x 20 cm) and placed into a glass tank containing 100 ml butanol/ acetic acid/ water with ratio either 2:1:1 or 4:1:1 by vol. The tank was sealed with a glass lid and the plate was removed when the solvent front was approximately 2 cm from the top of the plate. Fluorescent spots were examined and recorded under a 254-nm UV lamp in the Camlab DocIt system and unlabelled sugars were stained with thymol.

2.10 Detection of compounds on paper or TLC

2.10.1 Silver nitrate stain

When completely dry, paper electrophoretograms and paper chromatograms were dipped through three solutions (a − c). The paper was dried for 15 min each time before it was dipped through the next solution. Papers were dipped twice or three times through solution b.

(a) $AgNO_3$ (5 mM in acetone; a small volume of H_2O was used to redissolve any precipitate).

(b) NaOH (0.125 mM in 96% ethanol).

(c) $Na_2S_2O_3$ (10% w/v in H_2O).

The paper was washed with tap water for 1 h and then dried overnight.

2.10.2 Aniline hydrogen-phthalate stain

A stock of acetone/diethyl ether/water (49:49:2 by vol.) containing 1.6% w/v phthalic acid was prepared. Prior to use, aniline (0.5 ml/100 ml of stock) was added to the stock solution. The paper was dipped through the solution, dried and heated in an oven at 105°C for 5 to 10 min.

2.10.3 Thymol stain

A 0.5% (w/v) thymol solution was prepared in ethanol. Concentrated H_2SO_4 to a final concentration 5.0% of v/v was added to the solution. The TLC plate was quickly dipped through this solution, dried and then heated in an oven at 120°C for 5 min.

2.10.4 Ethanolic bromophenol blue stain

When completely dry, paper electrophoretograms and paper chromatograms were washed a few times in butanol/acetone (1:1 by vol.) to remove remaining acetic acid on the paper then re-dried. A 0.04% w/v bromophenol blue solution was prepared in ethanol. When dissolved, collidine (60 µl collidine per 100 ml bromophenol blue solution) was added to the solution to raise the pH. The paper was dipped through the solution, dried and yellow-stained compounds were subjected to elution from paper and C_{18} purification. If decolourisation was needed, the stained paper was washed in ethyl acetate followed by acetone a few times.

2.11 Analysis of compounds by HPLC

2.11.1 Luna C_{18} column

A portion of digested pAMAC•pectin and/or pAMAC•AIR was diluted with H_2O or freshly delactonised with NaOH (refer Section 2.2.8). HPLC separation was

performed on a Luna C_{18}-silica column (250 × 4.6 mm, 5µ C_{18}(2) 100Å) from Phenomenex. Eluent A was 500 mM acetic acid (adjusted to pH 5 with NaOH) and eluent B was acetonitrile. The column was pre-conditioned with 90% A, 10% B for 30 min. The sample (20 µl) was injected and the following elution conditions were used: 0–5 min: 90% A, 10% B, isocratic; 5–15 min: 90% A, 10% B to 87.5% A, 12.5% B, linear gradient; 15–30 min: 87.5% A, 12.5% B, isocratic; 30–35 min: 87.5% A, 12.5% B to 85% A, 15% B, linear gradient; 35–40 min: 85% A, 15% B, isocratic; 40–50 min: 85% A, 15% B to 75% A, 25% B, linear gradient; 50–60 min: 75% A, 25% B to 90% A, 10% B, linear gradient; 60–65 min: 90% A, 10% B, isocratic. The flow rate used was 1 ml/min at ambient room temperature. A fluorescence detector (RF 2000, Dionex) was used with an excitation wavelength of 442 nm and an emission wavelength of 520 nm.

2.11.2 Dionex PA1 column

HPLC separation of monosaccharides and disaccharides was performed on a PA1 column. Eluent A was H_2O and eluent B was 1 M NaOH. The column was pre-conditioned with 98% A, 2% B for 30 min. The sample (20 µl) was injected and the following elution conditions were used: 0–3 min: 98% A, 2% B, isocratic; 3–3.01 min: 98% A, 2% B to 100% A, linear gradient; 3.01–40 min: 100% A, isocratic; 40–75 min: 100% A to 20% A, 80% B, non-linear gradient; 75–81 min: 20% A, 80% B, isocratic; 81–82 min: 20% A, 80% B to 98% A, 2% B, linear gradient; 82–90 min: 98% A, 2% B, isocratic. The flow rate used was 1 ml/min and at ambient room temperature and a pulsed amperometric detector (PAD) was used.

2.11.3 Dionex PA100 column

Acidic sugars were separated and analysed by HPLC on a PA100 column (from Dionex). Eluent A was 1 M NaOAc and eluent B was 100 mM NaOH. The column was pre-conditioned with 20% A, 80% B. The sample (20 µl) was injected and the following elution conditions were used: 0–2 min: 20% A, 80% B, isocratic; 2–40 min: 20% A, 80% B to 70% A, 30% B, linear gradient; 40–41 min: 70% A, 30% B to 100% A, linear gradient; 41–46 min: 100% A, isocratic; 46–47 min: 100% A–20% A, 80% B, linear gradient; 47–52 min: 20% A, 80% B, isocratic. The flow rate used was 1 ml/min and at ambient room temperature and a pulsed amperometric detector (PAD) was used.

3. Results

3.1 Preparation and analysis of standard markers for recognizing the chemical fingerprints of ˙OH, EPG and PL attack

3.1.1 pAMAC-labelling of reducing monosaccharides and oligosaccharides

3.1.1.1 Electrophoresis at pH 6.5

Neutral and acidic monosaccharides and oligosaccharides were successfully labelled with pAMAC at the reducing terminus to produce useful markers. These compounds were examined by pH 6.5 electrophoresis and visualised under a 254-nm UV lamp. Neutral monosaccharide labelling (to produce Glc-pAMAC and Gal-pAMAC) resulted in spots that were approximately neutral (or moved slightly towards the cathode when compared with the free glucose; Figure 3.1.1 (i)). Uronic acid labelling (to produce GalA-pAMAC, $GalA_2$-pAMAC and $GalA_3$-pAMAC) resulted in fluorescent anionic spots (Figure 3.1.1 (ii) & (iii)).

Uronic acids labelled with pAMAC were prone to lactonise. When GalA-pAMAC, $GalA_2$-pAMAC and $GalA_3$-pAMAC were subjected to electrophoresis at pH 6.5 without a delactonisation step, each marker migrated as a number of fluorescent spots (Figure 3.1.1 (ii)). Two spots were formed from GalA-pAMAC and three spots each were formed from $GalA_2$-pAMAC and $GalA_3$-pAMAC. The fastest-migrating spot (fluorescing greenish) was the acidic form of the UA-pAMAC derivative while the slower migrating spots were presumed to be lactones. These lactone spots (fluorescing greenish and/or blue) could be converted into the fastest-migrating one by brief treatment with NaOH at pH > 11, which cleaves the lactone rings. The acidic forms of GalA-pAMAC, $GalA_2$-pAMAC and $GalA_3$-pAMAC were

well separated and distinguishable from each other (Figure 3.1.1 (iii)). Acidic $GalA_2$-pAMAC moved slower than acidic $GalA_3$-pAMAC and faster than GalA-pAMAC.

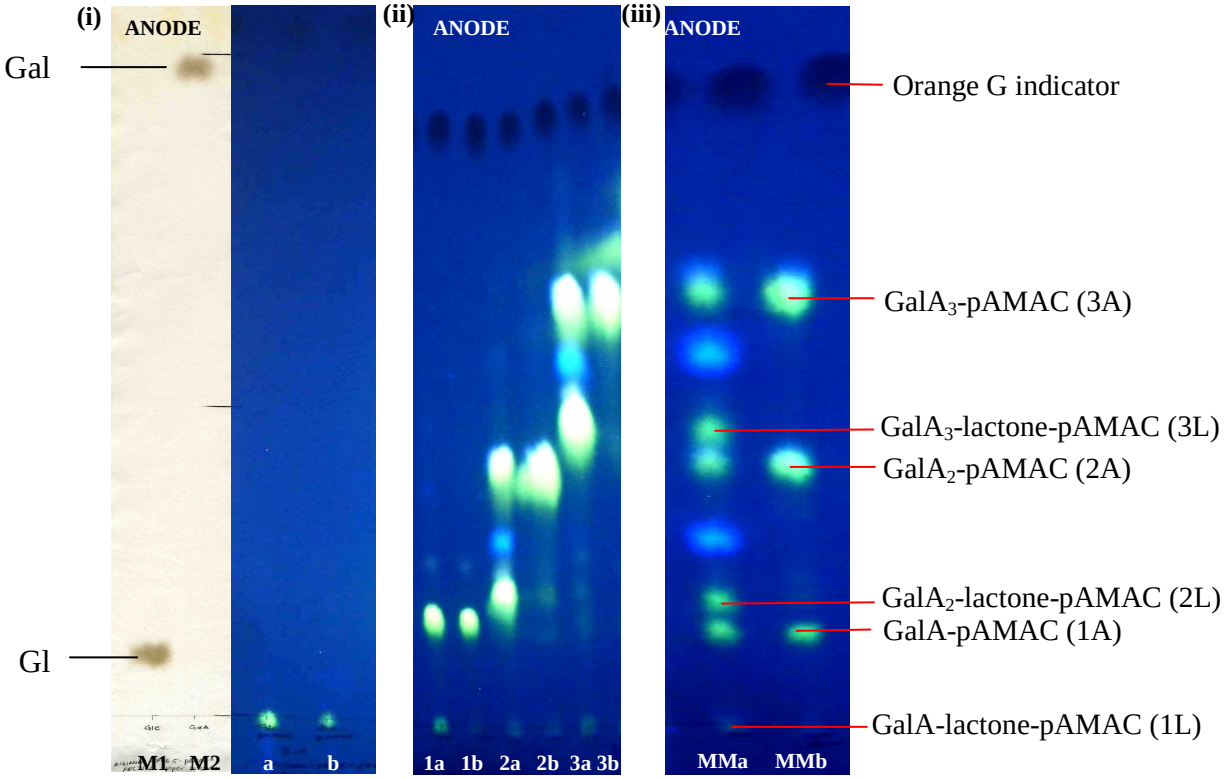

Figure 3.1.1 Approximately-neutral and anionic pAMAC-labelled sugars on a pH 6.5 electrophoretogram

Neutral and acidic monosaccharides and oligosaccharides were labelled with pAMAC; the products were then fractionated on a C_{18} column, and fractions with major fluorescent compounds were pooled. The image shows the fluorescent compounds obtained from each sugar labelling: (i) is the neutral monosaccharide pAMAC labelling while (ii) and (iii) are the uronic acid pAMAC labelling, with (a) Glc-pAMAC; (b) Gal-pAMAC; (1a and 1b) GalA-pAMAC before and after delactonisation; (2a and 2b) $GalA_2$-pAMAC before and after delactonisation; (3a and 3b) $GalA_3$-pAMAC before and after delactonisation; MMa and MMb are the mixture of GalA-pAMAC, $GalA_2$-pAMAC and $GalA_3$-pAMAC before and after delactonisation; free sugars were: (M1) Glc and (M2) GalA. Compounds on electrophoretogram were visualised with silver nitrate staining. Electrophoresis was at pH 6.5, 4.0 kV, 45 min and then fluorescent products were examined under a 254-nm UV lamp.

3.1.1.2 Analysis by HPLC on a C_{18} column

The UA-pAMAC markers were further analysed by HPLC on a Luna C_{18} column with a fluorescence detector. Without a delactonisation step, each UA-pAMAC marker produced two peaks, but a single peak if delactonised. Figure 3.1.2 (i) shows the result observed when a mixture of GalA-pAMAC, $GalA_2$-pAMAC and $GalA_3$-pAMAC was subjected to HPLC without being delactonised: six well-resolved peaks were formed which belonged to GalA-pAMAC, $GalA_2$-pAMAC and $GalA_3$-pAMAC and their lactones (based on peaks that eluted when each marker was run individually, with and without a delactonisation step). Amongst the acidic forms, GalA-pAMAC has a longer retention time than $GalA_2$-pAMAC, while $GalA_3$-pAMAC has the shortest retention time. This observation agreed with the expected polarity properties of each sugar where GalA-pAMAC, the simplest compound, is the most hydrophobic thus being retained longer on the column while $GalA_3$-pAMAC is the most hydrophilic compound thus easily eluted from the column. For the same reason, the acidic form of any UA-pAMAC has a shorter retention time than its less hydrophilic lactone form. Lactonisation evidently caused the compound to be more hydrophobic than the acidic form thus the lactone form was retained longer on the C_{18} column. Delactonisation of the same mixture produced three very well-resolved peaks (Figure 3.1.2 (ii)). The shortest retention time was for the acidic form of $GalA_3$-pAMAC and the longest was for the acidic form of GalA-pAMAC. The retention times of these peaks differed slightly from run to run, but could still be well interpreted.

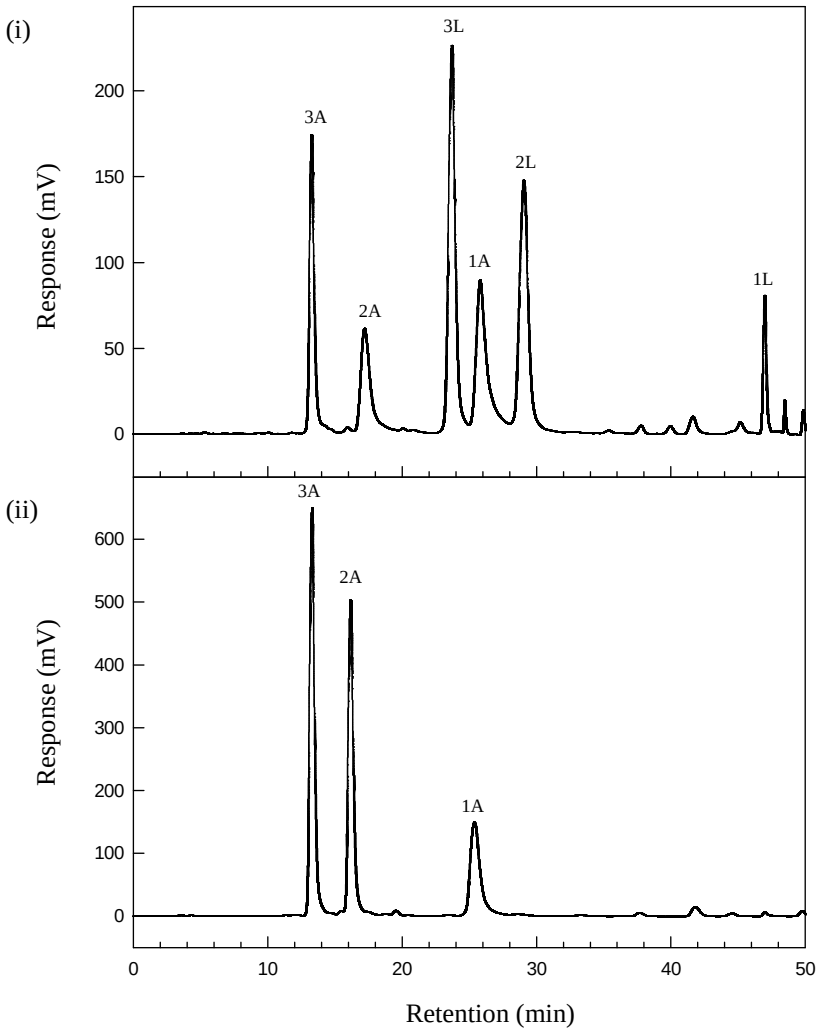

Figure 3.1.2 HPLC-resolution of a marker mixture of GalA-pAMAC, $GalA_2$-pAMAC and $GalA_3$-pAMAC on a Luna C_{18} column

Two samples of a marker mixture of GalA-pAMAC, $GalA_2$-pAMAC and $GalA_3$-pAMAC were analysed by HPLC: (i) not delactonised; (ii) delactonised. Peaks: (3A) $GalA_3$-pAMAC; (2A) $GalA_2$-pAMAC; (3L) $GalA_3$-lactone-pAMAC; (1A) GalA-pAMAC; (2L) $GalA_2$-lactone-pAMAC; and (1L) GalA-lactone-pAMAC. Different proportions of GalA-pAMAC, $GalA_2$-pAMAC and $GalA_3$-pAMAC were used to form the mixtures. Fluorescence detection was with excitation at 442 nm and emission at 520 nm.

3.1.1.3 Analysis of individual fluorescent spots by HPLC

Further verification was performed for individual fluorescent spots by HPLC. Each fluorescent spot was eluted from an electrophoretogram and submitted to HPLC analysis. GalA-pAMAC, $GalA_2$-pAMAC, $GalA_3$-pAMAC and their lactone forms each resulted in a peak matching its expected retention time (Figure 3.1.3). The lactone form of each acidic compound may present as a minor compound in the sample or vice versa because lactonisation is a reversible process and acetic acid as eluent in this HPLC system might promote lactonisation.

The eluted blue-fluorescing compounds (2B and 3B) were detected with low sensitivity on HPLC, probably because the detector (λ_{em}= 520 nm) was only detecting the greenish-fluorescing compounds. The blue fluorescence of compound 2B and 3B suggests that the lactonisation had occurred in the pAMAC moiety, not the sugar moiety. The blue-fluorescing compounds were not of special interest and could be converted to a non-lactone form by simple treatment with NaOH.

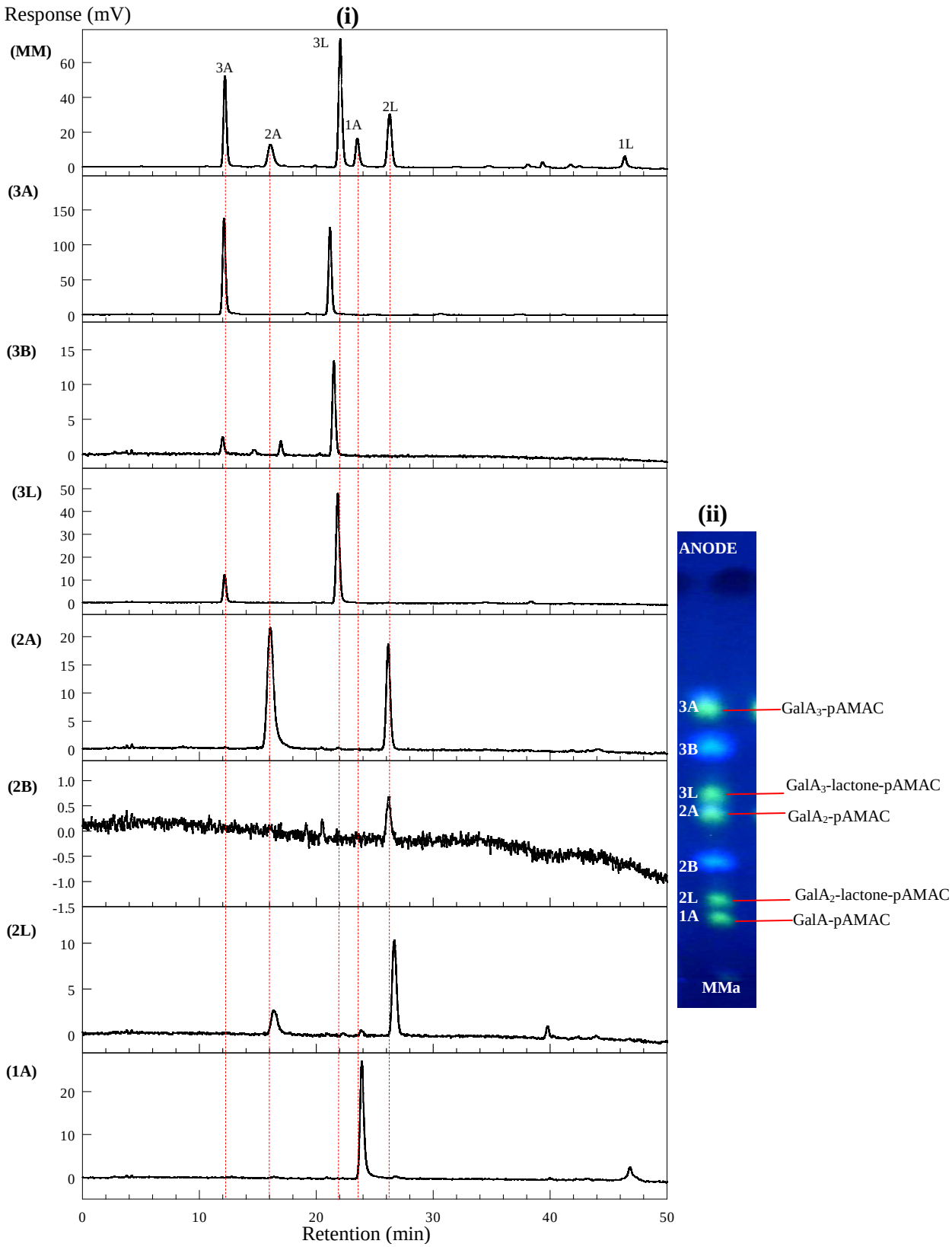

Figure 3.1.3 HPLC-resolution of individual eluted spots on a Luna C_{18} column

(i) HPLC profile of individual spots of: 1A, 2L, 2B, 2A, 3L, 3B and 3A, which were eluted from (ii) the electrophoretogram (shown on the right). Each eluted compound was analysed by HPLC. Marker mixture (MM) was run before the samples for reference. Fluorescence detection was with excitation at 442 nm and emission at 520 nm. The electrophoretogram was part of Figure 3.1.1 (iii): MM is a marker mixture which had not been delactonised.

3.1.1.4 Susceptibility of $GalA_2$-pAMAC marker to Driselase digestion

A Driselase-resistant uronic acid dimer labelled with pAMAC at any position of the sugar (pAMAC•UA_2), other than carbon-1 of the reducing terminus, is the proposed chemical fingerprint for $^{\bullet}OH$ attack on homogalacturonan. Therefore, it was important to establish that a dimer marker ($GalA_2$-pAMAC) labelled at carbon-1 of its reducing terminus is susceptible to Driselase. As shown in Figure 3.1.4, Driselase quickly digested the acidic form of the marker; subsequently, it digested the lactone form, but over a much longer period of time. For these reasons, it was essential to freshly delactonise the $GalA_2$-pAMAC marker with NaOH before it was subjected to Driselase digestion for up to 7 days. As predicted, $GalA_2$-pAMAC was susceptible to Driselase and the digestion product co-migrated with the authentic monomer marker GalA-pAMAC (Figure 3.1.5).

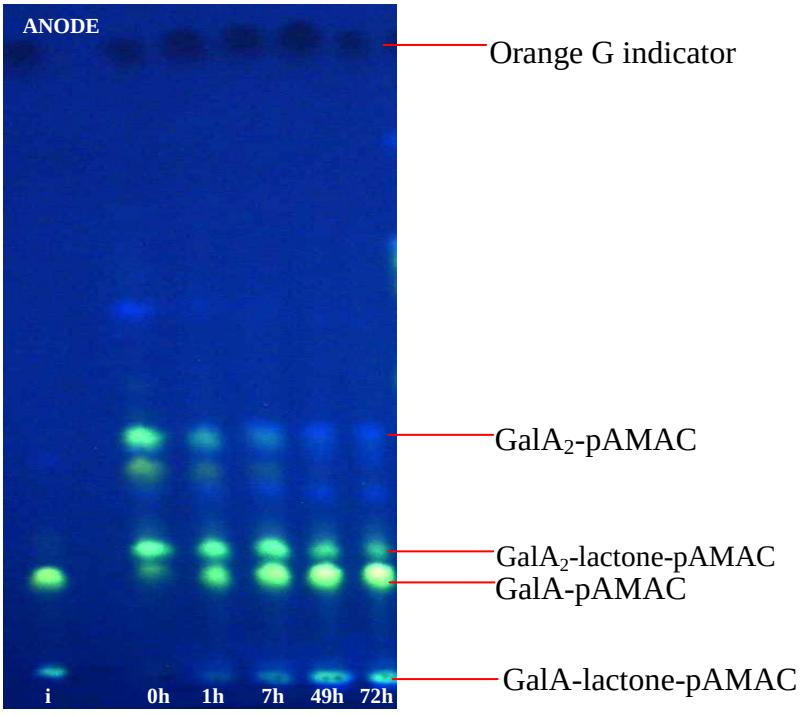

Figure 3.1.4 Digestion of non-delactonised-$GalA_2$-pAMAC marker as revealed on a pH 6.5 electrophoretogram

The $GalA_2$-pAMAC marker and its lactone were digested with Driselase for 0 h, 1 h, 7 h, 49 h and 72 h. Digested samples were electrophoresed together with marker (i) GalA-pAMAC. Electrophoresis was at pH 6.5, 4.0 kV, 45 min and then fluorescent products were examined under a 254-nm UV lamp.

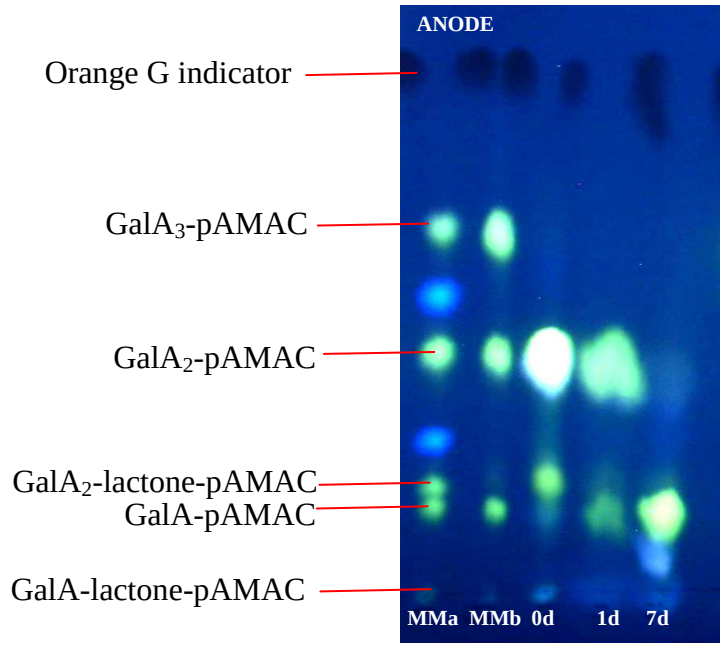

Figure 3.1.5 Digestion of delactonised-GalA$_2$-pAMAC marker as revealed on a pH 6.5 electrophoretogram

The GalA$_2$-pAMAC was delactonised and digested with Driselase for 0 day, 1 day and 7 day. Digested samples were electrophoresed together with markers (MMa and MMb are the marker mixture before and after delactonisation). Electrophoresis was at pH 6.5, 4.0 kV, 45 min and then fluorescent products were examined under a 254-nm UV lamp.

3.1.2 Preparation of ΔUA-GalA

3.1.2.1 Electrophoresis at pH 6.5 and Driselase-stability analysis

Amongst all cell wall-degrading enzymes, PL is the only enzyme known to produce an unsaturated uronic acid residue. Previous research in this lab by R. A. M. Vreeburg & S. C. Fry (unpublished) has shown that PL-treated homogalacturonan left a resistant dimer (ΔUA-GalA) after Driselase treatment. Therefore, a preparation of marker ΔUA-GalA is useful to validate the evidence of PL action in this proposed fingerprint methodology.

PL treatment of homogalacturonan solution resulted in the production of oligomers with an unsaturated uronic acid residue on the non-reducing end. The degree of polymerisation decreased rapidly with increasing digestion time to the smallest breakdown product, a dimer (ΔUA-GalA), as shown in Figure 3.1.6. The ΔUA-GalA migrated as an anionic spot in a position between free $GalA_2$ and $GalA_3$ on the pH 6.5 electrophoretogram. One additional step was applied to the ΔUA-GalA in order to establish its stability to Driselase digestion: the 100-min sample containing ΔUA-GalA was digested with Driselase for up to 7 days and subjected to pH 6.5 electrophoresis. Based on previous experiment by R. A. M. Vreeburg & S. C. Fry (unpublished), this result was as expected; the ΔUA-GalA itself was completely stable to Driselase digestion (Figure 3.1.7). Therefore, the stability of this dimer was verified.

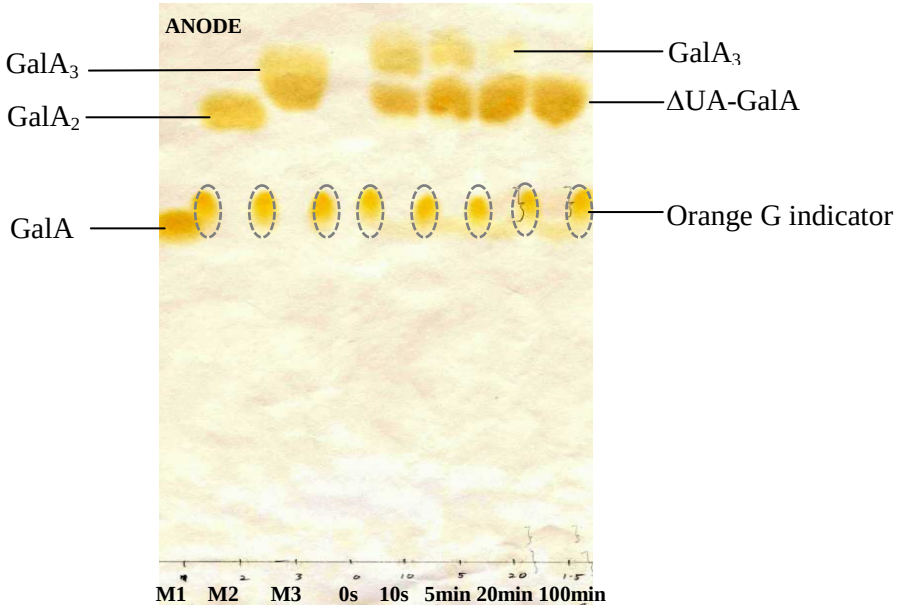

Figure 3.1.6 Anionic products of HG digested with PL and analysed on a pH 6.5 electrophoretogram

The homogalacturonan was digested with PL for 0 s, 10 s, 5 min, 20 min and 100 min. Digested samples were electrophoresed together with markers (M1 to M3). Electrophoresis was at pH 6.5, 4.0 kV, 45 min and products were stained with aniline hydrogen-phthalate.

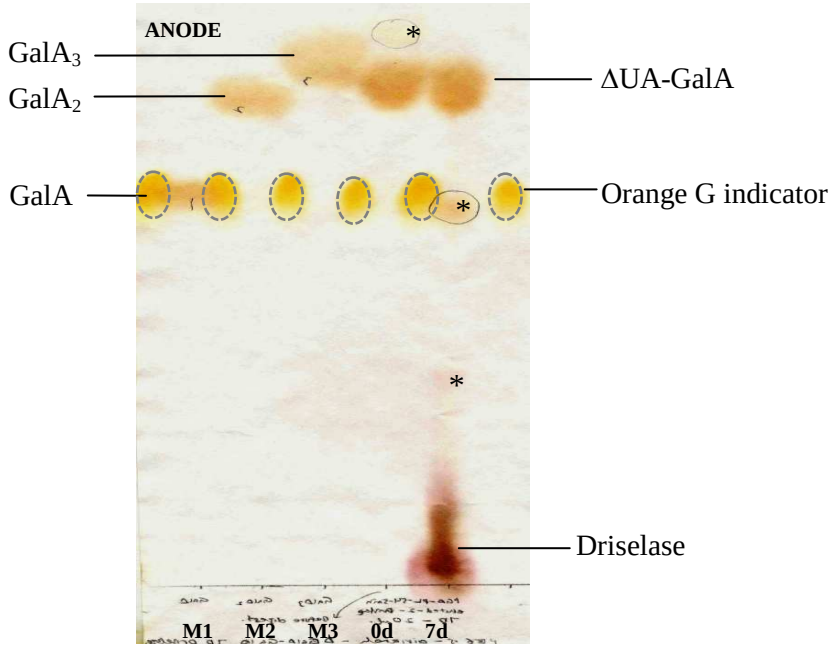

Figure 3.1.7 Anionic products of digestion of ΔUA-GalA with Driselase, analysed on a pH 6.5 electrophoretogram

The 100-min sample containing ΔUA-GalA (see Figure 3.1.6) was digested with Driselase for 0 or 7 days, and electrophoresed together with markers (M1 to M3). A faint spot marked as (*) in 0d sample was impurity contained in the 100-min sample (possibly $GalA_3$ and was digested to GalA and another by-product (*) by Driselase in the 7d sample). Electrophoresis was at pH 6.5, 4.0 kV, 45 min and products were stained with aniline hydrogen-phthalate.

3.1.2.2 Analysis of ΔUA-GalA by HPLC

The Driselase-resistant ΔUA-GalA was eluted from the electrophoretogram and analysed by HPLC on a PA100 column. The identification of ΔUA-GalA was achieved by comparing its elution pattern with those of free GalA, $GalA_2$ and $GalA_3$. ΔUA-GalA was well resolved from GalA, $GalA_2$ and $GalA_3$ (Figure 3.1.8). The retention times of these peaks differed slightly from run to run on a PA100 column, but could still be well interpreted.

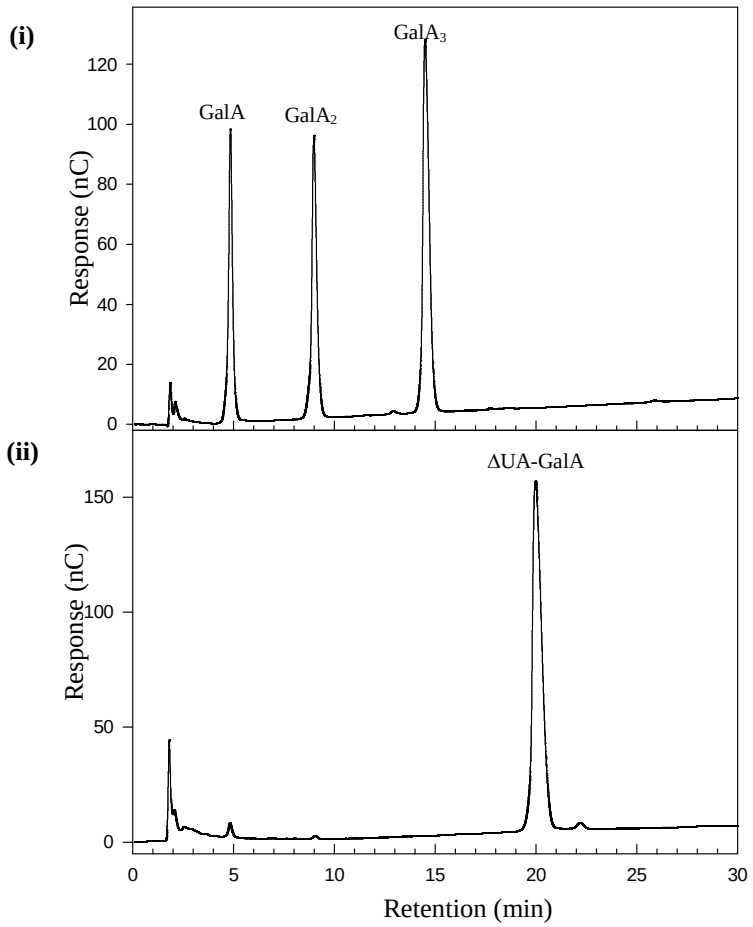

Figure 3.1.8 HPLC-Resolution of a Driselase-resistant ΔUA-GalA on a PA100 column

The Driselase-resistant ΔUA-GalA was eluted from an electrophoretogram and was analysed by HPLC on a PA100 column. Resolution profile for (ii) ΔUA-GalA was compared with the resolution profile of (i) free GalA, $GalA_2$ and $GalA_3$. PAD was used for this HPLC system.

3.1.3 Preparation of GalA-GalO

3.1.3.1 Electrophoresis at pH 6.5, TLC and Driselase-stability analysis

In experiments by Fry *et al.* (2001), L-[^{3}H]galactonate, the expected Driselase digestion product of NaB^3H_4-reduced pectin, was undetectable. Thus Driselase fails to cleave the glycosidic bond between GalA and GalO and is assumed to leave an informative dimeric product, GalA-GalO on digestion of pectin. A preparation of

marker GalA-GalO is useful to validate the evidence of EPG action in my proposed fingerprint methodology.

Treatment with $NaBH_4$ in the presence of NH_3 successfully reduced the reducing end of $GalA_2$ to form GalA-GalO. This was verified by the inability of aniline hydrogen-phthalate to stain the $NaBH_4$-reduced sample as this stain is only able to stain reducing sugars, not alditols (Fry, 2000; Figure 3.1.9). Surprisingly, it was also not able to be stained by silver nitrate, a 'universal' and highly sensitive sugar staining method. The electrophoretogram in Figure 3.1.9 also shows that a minor compound, possibly $GalA_2$-lactone, was formed in the control sample. This might due to addition of acidified $NaBH_4$ into the sample in which will promotes lactonisation.

The non-reduced $GalA_2$ (and its lactone) and GalA-GalO were then digested with Driselase for 7 days, run on TLC, and the digestion products were stained with thymol (Figure 3.1.10). As expected, the non-reduced-$GalA_2$ was digested to free GalA but Driselase failed to cleave the glycosidic bond between GalA and GalO; it left GalA-GalO as a Driselase-resistant, dimeric product which migrated between GalA and $GalA_2$. There were also impurities and possibly lactones in the digested sample, which were not of interest. The compound of interest, GalA-GalO, was purified from the TLC plate for further analysis.

GalA-GalO was prone to lactonise. When GalA-GalO from a TLC plate was subjected to electrophoresis at pH 6.5 without a delactonisation step, and visualised with bromophenol blue staining, it migrated much slower than the free $GalA_2$ and also slower than the free GalA (Figure 3.1.11). Based on its structure and its charge

properties (two negative charges from —COOH groups) at pH 6.5, this migration was not as expected for an acidic dimer. Therefore, the Driselase-resistant GalA-GalO was routinely delactonised with NaOH before it was subjected to electrophoresis at pH 6.5 and visualised with bromophenol blue staining (Figure 3.1.11). The previously slower-migrating spot was converted to the faster-migrating spot, in a position between the free $GalA_2$ and the orange G indicator (Figure 3.1.11), as expected for a dianionic disaccharide.

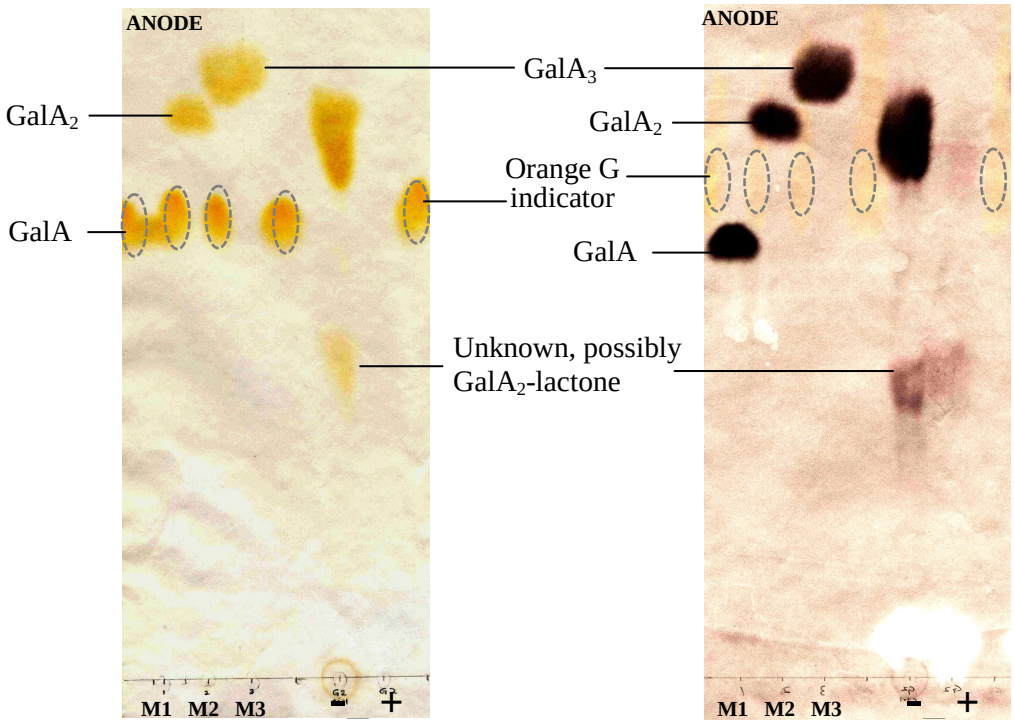

Figure 3.1.9 Anionic products of $NaBH_4$-reduced $GalA_2$ analysed on a pH 6.5 electrophoretogram

$GalA_2$ was reduced with $NaBH_4$ (+) electrophoresed together with the control (-) and markers (M1 to M3). Sample (+) was loaded 2X more than sample (-). Electrophoresis was at pH 6.5, 4.0 kV, for 45 min and products were stained with aniline hydrogen-phthalate (left) and silver nitrate (right).

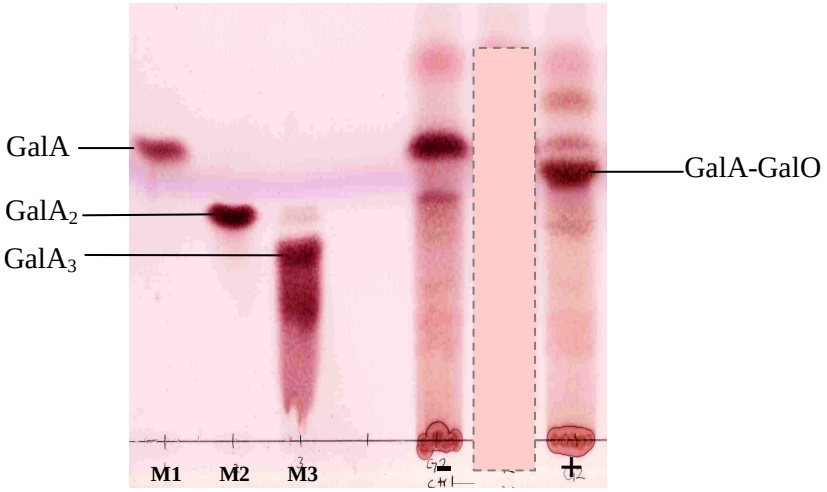

Figure 3.1.10 Products of Driselase-digested $GalA_2$ and GalA-GalO on TLC

The (-) $GalA_2$ and (+) GalA-GalO were digested with Driselase for 7 days. Digested samples were loaded onto a silica-gel plate, and run for 7 hours in (B/A/W; 2/1/1) together with markers (M1 to M3). Products were stained with thymol.

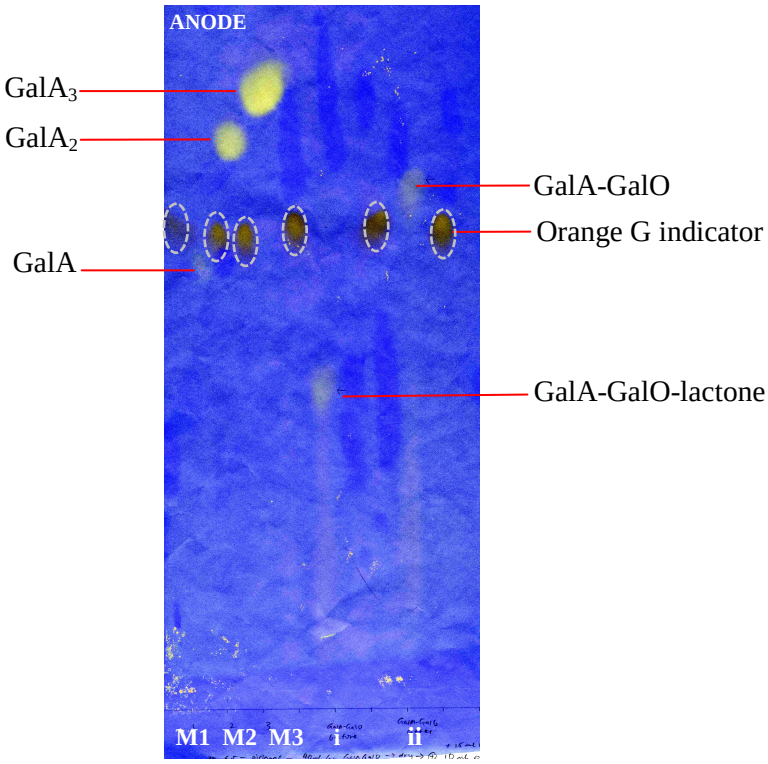

Figure 3.1.11 Anionic products of GalA-GalO on a pH 6.5 electrophoretogram

Driselase resistant GalA-GalO was eluted from the TLC plate in Figure 3.1.10 and electrophoresed together with the markers (M1 to M3). GalA-GalO was: (i) not delactonised; (ii) delactonised before being loaded onto the electrophoretogram. Electrophoresis was at pH 6.5, 4.0 kV, for 45 min and products were stained with bromophenol blue.

3.1.3.2 Analysis of GalA-GalO by HPLC

The Driselase-resistant, 'fingerprint' compound, GalA-GalO, purified from a TLC plate, was analysed by HPLC on a PA100 column. The identification of the GalA-GalO was achieved by comparing its elution pattern with markers including GalA, $GalA_2$, $GalA_3$, GalO, and also ΔUA-GalA. GalA-GalO was well resolved from the rest (Figure 3.1.12). As this HPLC system was run under alkaline condition, the formation of lactone was not a concern. The retention time of these peaks differed slightly from run to run, but could still be well interpreted.

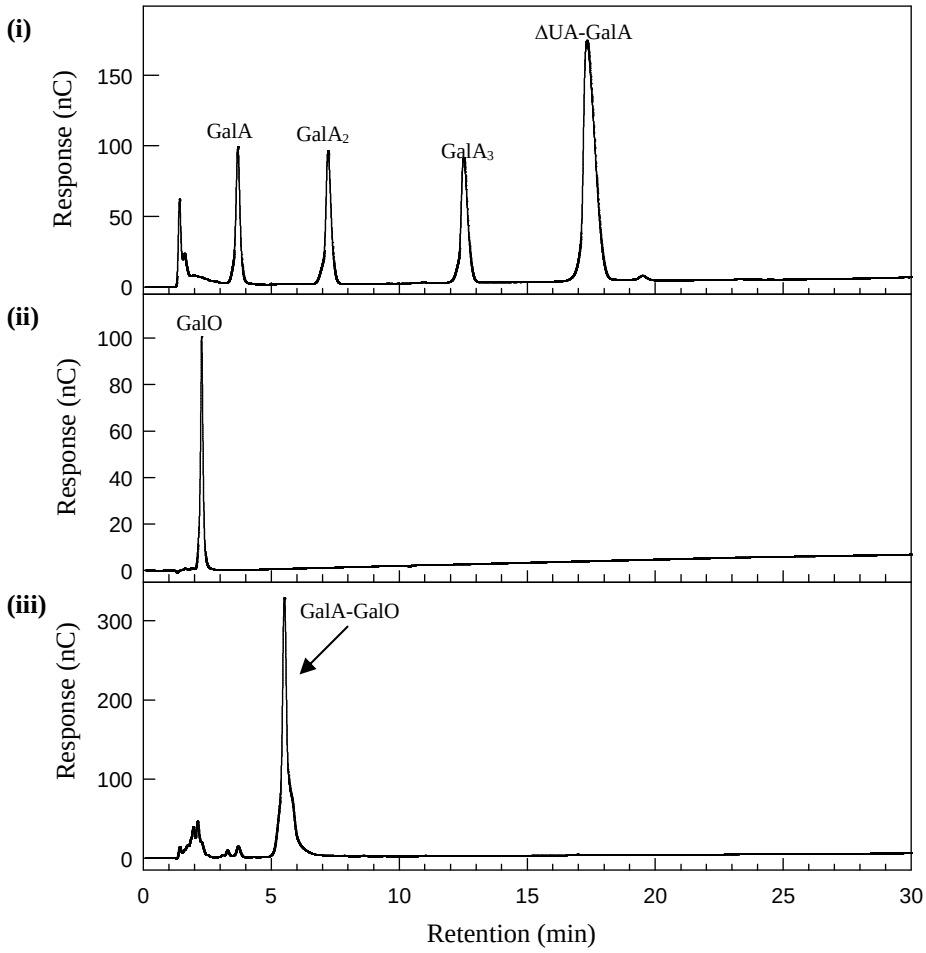

Figure 3.1.12 HPLC-resolution of a Driselase-resistant GalA-GalO on a PA100 column

The Driselase-resistant GalA-GalO was eluted from a TLC plate and was analysed by HPLC on a PA100 column. HPLC-resolution profile for (iii) GalA-GalO was compared with the HPLC-resolution profile of (i) GalA, $GalA_2$, $GalA_3$ and ΔUA-GalA, and (ii) GalO. PAD was used for this HPLC system.

3.2 pAMAC labelling of ˙OH-treated pectin (pAMAC•pectin)

The pAMAC-labelling method was applied *in vitro* to pectin solutions that had been treated with ˙OH formed from H_2O_2/ascorbate/Cu^{2+} and the pectin was freed of unreacted 2-AMAC by ethanol precipitation. ˙OH-treated pectin was successfully labelled with pAMAC which resulted in a clear single immobile (i.e. polysaccharide) fluorescent spot on a TLC plate compared with the untreated pectin (Figure 3.2.1). Both ˙OH-treated and ˙OH-untreated pectin had previously been treated with NaOH and $NaBH_4$ to remove any methyl esters and naturally existing oxo groups including the reducing ends, thus preventing any 2-AMAC labelling other than of ˙OH-introduced oxo groups. At the same time, the pre-treatment of the pectin with NaOH and $NaBH_4$ promoted gel formation. To avoid this, the NaOH and $NaBH_4$ were used at the least possible concentrations based on the extreme assumption that each mol of GalA residues present in the pectin solution needs 1 mol of NaOH and 1 mol of $NaBH_4$.

Figure 3.2.1 Fluorescent spot of ˙OH-treated pectin obtained after pAMAC labelling

Citrus pectin was treated with Fenton reagent (b) or untreated (c). The products for both samples after the pAMAC labelling and ethanol-precipitation were loaded onto a silica-gel plate together with (a) 2-AMAC itself. The TLC was run overnight in B/A/W (2:1:1) and examined under a 254-nm UV lamp.

3.3 Analysis of Driselase digestion products of pAMAC•pectin

3.3.1 Analysis by electrophoresis at pH 6.5

The Driselase-generated pAMAC•pectin digestion products ran as anionic compounds on electrophoresis at pH 6.5 (Figure 3.3.1). Interesting fluorescent compounds were mostly eluted from a C_{18} column in the 20% methanol fraction. When the Driselase-digested sample was not subjected to delactonisation, four major compounds (1A*, 2L*, X* and 2A*) were formed as greenish fluorescent spots. In addition, there was a bright fluorescent blue spot (2B*) migrating faster than X*. When the sample was freshly delactonised before being subjected to pH 6.5 electrophoresis, the 1A* spot remained as it was; the 2L* and 2B* were decreased in intensity while the X* and 2A* spots became more intense. Figure 3.3.1 also shows that there was no significant difference whether the samples were digested with Driselase for 7 or 14 days. Therefore, the Driselase digestion was established for 14 days in further experiments.

1A* is proposed to be UA•pAMAC as it co-migrated with authentic marker GalA-pAMAC. 2L* co-migrated with $GalA_2$-lactone-pAMAC, and at least half of the 2L* compound(s) was successfully delactonised with NaOH, but some still remained as a streak on the electrophoretogram. Therefore, the 2L* spot is proposed to contain not only pAMAC•UA_2-lactone(s) that could be delactonised to the acidic form (2A*) but also compound(s) that were resistant to delactonisation. X* migrated faster than the authentic marker $GalA_2$-lactone-pAMAC and is clearly not a lactone of a dimer because it increased in intensity after delactonisation; it is possibly a pAMAC•UA_2 with different ionic properties from 2A* at pH 6.5. Also, X* could possibly a

pAMAC•UA; however, subsequent HPLC analysis suggests that this is unlikely as it has a very short retention time (Figure 3.3.3.). As the intensity of the X* spot also increased after the sample had been delactonised, it is proposed that a compound migrating slower than X* must be a lactone form of X*. There were two most plausible candidates: X* arose either from the spot at the origin (based on the migration pattern and distance of migration between an acidic compound and its lactone on the electrophoretogram), or it arose from 2L* (based on HPLC analysis of eluted 2L* compound which contained some X*; Section 3.3.3 & Figure 3.3.3).

2A* is proposed to be a pAMAC•UA_2 as it co-migrated with the marker $GalA_2$-pAMAC and these two structures were predicted to have similar ionic properties. 2A* is clearly not $GalA_2$-pAMAC itself (dimer with pAMAC at reducing terminus) because this would have been digested by Driselase to GalA-pAMAC and free GalA within 7 days.

In addition to the four major fluorescent greenish compounds, the blue-fluorescing spot, 2B*, which migrated between X* and 2A*, decreased in intensity when the sample was delactonised although some remained. This observation suggests that 2B* contained a lactone ring (possibly the lactonisation occurred in the AMAC moiety, not the sugar moiety) that can readily delactonise after NaOH treatment; most probably it was converted to 2A* (based on previous analysis with $GalA_2$-pAMAC marker; Section 3.1.1.1 & Figure 3.1.1).

The $^{\bullet}OH$ attack at position 1 or 4 would rapidly cleave the polysaccharide chain thus resulted in new reducing termini (as shown in Figure 1.3.2; Lindsay & Fry, 2007). The reducing terminus newly introduced by $^{\bullet}OH$ attack at carbon-1 is

suggested would not able to be labelled with 2-AMAC as it would form a carboxylate lactone terminus (Figure 1.3.2). On the other hand, the newly introduced reducing terminus formed when $^{\bullet}$OH attacks at carbon-4 is able to be labelled with 2-AMAC (to produce ((GalA)$_n$-GalA•pAMAC). This situation might enable Driselase digestion to yield a fluorescent monosaccharide (UA•pAMAC) as Driselase possess endo-polygalacturonase and α-D-galacturonidase. The formation of UA•pAMAC (spot 1A*) probably occurred via this reaction.

On the other hand, if $^{\bullet}$OH attacks at position 2 or 3, it is expected to give a relatively stable glycosulose residue (Figure 1.3.2). The formation of compounds of the type pAMAC•UA$_2$ (spot 2A*) and their lactones (pAMAC•UA$_2$-lactone; spot 2L*) after the digestion was suggested to occur when pAMAC labelled the 2-epimer (α-D-TalA) and/or of the 3-epimer (α-D-GulA) formed when $^{\bullet}$OH attacked at position 2 or 3 of an α-D-GalA residue. Driselase probably lacks the α-taluronidase and α-guluronidase activity. It could also be pAMAC•GalA-GalA and/or its 4-epimer, pAMAC•GlcA-GalA (pAMAC labelling of an oxo group newly introduced at carbon-4), which both are suggested to resistant to Driselase. Therefore, it is possible that these dimeric fluorescent compounds could be pAMAC•GalA-GalA and/or its 2-, 3- and 4-epimers (pAMAC•TalA-GalA, pAMAC•GulA-GalA and pAMAC•GlcA-GalA respectively) and their lactones as they co-migrated with the dimer marker of GalA$_2$-pAMAC and its lactone. pAMAC•GalA-GalA, pAMAC•TalA-GalA, pAMAC•GulA-GalA and pAMAC•GlcA-GalA are likely to have similar ionic properties to GalA$_2$-pAMAC at pH 6.5.

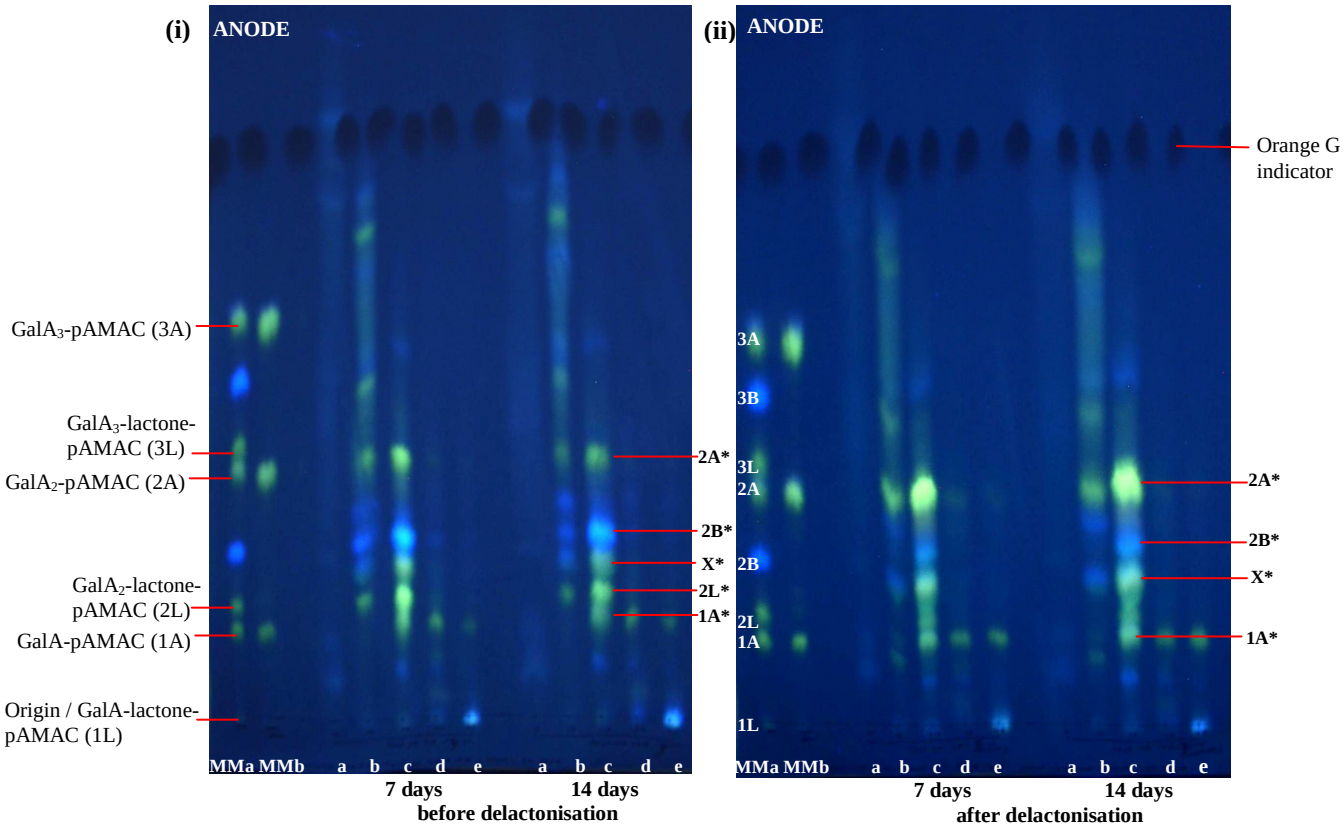

Figure 3.3.1 Anionic compounds of Driselase-digested pAMAC•pectin on a pH 6.5 electrophoretogram

Pectin was successively treated with $^{\bullet}OH$, 2-AMAC, acetone and finally Driselase for 7 and 14 days; the products were then fractionated on a mini Supelco C_{18} column. The image shows the fluorescent fractions obtained: (a to e) 0% to 40% methanol fraction; before and after being delactonised; MMa and MMb are the marker mixture before and after delactonisation. Electrophoresis was at pH 6.5, 4.0 kV, 45 min and then products were examined under a 254-nm UV lamp.

3.3.2 Analysis of pAMAC•pectin by HPLC on a C_{18} column

Analysis of digested pAMAC•pectin by HPLC was conducted in order to identify 1A*, 2L*, X*, 2A* (and possibly also 2B*). The 20% methanol fraction from the C_{18} column, not delactonised, was analysed by HPLC on a Luna C_{18} column with a fluorescence detector. At least four major, interesting peaks were resolved (Figure 3.3.2 (i)), each of which was corresponded to a specific spot on the electrophoretogram (Figure 3.3.2 (ii).

1A*, 2L* and 2A* had co-migrated on HVPE with authentic markers (1A, 2L and 2A respectively; Figure 3.3.1). Therefore, the peak with the 25.8 min retention time was suggested to correspond to 1A*, that with the 29.4 min retention to 2L*, and that with the 17.3 min retention time to 2A*. This left X* and 2B* to be matched with other peaks resolved by HPLC (one major peak and at least five minor peaks). It had been shown that the fluorescence detector is less sensitive to the blue fluorescent compound (see Section 3.1.1.3). As a result, the remaining major peak, with the shortest retention time (9.70 min), was suggested to correspond to the X* spot.

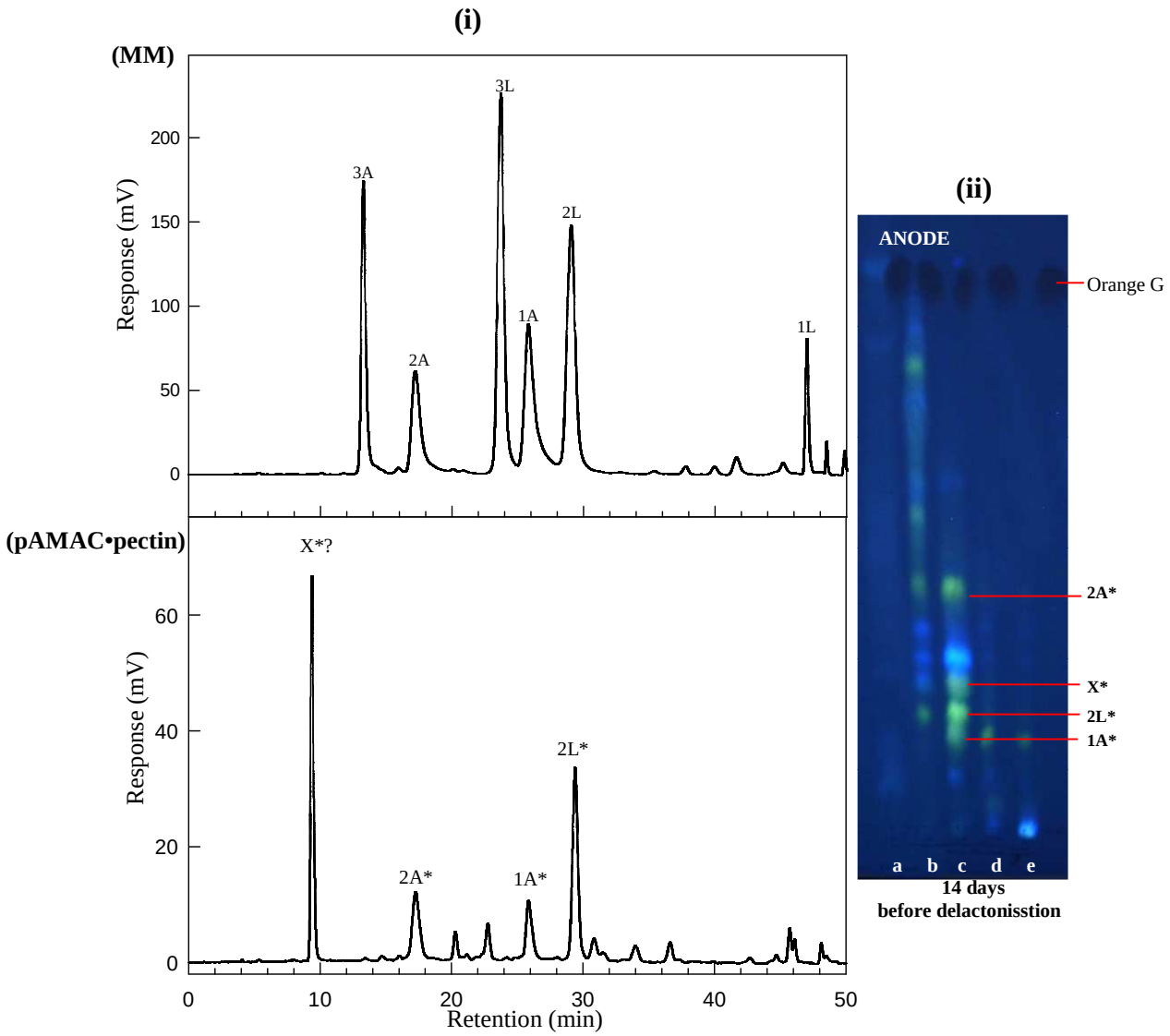

Figure 3.3.2 HPLC-resolution of the 20% methanol fraction of Driselase-digested pAMAC•pectin, not delactonised, on a Luna C_{18} column

(i) HPLC profile pAMAC•pectin is a 20% methanol fraction, not delactonised, from a 14-day digested sample. HPLC profile MM is a marker mixture that was run before the samples for reference. Labels on top of the peaks correspond to the suggested fluorescent spots on the electrophoretogram (b). Fluorescence detection was with excitation at 442 nm and emission at 520 nm. The electrophoretogram is part of Figure 3.3.1: (a to e) 0% to 40% methanol fraction, before being delactonised.

3.3.3 Analysis of individual fluorescent spots by HPLC

Further verification was performed for 1A*, 2L*, X*, 2A* and 2B* by HPLC. Each fluorescent spot was individually eluted from the electrophoretogram and submitted to HPLC analysis. 1A* and 2A* resulted in peaks matching their respective authentic marker retention times (Figure 3.3.3), thus supporting the suggestion: 1A* is pAMAC•UA while 2A* is pAMAC•UA_2. The unique compound, X*, as expected, resulted in a unique peak with the shortest retention time.

2L*, suggested to be pAMAC•UA_2-lactone, gave a peak matching the acidic form of the dimer marker, $GalA_2$-pAMAC. This is plausible because 2L* could contain both the acidic and lactone forms after it was eluted from the paper as lactonisation is a reversible process. 2L* also gave an additional peak matching the X* retention time. This result has two possible explanations: (a) 2L* was (or contained) a lactone of X*, so that it migrated slightly slower than the X* on an electrophoretogram, or (b) there was cross contamination between 2L* and X* during the elution process and X* is detected on HPLC with high sensitivity. The first is the most possible explanation because the intensity of the X* spot increased whilst the intensity of the 2L* spot decreased after the sample had been delactonised, which may suggests X* arose from 2L*.

At least three main peaks were resolved from the eluted blue fluorescent compound (2B*): a peak previously established to correspond to X*, a peak matching authentic $GalA_2$-pAMAC, and an unidentified peak with a retention time of 37.2 min. This result showed that the blue fluorescent compound not only contained

the lactone form of a dimer, i.e. pAMAC•UA_2-lactone, but also contained X* and other sugar derivatives.

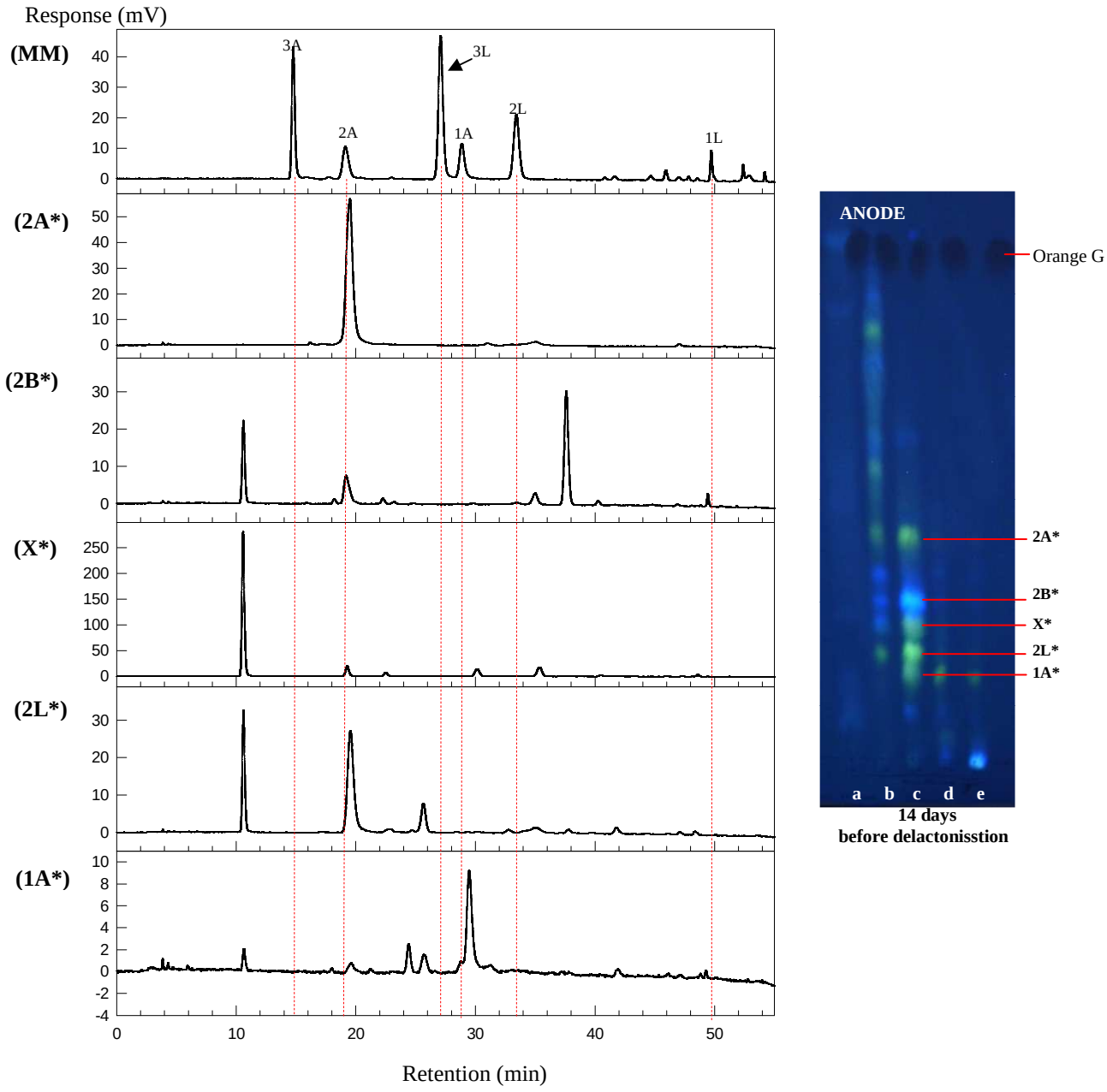

Figure 3.3.3 HPLC-resolution of the individual eluted electrophoretogram spots of the 20% methanol fraction from Driselase-digested pAMAC•pectin

Individual spots of 1A*, 2L*, X*, 2B* and 2A* were eluted from the electrophoretogram (shown on the right) and were analysed by HPLC. Marker mixture was run before the samples for reference. Fluorescence detection was with excitation at 442 nm and emission at 520 nm. The electrophoretogram is part of Figure 3.3.1: (a to e) 0% to 40% methanol fraction, before being delactonised.

3.4 *In-vivo* application of developed labelling method

3.4.1 Fruit selection and firmness readings

Seven fruits (pear, mango, banana, apple, avocado, strawberry and strawberry tree fruit) were chosen to represent a wide range of fruit species as describe in introduction (Section 1.5). The firmness of each fruit at three empirically defined stages of softening (hard, medium and soft) was measured with a penetrometer (except strawberry tree fruit) as shown in Table 3.4.1.

Table 3.4.1 Firmness readings of fruits at three stages

Species	Firmness reading (newtons)		
	Stage 1 (Days after purchase)	**Stage 2 (Days after purchase)**	**Stage 3 (Days after purchase)**
Pear	16.5 ± 2.31 (0)	4.7 ± 1.15 (7)	2.83 ± 0.92 (14)
Mango	13.6 ± 2.13 (0)	5.47 ± 1.37 (7)	2.54 ± 0.82 (14)
Banana	11.9 ± 2.07 (0)	3.74 ± 1.08 (7)	1.78 ± 0.72 (14)
Apple	18.0 ± 2.62 (0)	18.6 ± 2.49 (14)	21.1 ± 2.68 (28)
Avocado	10.4 ± 1.83 (0)	2.76 ± 0.92 (6)	1.33 ± 0.58 (12)
Strawberry	13.0 ± 2.07 (-)	3.78 ± 1.09 (-)	1.29 ± 0.58 (-)
Strawberry tree fruit	Orange (-)	Red (-)	Blackish (-)

Data were obtained by penetrometer in newtons (N). Values are means (n=3) ± standard error. Stages of softening were at various days after purchase as stated in parentheses. Strawberry and Strawberry tree fruit were chosen based on their fruit colour but no firmness readings for Strawberry tree fruit are available as they were preserved frozen immediately after picking.

3.4.2 pAMAC labelling of fruit AIR (pAMAC•AIR)

AIRs from the seven fruits at each stage of softening were successfully labelled with pAMAC (producing pAMAC•AIR). Frozen AIR was labelled immediately upon thawing and ice-cold ethanol was used in washing and precipitation steps during the labelling process as a precaution to preserve any oxo groups on the pectin chain. pAMAC•AIR was delactonised and submitted to Driselase digestion for 14 days. The digestion products were then purified on a C_{18} column; a portion of the products from each pAMAC•AIR sample was delactonised and another equal portion was not delactonised (for comparison), then electrophoresed at pH 6.5 to separate the acidic fragments of pAMAC-labelled pectins from each other and from the neutral fragments of other cell wall components.

3.4.3 Analysis of Driselase digestion products of pAMAC•AIR by electrophoresis at pH 6.5

The fluorescent pAMAC•AIR digestion products ran as anionic and approximately-neutral compounds on electrophoresis at pH 6.5. Non-delactonised and delactonised samples (Figures 3.4.1 (i) & (ii)) were compared. In general, an acidic monomer (UA•pAMAC ($1A^F$)): a greenish-fluorescing spot which co-migrated with GalA-pAMAC), and an acidic dimer (pAMAC•UA_2 ($2A^F$)): a greenish-fluorescing spot which co-migrated with $GalA_2$-pAMAC), increased in intensity in all fruit samples after delactonisation. A similar increase in intensity happens to the approximately-neutral compounds at the origin, which could be any neutral sugar labelled with

pAMAC. However, these approximately-neutral compounds are not of interest and therefore are not further discussed in detail.

On the other hand, the intensity of the lactone form of the dimer (pAMAC•UA_2-lactone ($2L^F$): a greenish-fluorescing spot which co-migrated with $GalA_2$-lactone-pAMAC) decreased in intensity and formed a streak on paper electrophoresis after delactonisation while the other form of lactone dimer ($2B^F$: a blue-fluorescing spot which co-migrated with the dimer marker fluorescent blue conjugate) totally disappeared after delactonisation. Therefore, delactonisation prior to electrophoresis was essential to eliminate or at least decrease the lactone forms thus leaving predominantly an acidic monomer and an acidic dimer, and approximately-neutral compounds.

In addition, in some species, there was an unidentified spot with unique migration on paper (greenish-fluorescing spot labelled "X^F"), as observed in banana and strawberry tree fruit samples, before delactonisation. After delactonisation, this spot remained in the banana sample but became indistinct in the strawberry tree fruit sample as it formed a streak together with the $2L^F$.

There were also two minor highly anionic spots, suggested to be trimer compounds, labelled $3L^F$ and $3A^F$, observed in avocado and strawberry tree fruit. $3L^F$ is expected to contain a lactone while $3A^F$ is expected to be a fully acidic form of trimer as they co-migrated with $GalA_3$-lactone-pAMAC and $GalA_3$-pAMAC, respectively. However, neither compound is of key interest as they were minor and possibly resulted from an incomplete digestion. The qualitative comparison of non-

delactonised and delactonised samples of digested pAMAC•AIR is summarized in Table 3.4.2.

As the pattern of Driselase digestion products of pAMAC•AIR could be simplified if the sample was delactonised before electrophoresis, therefore, the analysis of changes in intensity of the interesting compounds between stages 1 and 3 was based on the delactonised sample as in Figure 3.4.1 (ii). In the analysis of authentic $^{\bullet}$OH-treated pectin labelled *in vitro* with pAMAC (Section 3.3), a very similar monomeric anion to $1A^F$ (Figure 3.4.1 (ii)) was generated (referred to as 1A* in *in-vitro* labelling in Section 3.3). However, the spot of $1A^F$ from AIR that increased in intensity from stage 1 to stage 3 of softening in most fruit samples could possibly be (or include) a GalA-pAMAC (pAMAC attached at the reducing terminus of a D-GalA group), which could correspond to the increasing number of D-GalA reducing termini during fruit ripening, caused by the actions of any or all of EPG, PL and $^{\bullet}$OH. Spot $1A^F$ obtained from AIR could therefore result from EPG and/or PL attack.

Regardless of this uncertainty, the dimeric compound $2A^F$ was definitely not the reducing-end-labelled dimer, $GalA_2$-pAMAC, since it has been established that Driselase would be able to hydrolyse $GalA_2$-pAMAC to GalA-pAMAC. Therefore, $2A^F$ is concluded to be a limit digestion product, i.e. the suggested "fingerprint" indicating the *in-vivo* action of $^{\bullet}$OH attack; it could possibly be pAMAC•GalA-GalA and/or its 2-, 3- and 4-epimers (pAMAC•TalA-GalA, pAMAC•GulA-GalA and pAMAC•GlcA-GalA respectively).

In general, the fluorescent spots increased in intensity during the softening process, i.e. from stage 1 to stage 3, except in apple and strawberry (Figure 3.4.1). The most noticeable changes were the increase of $1A^F$ and $2A^F$, whereas the approximately-neutral compounds had no obvious changes throughout. In pear, mango, banana, avocado and strawberry tree fruit, $1A^F$ significantly increased in intensity, especially when stage 3 and stage 2 (soft and medium-soft fruits) are compared with stage 1 (hard fruit). On the other hand, the apple and strawberry AIR samples did not show any clear evidence of $1A^F$ increasing at any stage. The putative fingerprint, $2A^F$, increased in mango, banana, avocado and strawberry tree fruit and was always either absent or very faint at stage 1. There was no evidence of $2A^F$ at any stage in apple or strawberry, and only detected at stage 2 in pear. When compare to mango, banana, avocado and strawberry tree fruit (tropical/sub-tropical climate species), pear, apple and strawberry on the other hand are temperate climate species. Therefore, differences in botanical origin may influence their ripening mechanism and cell wall regulation. The semi-quantitative analysis of digested pAMAC•AIR is summarized in Table 3.4.3.

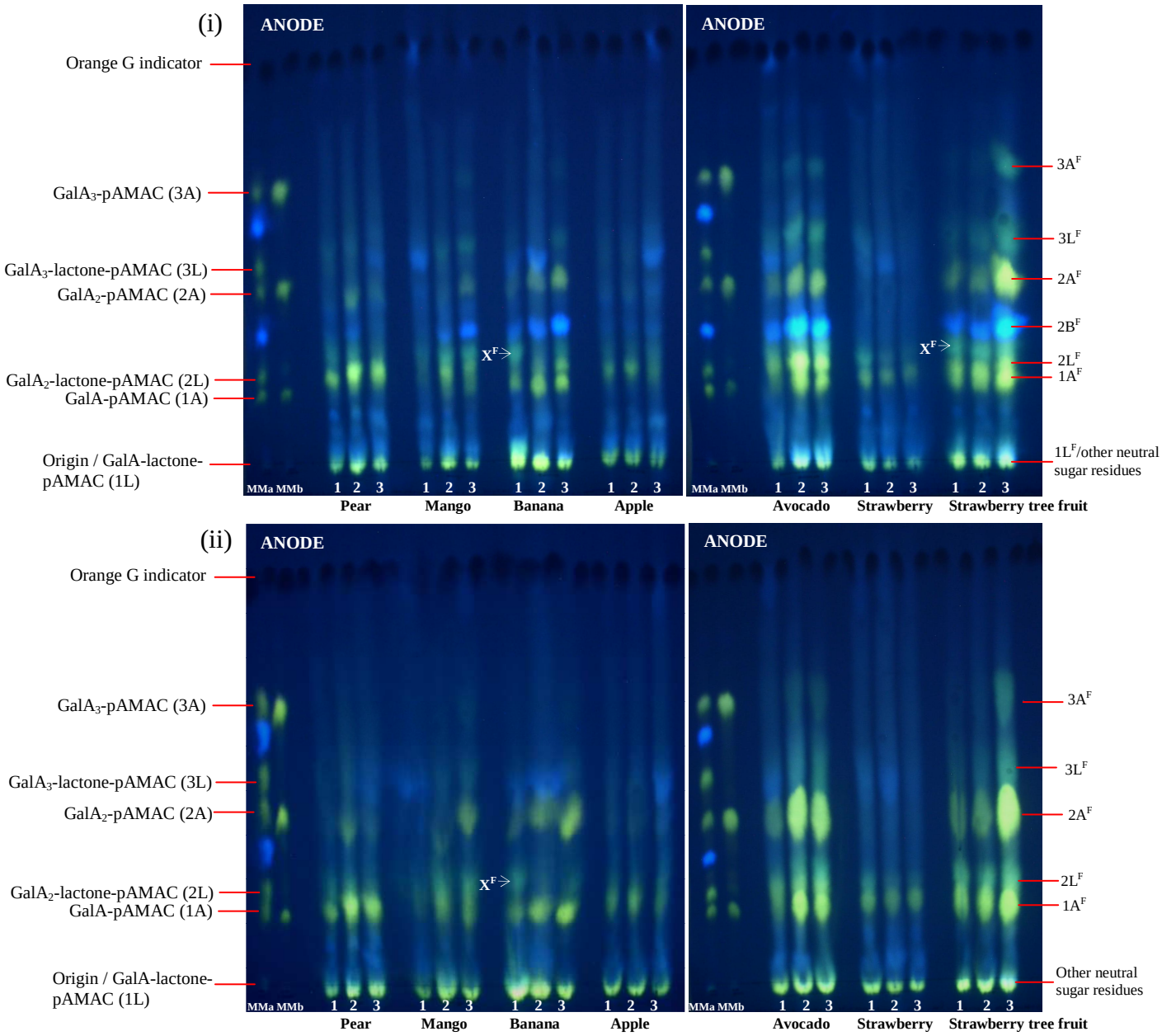

Figure 3.4.1 Driselase-digested products of pAMAC•AIR at pH 6.5 electrophoresis

Fruit AIRs were successively treated with AMAC, acetone and finally Driselase for 14 days; the products were then fractionated on a mini Supelco C_{18} column. C_{18}-fractions containing fluorescent compounds were pooled. The images show the (i) not delactonised and (ii) delactonised samples of total fluorescent material obtained from: (1) stage 1, i.e. the hard fruit; (2) stage 2, i.e. the medium-soft fruit; and (3) stage 3, i.e. the soft fruit; MMa and MMb are the marker mixture before and after delactonisation. The fluorescing spots ($1A^F$, $2L^F$, $2B^F$, $2A^F$, $3L^F$, $3A^F$) were as described in Section 3.4.3. Electrophoresis was at pH 6.5 and 4.0 kV for 45 min and then products were examined under a 254-nm UV lamp.

Table 3.4.2 Qualitative comparison of non-delactonised and delactonised samples of digested pAMAC•AIR at stage 3 of softening

Species	Fluorescent intensity scoring of Driselase-digested products of pAMAC•AIR						
	$1A^F$	**$2L^F$**	**X^F**	**$2B^F$**	**$2A^F$**	**$3L^F$**	**$3A^F$**
Pear (non-delactonised)	√	–	–	–	√	–	–
Pear (delactonised)	√√	–	–	–	√√ **(Stage 2)**	–	–
Mango (non-delactonised)	√	√	–	√	√	–	–
Mango (delactonised)	√√	streak	–	–	√√	–	–
Banana (non-delactonised)	√	√	√	√	√	–	–
Banana (delactonised)	√√	-	√ **(Stage 1)**	–	√√	–	–
Apple (non-delactonised)	√	–	–	–	–	–	–
Apple (delactonised)	√√	–	–	–	–	–	–
Avocado (non-delactonised)	√	√	–	√	√	√	√
Avocado (delactonised)	√√	streak	–	–	√√	streak	streak
Strawberry (non-delactonised)	√	-	–	–	–	–	–
Strawberry (delactonised)	√√	-	–	–	–	–	–
Strawberry tree fruit (non-delactonised)	√	√	√	√	√	√	√
Strawberry tree fruit (delactonised)	√√	streak	streak	–	√√	√	√

Data were obtained by scoring the presence (√) or absence (-) of the fluorescent compounds on electrophoretograms before and after delactonisation (Figure 3.4.1). (√√) indicates higher-intensity fluorescent spots. This data only refer to the comparisons of fluorescent spot intensity at stage 3 of softening with exception for banana (X^F) and pear ($2A^F$).

Table 3.4.3 Characteristics of seven anionic, pAMAC•AIR products obtained after Driselase digestion

Driselase-digested products of pAMAC•AIR	Proposed nature of product
$1A^F$ (UA•pAMAC)	Monomer; not lactone; greenish-fluorescing spot
$2L^F$ (pAMAC•UA_2-lactone)	Dimer; lactone; greenish-fluorescing spot
X^F (pAMAC•UA_2)	Dimer; not lactone; greenish-fluorescing spot
$2B^F$ (pAMAC-lactone •UA_2)	Dimer; lactone within AMAC moiety; blue-fluorescing spot
$2A^F$ (pAMAC•UA_2)	Dimer; not lactone; greenish-fluorescing spot
$3L^F$ (pAMAC•UA_3-lactone)	Trimer; lactone; greenish-fluorescing spot
$3A^F$ (pAMAC•UA_3)	Trimer; not lactone; greenish-fluorescing spot

Data of probable identities of seven spots are obtained based on electrophoretic mobilities at pH 6.5 electrophoresis and when examined under a 254-nm UV lamp.

Table 3.4.4 Semi-quantitative analysis of anionic compounds, $1A^F$ and $2A^F$, based on the delactonised samples shown in Figure 3.4.1

Species	Compounds of interest	Fluorescent intensity scoring at different stages of softening		
		Stage 1	Stage 2	Stage 3
Pear	$1A^F$	□	■	■
	$2A^F$	–	■	–
Mango	$1A^F$	□	■	■
	$2A^F$	–	□	■
Banana	$1A^F$	□	■	■
	$2A^F$	□	◪	■
Apple	$1A^F$	□	□	□
	$2A^F$	–	–	–
Avocado	$1A^F$	□	■	■
	$2A^F$	□	■	■
Strawberry	$1A^F$	□	□	□
	$2A^F$	–	–	–
Strawberry tree fruit	$1A^F$	□	□	■
	$2A^F$	□	□	■

Data were obtained by visually scoring the intensity of the fluorescent spots from the electrophoretogram in Figure 3.4.1, as: (-) absence; (□) faint; (◪) medium and (■) intense. These data only refer to the comparisons of fluorescent spot intensity within a species.

3.5 Analysis of Driselase digestion products of pAMAC•AIR by HPLC

3.5.1 Attempt to identify individual fluorescent spots by HPLC

Further characterisation was performed for individual fluorescent compounds $1A^F$, $2L^F$, X^F, $2B^F$ and $2A^F$ as labelled on the pH 6.5 electrophoretograms (Figure 3.4.1). The same compounds from the same fruit each from non-delactonised and delactonised samples were eluted, pooled and submitted to HPLC analysis (Table 3.5.1; Figure 3.5.1). Suprisingly, apparently identical electrophoretogram spots from different species gave different patterns. For example, compound $1A^F$ from non-

delactonised samples (expected to be an acidic monomer as it co-migrated on the electrophoretogram with 1A) was resolved into: a peak approximately matching authentic 3L for pear, apple and strawberry; peaks matching authentic 1A and 1L for avocado; and peaks matching at least two of these authentic compounds for mango, banana and strawberry tree fruit. In addition, there are also unidentified peaks, mostly with shorter retention times. However, later in Section 3.5.2, an experiment to distinguished $1A^F$ from authentic 3L was conducted. In that experiment, fractions contained $1A^F$ was mixed with authentic marker mixture contained 3L; compounds $1A^F$ and authentic 3L resolved as two distinguishable peaks. Thus, spot $1A^F$ is proven not to contain a trimer lactone.

Spot $2L^F$ (expected to contain a lactone form of a uronic acid dimer as it co-migrated with 2L) was eluted only from the electrophoretogram in non-delactonised avocado sample. In other samples, the spots either faintly present or formed a streak. $2L^F$ from avocado resulted in peaks matching authentic 2A and 2L, as expected. Both forms, fully acidic and lactonised, may present in this sample because lactonisation is a reversible process.

Electrophoretogram spot X^F, a greenish-fluorescing spot migrating slightly faster than authentic 2L and observed in banana and strawberry tree fruit samples, was resolved into several peaks. In the non-delactonised banana sample, one of the peaks matched authentic 3L, while in the delactonised sample, two of the peaks matched authentic 2A and 3L. Spot X^F from strawberry tree fruit (the non-delactonised sample) resulted in peaks matching authentic 2A, 1A, 2L and another unidentified peak. All X^F analyses resulted in very small peaks. This result suggests

that X^F from this *in-vivo* labelling is not the same as X* found after *in-vitro* labelling (see section 3.3.3) even though both have approximately similar migration properties on the electrophoretogram.

$2B^F$ is a blue-fluorescing spot on the electrophoretogram, expected to be a lactone form of dimer as it co-migrated with the blue-fluorescing form of authentic 2L. This blue-fluorescing spot is similar to 2B* from the *in-vitro* labelling (Section 3.3.3) and the fluorescence detector used in this HPLC system is expected to be less sensitive towards blue-fluorescing compound than to greenish-fluorescing compound. In pAMAC•AIR, $2B^F$ was only present in the non-delactonised samples. $2B^F$ spot was observed in mango and banana, and present with high intensity in avocado and strawberry tree fruit. Eluted $2B^F$ from all these samples resulted in small peak that matched authentic 2L. This is because $2B^F$ is a lactone form of dimer and may present as fully acidic and/or its lactonised form. However, $2B^F$ was not of special interest and could be converted to an acidic form of dimer when delactonised.

The putative fingerprint for $^{\bullet}OH$ attack, $2A^F$, which co-migrated on the electrophoretogram with authentic 2A, resulted in peaks matching authentic 2A and/or 2L in all eluted samples, except for delactonised pear sample where no peaks were detectable. Again, both forms, acidic and lactone, may present in this sample because lactonisation is a reversible process.

Table 3.5.1 Analysis by HPLC of individual fluorescent spots of Driselase digestion products of pAMAC•AIR

Fruit source		Identities and relative area reading of Driselase-digested products of pAMAC•AIR				
		$1A^F$	$2L^F$	X^F	$2B^F$	$2A^F$
Non-delactonised	**Pear**	– : 54% 3L : 40%	/	/	/	2A : 88% 2L : 6%
	Mango	– : 36% 3L : 21% 1A : 13% – : 15%	/	/	2L : 100%	2A : 32% 2L : 61%
	Banana	– : 7% 3L : 75% 1L : 15%	/	– : 67% – : 9% 3L : 5% – : 3% – : 14%	2L : 83%	2A : 29% 2L : 55%
	Apple	– : 56% 3L : 33%	/	/	/	/
	Avocado	1A : 90% 1L : 10%	2A : 23% 2L : 58%	/	2L : 64%	2A : 34% 2L : 45%
	Strawberry	– : 15% – : 25% 3L : 60%	/	/	/	/
	Strawberry tree fruit	– : 7% 3L : 14% 1A : 64% 1L : 11%	/	2A : 64% 1A : 8% 2L : 7% – : 15%	2L : 91%	2A : 32% 2L : 59%
Delactonised	**Pear**	– : 44% 1A : 45% – : 11%	/	/	/	Unable to detect any peak
	Mango	3L : 38% 1A : 33% – : 29%	/	/	/	2A : 22% 2L : 78%
	Banana	3L : 4% 1A : 80% 1L : 10%	/	2A : 75% 3L : 16%	/	2A : 46% 2L : 38%
	Apple	– : 56% 3L : 44%	/	/	/	/
	Avocado	1A : 89% 1L : 11%	/	/	/	2A : 28% 2L : 62%
	Strawberry	– : 23% – : 61%	/	/	/	/
	Strawberry tree fruit	– : 7% – : 14% 1A : 68% 1L : 9%	/	/	/	2A : 37% 2L : 60%

Individual eluted spots of $1A^F$, $2L^F$, X^F, $2B^F$ and $2A^F$ were eluted from the electrophoretograms shown in Figure 3.4.1 and analysed by HPLC on a C_{18} column. Samples marked as (/) were not analysed and (–) is defined as an unidentified peak as it did not match any authentic marker. Data were extracted from the HPLC profiles shown in Figure 3.5.1. Data above show the: authentic marker most closely matching its HPLC retention time : relative area reading of the peak. For example, eluted spot of $1A^F$ from the non-delactonised pear sample gave two main peaks on HPLC: one which did not co-elute with any authentic marker and accounting for 54% of the total area reading of that sample; one approximately co-eluting with 3L and accounting for 40% of the total area reading of that sample; the latter observation does not imply that the compound detected is 3L (see Section 3.5.2). Authentic markers 1L, 1A, 2L, 2A, 3L, and 3A were as defined in Figure 3.4.1.

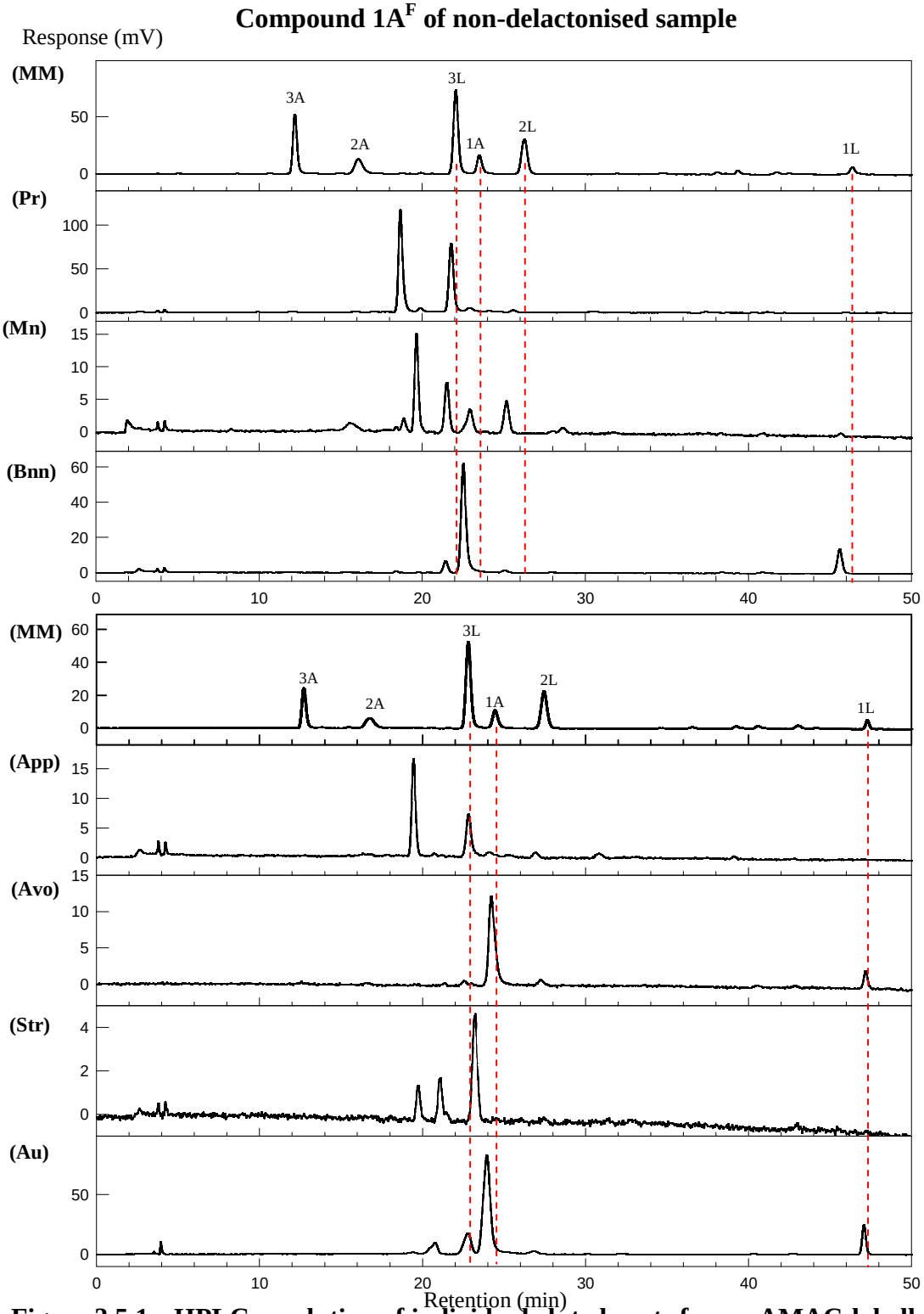

Figure 3.5.1 HPLC-resolution of individual eluted spots from pAMAC-labelled AIR on a Luna C_{18} column

Individual eluted spots of $1A^F$, $2L^F$, X^F, $2B^F$ and $2A^F$ from non-delactonised and delactonised sample: (Pr) pear, (Mn) mango, (Bnn) banana, (App) apple, (Avo) avocado, (Str) strawberry and (Au) strawberry tree fruit were eluted from electrophoretograms shown in Figure 3.4.1 and analysed by HPLC. MM is a marker mixture that was run in between samples for reference. Authentic markers 1L, 1A, 2L, 2A, 3L, and 3A are as defined in Figure 3.4.1. Fluorescence detection was with excitation at 442 nm and emission at 520 nm. Chromatograms continued overleaf.

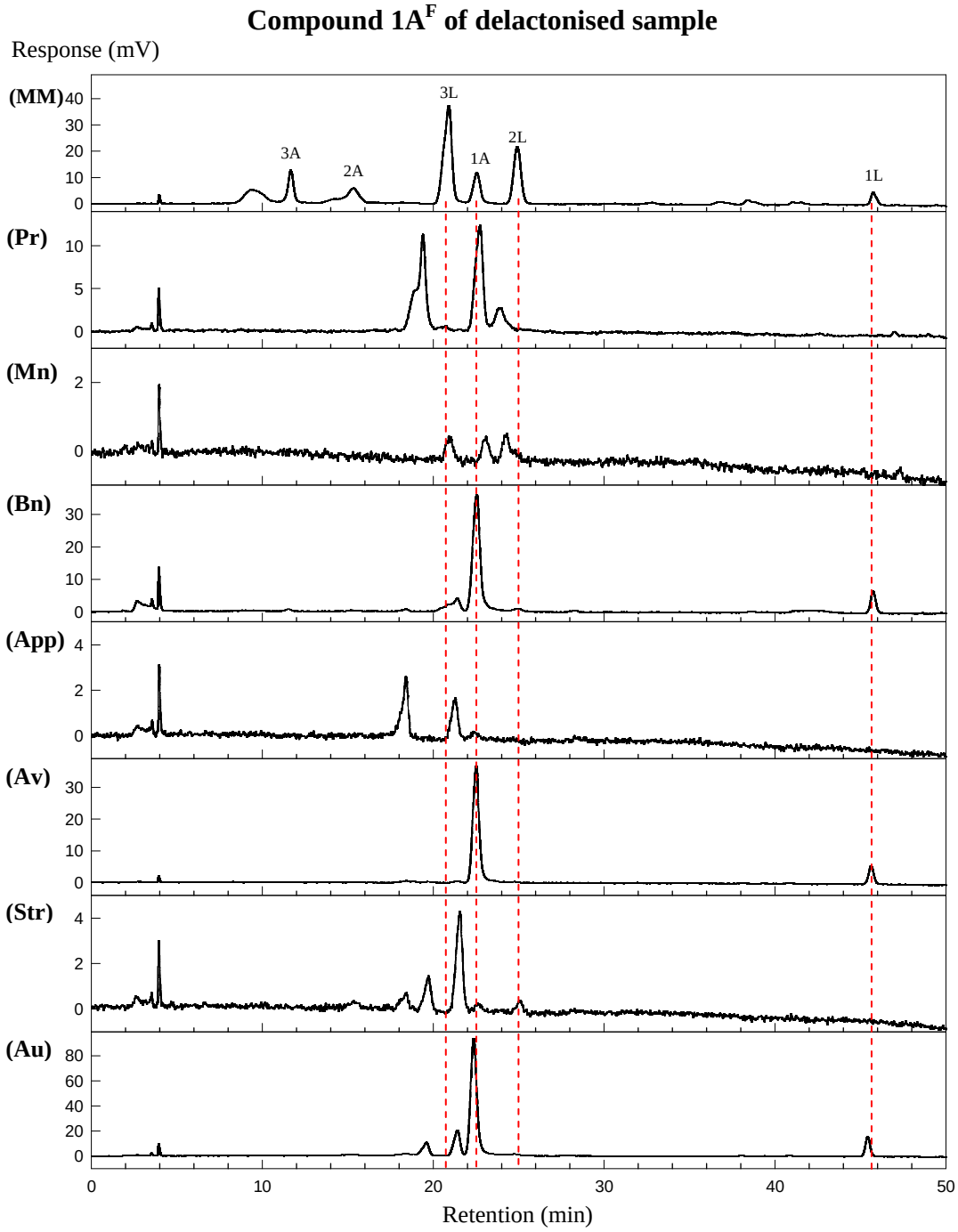

Figure 3.5.1 Continued.

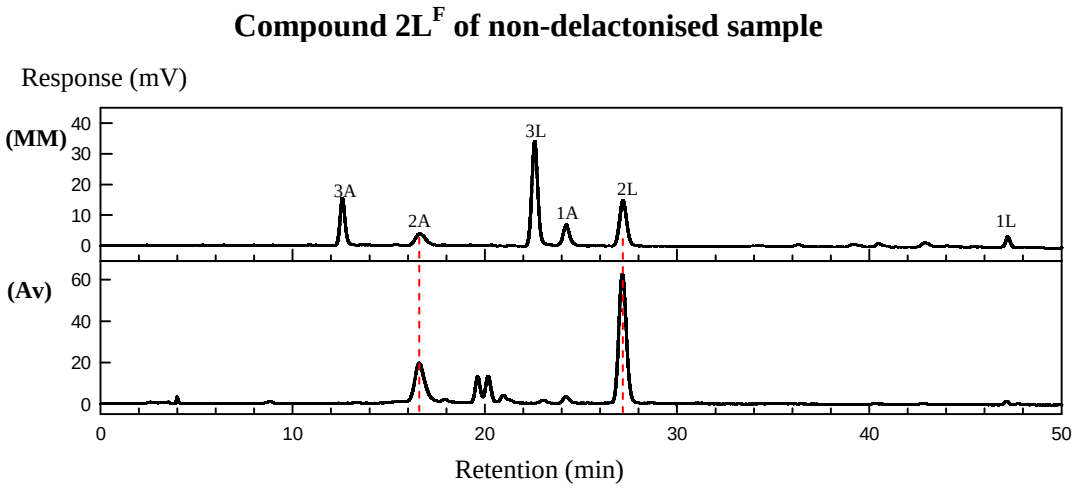

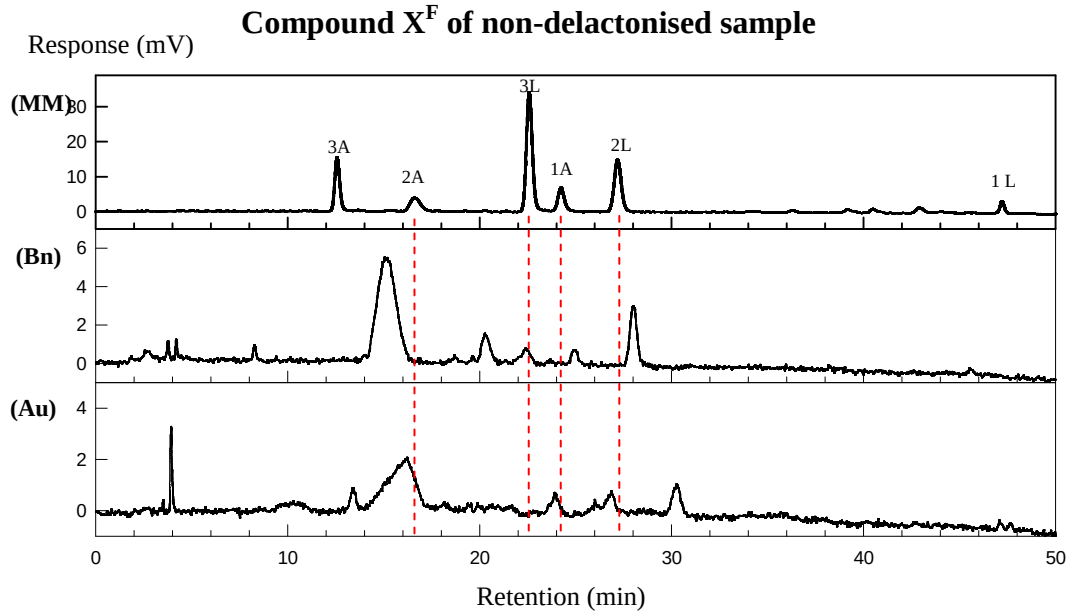

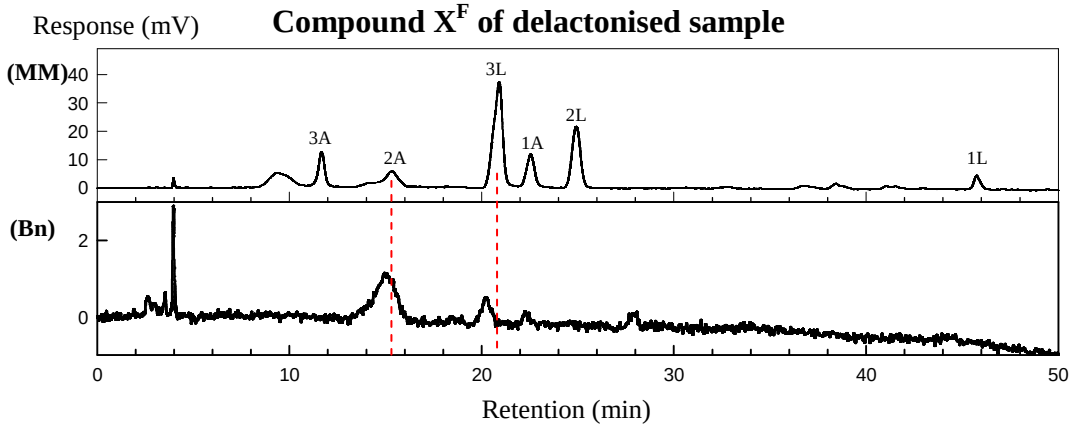

Figure 3.5.1 Continued.

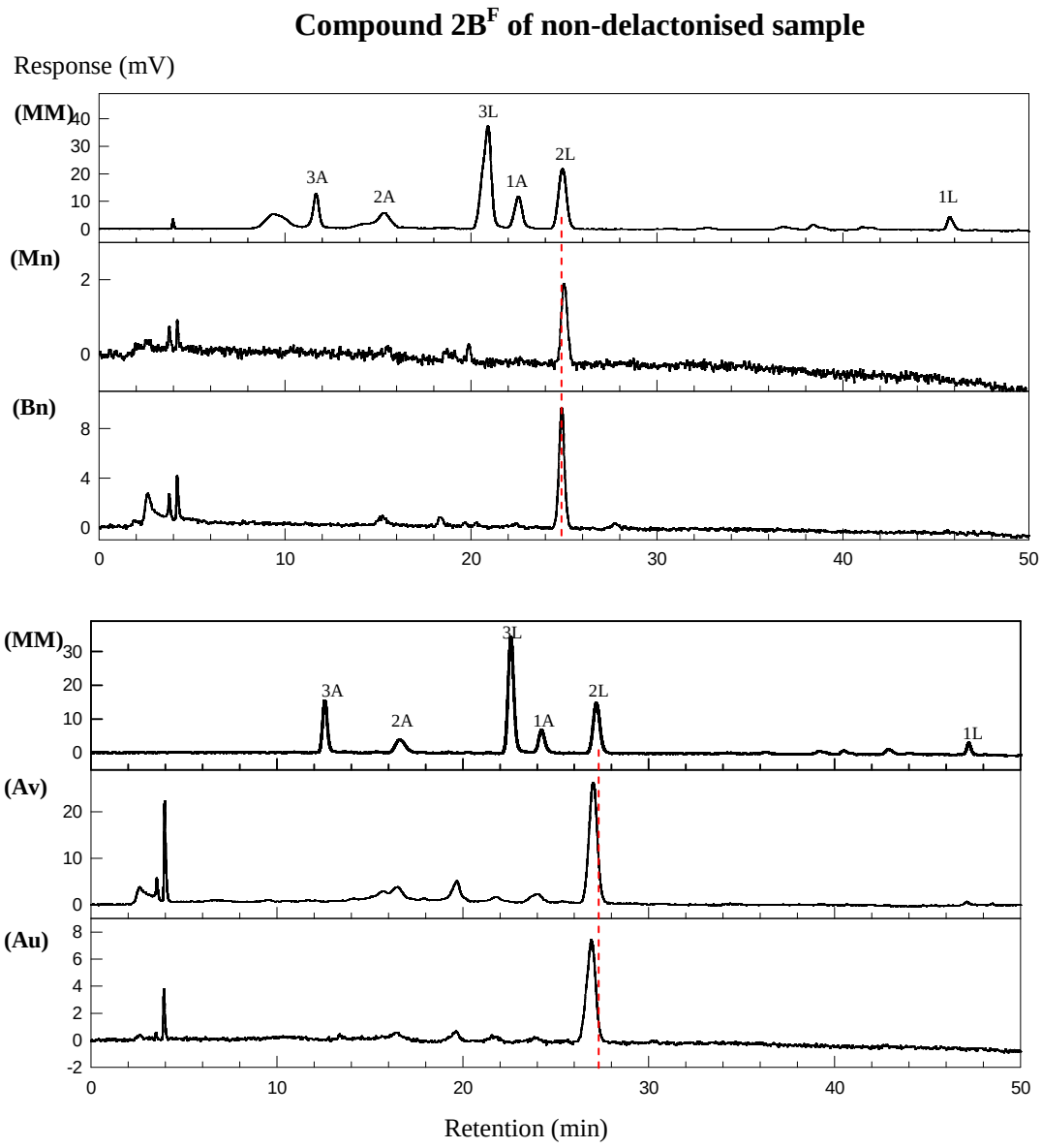

Figure 3.5.1 Continued.

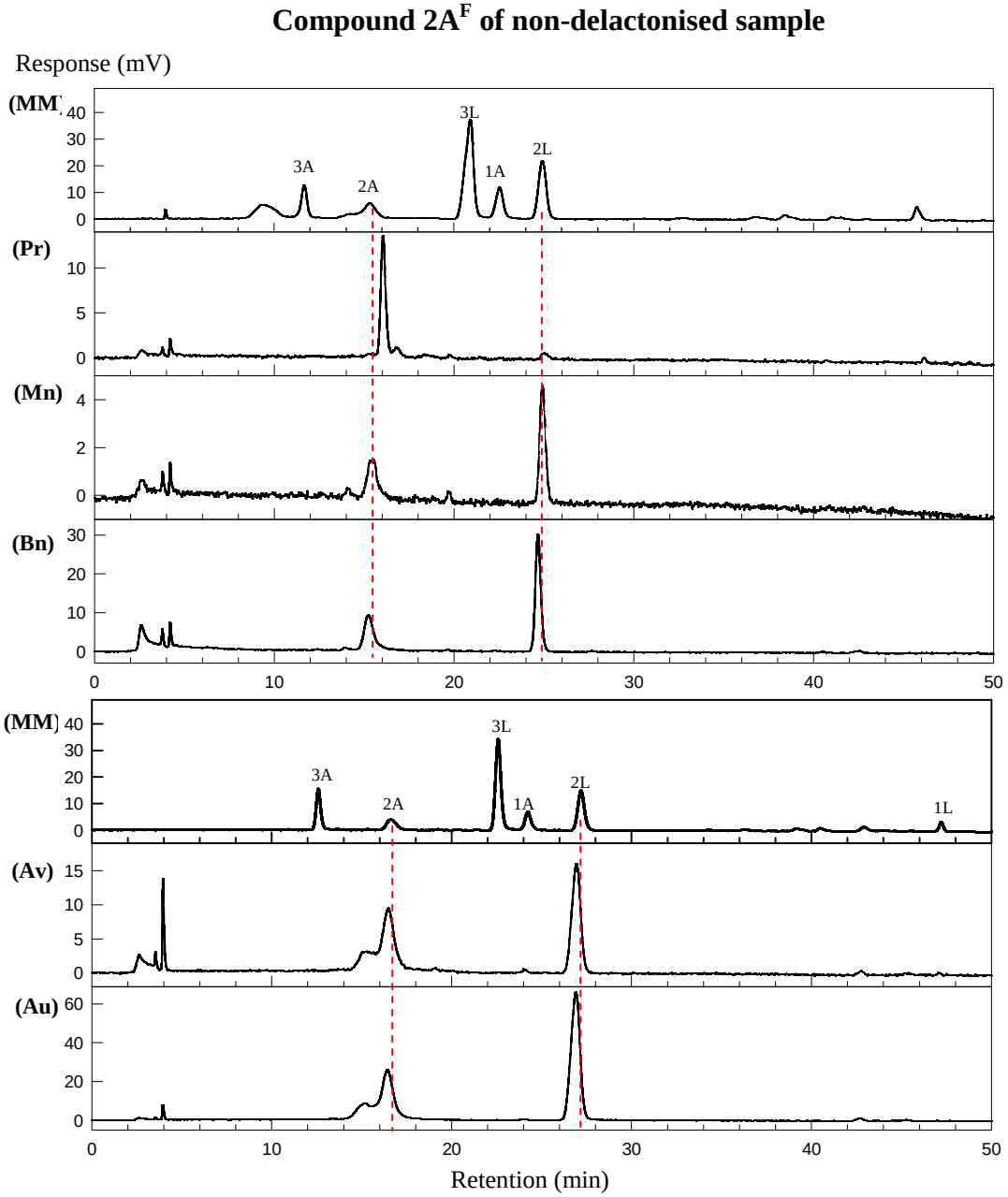

Figure 3.5.1 Continued.

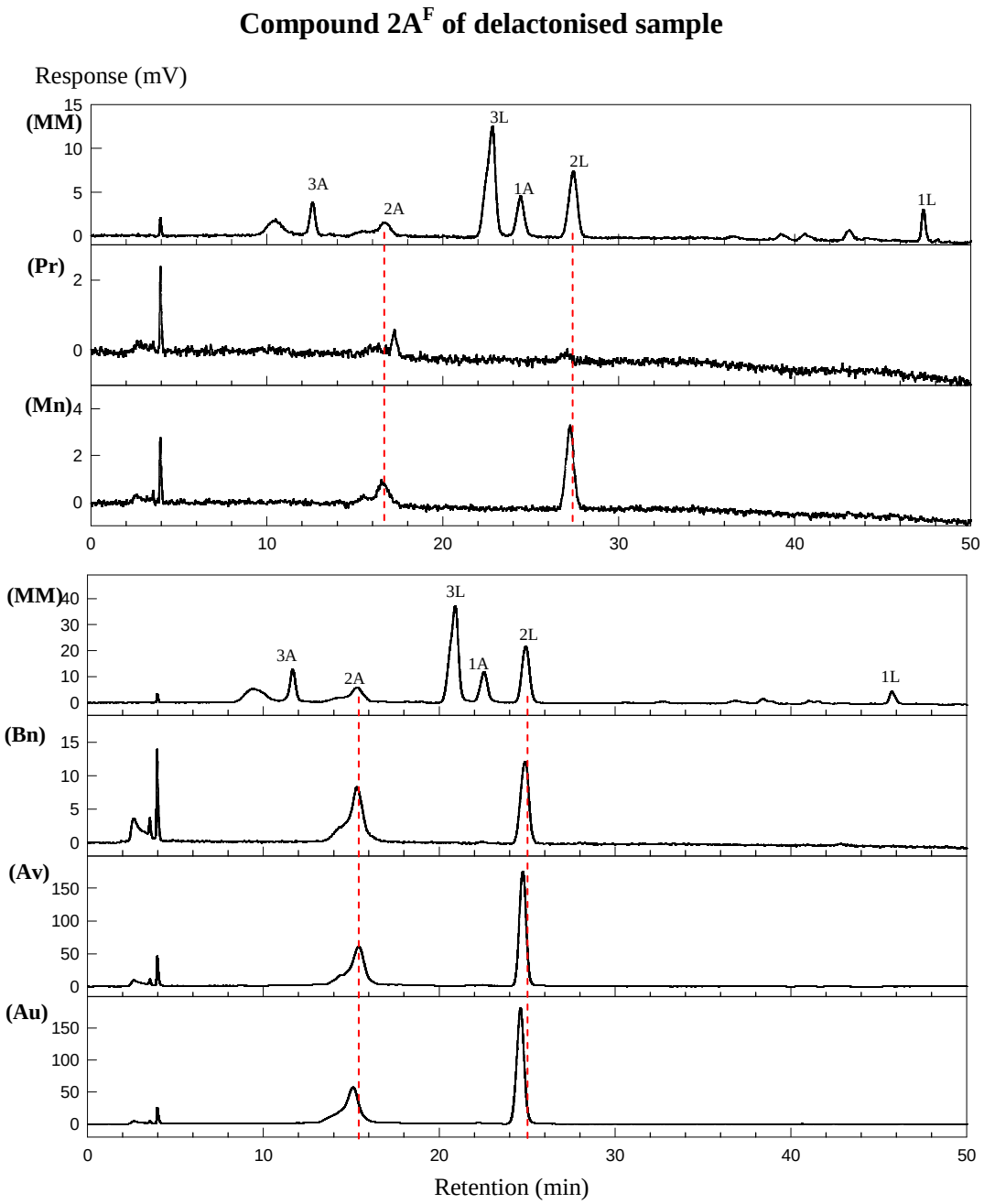

Figure 3.5.1 Continued.

3.5.2 Attempt to distinguish $1A^F$ from authentic 3L by HPLC

In Section 3.5.1, a monomeric compound, $1A^F$, was found to produce peaks (when eluted $1A^F$ was analysed by HPLC) that matched authentic marker 1A and/or 1L as expected, but also surprisingly resulted in a peak that matched authentic 3L. This peak was found in all seven fruit samples except in avocado (see Table 3.5.1). However, based on the electrophoretogram in Figure 3.4.1, it was impossible that eluted compound $1A^F$ from any sample would contain a trimer lactone judging by the migration pattern of monomeric and trimeric compounds on pH 6.5 electrophoresis. Therefore, it was important to establish whether the peak that matched authentic 3L produced from eluted $1A^F$ is a trimer lactone.

In order to test this hypothesis, a C_{18} fraction containing $1A^F$ from several species (pear, mango and banana) was mixed with authentic marker mixture containing 3L and analysed by HPLC. Each C_{18} fraction used in this experiment not only contained $1A^F$, but also other fluorescent compounds. However, the main interest is in the compound producing a peak labelled "$1A^F$" (Figure 3.5.2). Different concentrations of authentic marker mixture were added to each sample to make both the sample and the marker about the same concentration. Compounds $1A^F$ and authentic 3L resolved as two distinguishable peaks that were eluted very close to each other in all samples (Figure 3.5.2). Thus, this has established that $1A^F$ is not a trimer lactone.

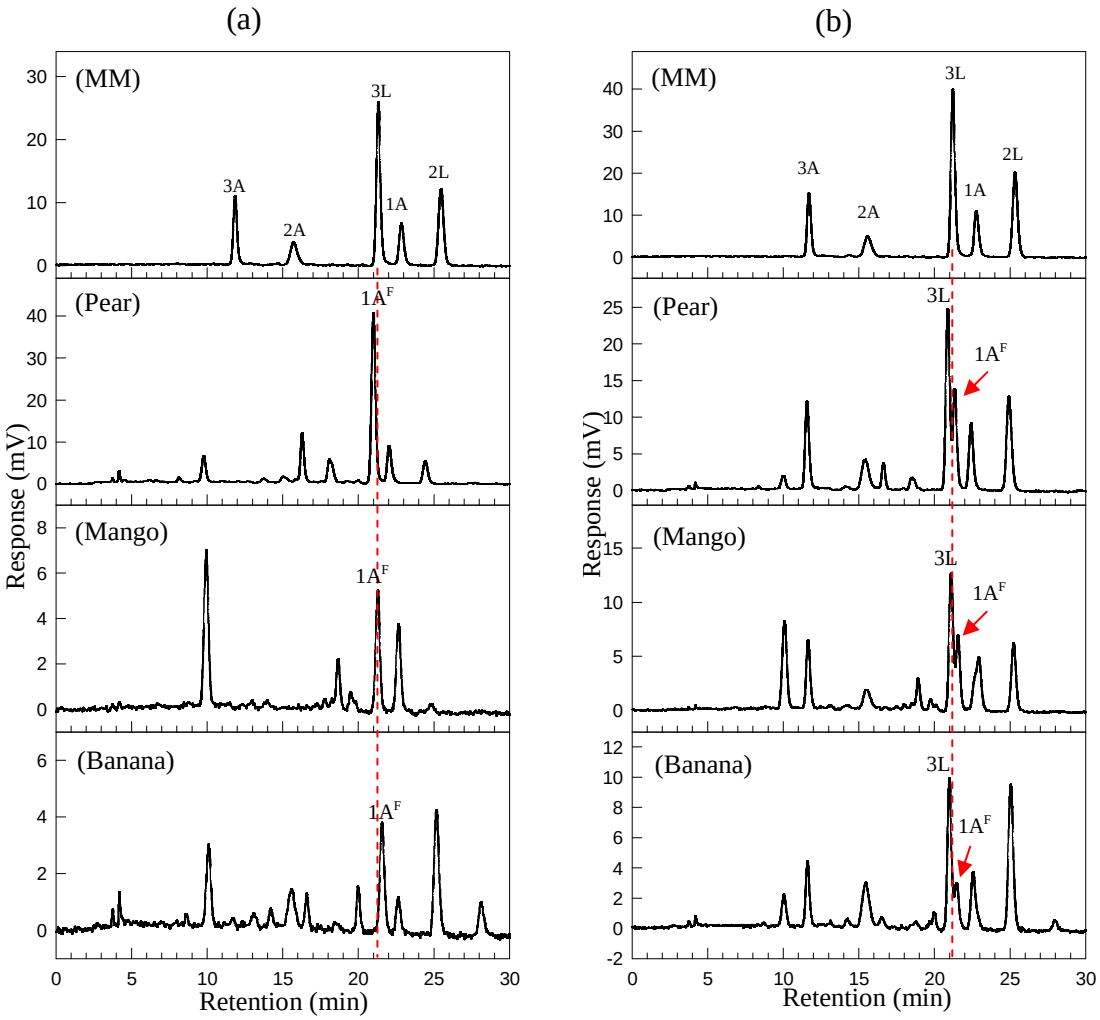

Figure 3.5.2 HPLC-resolution of several Driselase-digested pAMAC•AIR samples on a Luna C_{18} column in an attempt to distinguish $1A^F$ from authentic 3L

(a) is a profile of pear, mango and banana fractions contained $1A^F$, from a 14-day digested sample of pAMAC•AIR that was analysed by HPLC and (b) is the same fraction but mixed with authentic marker mixture contained 3L. MM is a marker mixture. Authentic markers 1L, 1A, 2L, 2A, 3L and 3A are as defined in Figure 3.4.1. Fluorescence detection was with excitation at 442 nm and emission at 520 nm.

3.5.3 Quantitative analysis of Driselase digestion products of pAMAC•AIR by HPLC

The digested products of seven fruits of pAMAC•AIR, each at three stages of softening, were analysed quantitatively by HPLC on a C_{18} column (Table 3.5.2; Figure 3.5.3). Selected peaks resolved from each sample were quantified by total relative area readings represent a total of 1^F or 2^F present in 20 mg fresh weight of fruit. The peaks were selected based on the expected compound(s) present in a particular sample that matched the retention times of expected authentic markers. There are two particularly interesting compounds in this analysis. One is $1A^F$, the monomer compound co-migrating with GalA-pAMAC that could have resulted from $^{\bullet}OH$, EPG and/or PL attack. Another is $2A^F$, the dimer compound co-migrating with $GalA_2$-pAMAC and proposed to be the end-product of Driselase digestion, i.e. the suggested "fingerprint" indicating the *in-vivo* action of $^{\bullet}OH$ attack.

This quantitative analysis by HPLC involved non-delactonised samples; therefore, the peaks of interest might contain both lactone and acidic compounds. For that reason, in order to get a relative quantity of the uronic monomers: 1^F is a total relative area reading of peaks that matched the retention times of authentic markers 1A, 1L, 3L and several other unidentified peaks (based on Section 3.5.1 analysis). For the dimers, 2^F is a total relative area reading of peaks that matched the authentic markers 2A and 2L retention times. The quantitative analysis of digested pAMAC-labelled AIR is summarized in Table 3.5.2.

In general, the quantitative data agreed with the qualitative data as discussed in Section 3.4.3 and summarized in Table 3.4.4. Compound 1^F showed an increasing pattern in mango, banana, avocado and strawberry tree fruit, at least when stage 1 was compared to stage 3 and remains consistent in apple throughout all three stages. For pear, the total relative area reading of 1^F is higher at stage 2 of softening and about the same level at stage 1 and stage 3. On the other hand, strawberry showed the highest reading at stage 1 and a lowest at stage 2.

Compound 2^F also showed an increasing pattern at least when stage 1 was compared to stage 3 in mango, banana, avocado and strawberry tree fruit; and was only detected in stage 1 and stage 2 with similar amount in pear. On the other hand, 2^F is highest at stage 1 and lowest at stage 2 in apple and strawberry. Overall, both 1^F and 2^F showed a significant increase from stage 1 to stage 3 of softening in mango, banana, avocado and strawberry tree fruit but not in pear, apple and strawberry. Pear, apple and strawberry are temperate climate species amongst all seven species used in this study and this might influence their ripening mechanism and cell wall regulation.

Table 3.5.2 Quantitative analysis of the two interesting compounds among Driselase digestion products of pAMAC•AIR

Fruit source	Compounds of interest (acidic and lactone of monomer and dimer)	Total relative area reading of peaks of interest (%)		
		Stage 1	Stage 2	Stage 3
Pear	1^F	32.1	56.1	34.5
	2^F	2.87	2.06	Not been detected
Mango	1^F	7.23	12.8	15.3
	2^F	Not been detected	4.83	24.6
Banana	1^F	6.97	18.9	33.3
	2^F	3.17	11.4	28.8
Apple	1^F	17.8	16.6	14.9
	2^F	4.65	1.84	3.66
Avocado	1^F	8.43	31.8	24.3
	2^F	16.4	42.4	40.9
Strawberry	1^F	21.9	12.2	17.1
	2^F	2.24	0.79	1.16
Strawberry tree fruit	1^F	19.6	29.2	29.7
	2^F	10.0	11.8	48.3

A portion of Driselase digestion products of pAMAC-labelled AIR representing 20 mg fresh weight fruit were analysed by HPLC on a C_{18} column. Data were extracted from HPLC graphs shown in Figure 3.5.3 in which selected peaks were quantified by a total relative area reading. 1^F is a total relative area reading of peaks that matched the authentic markers 1A, 1L, 3L and several other unidentified peaks, labelled as (↓,↓,↓,↓) in Figure 3.5.3. 2^F is a total relative area reading of peaks that matched the authentic markers 2A plus 2L. This data only refer to the comparisons of detected fluorescent compound within a species.

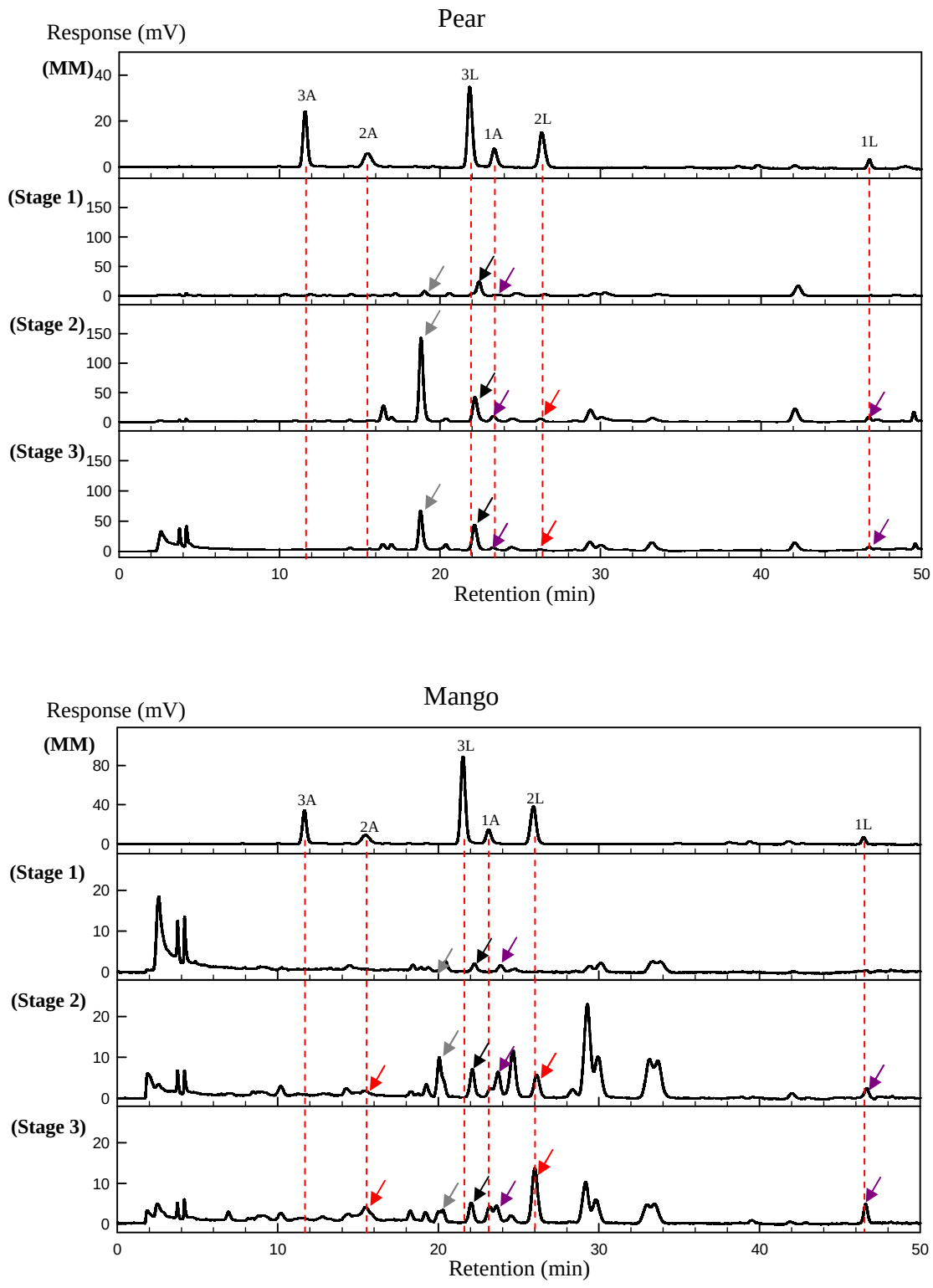

Figure 3.5.3 HPLC-resolution of Driselase-digested pAMAC•AIR for quantitative analysis on a Luna C_{18} column

Digested products of pAMAC•AIR sample: pear, mango, banana, apple, avocado, strawberry and strawberry tree fruit were analysed by HPLC. MM is a marker mixture that was run in between samples for reference; (↓,↓,↓,↓) are peaks taken together as '1F' and (↓) are peaks taken together as 2^F. Authentic markers 1L, 1A, 2L, 2A, 3L, and 3A were as defined in Figure 3.4.1. Fluorescence detection was with excitation at 442 nm and emission at 520 nm. Chromatograms continued overleaf.

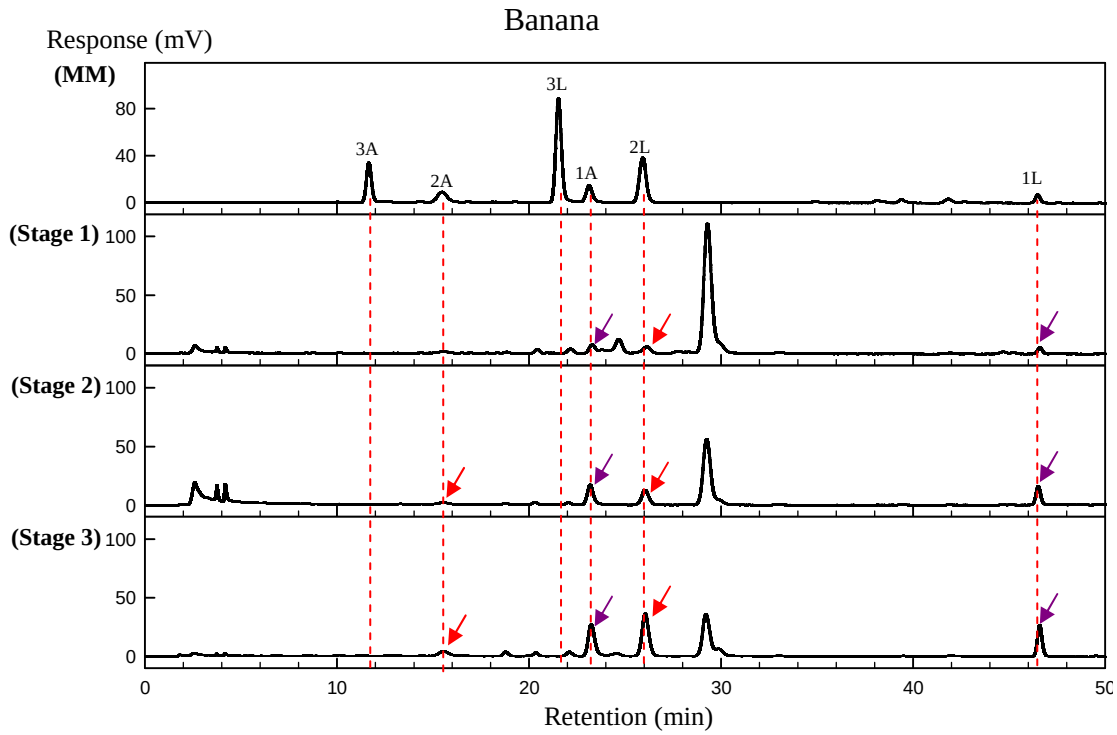

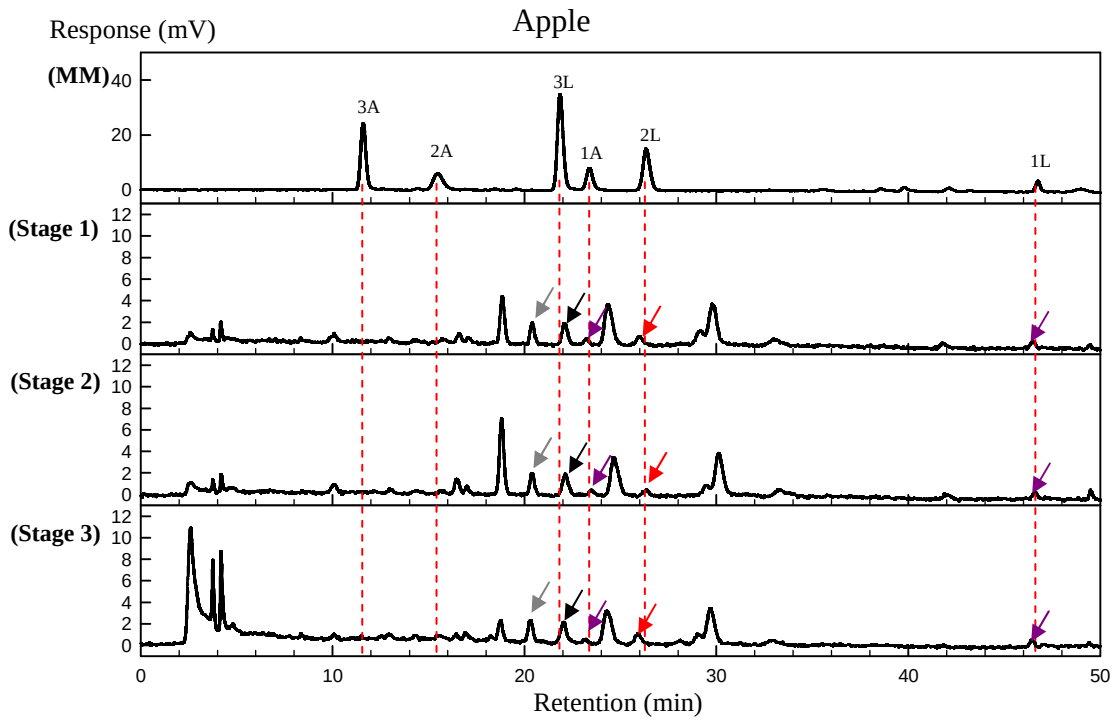

Figure 3.5.3 Continued.

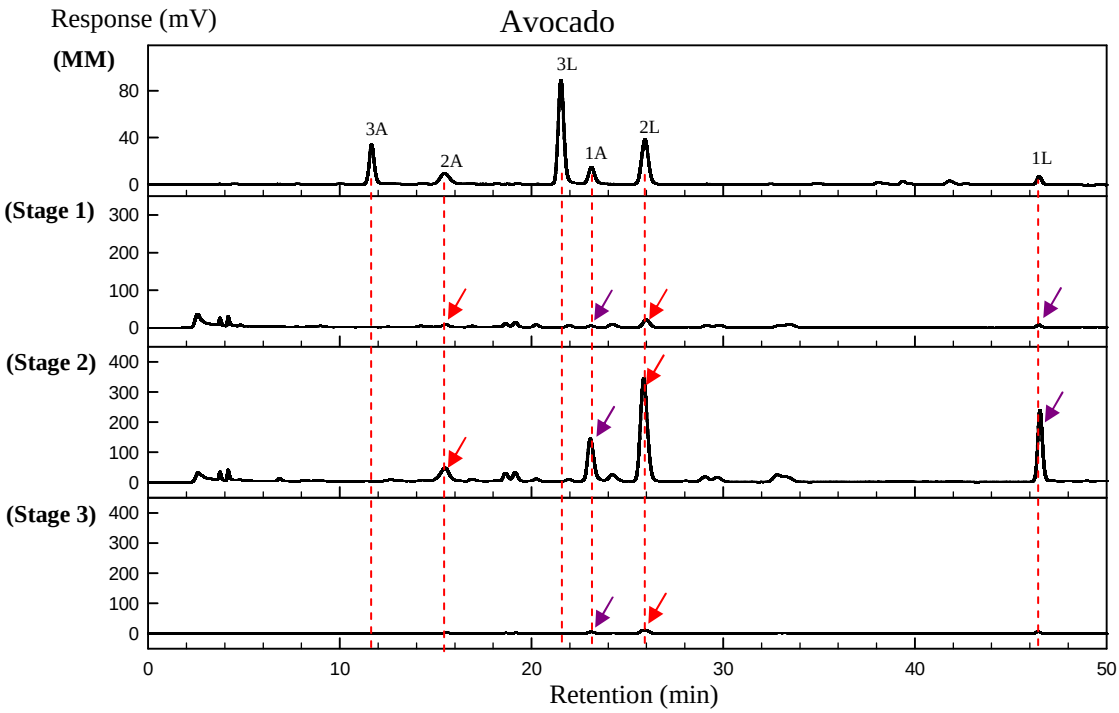

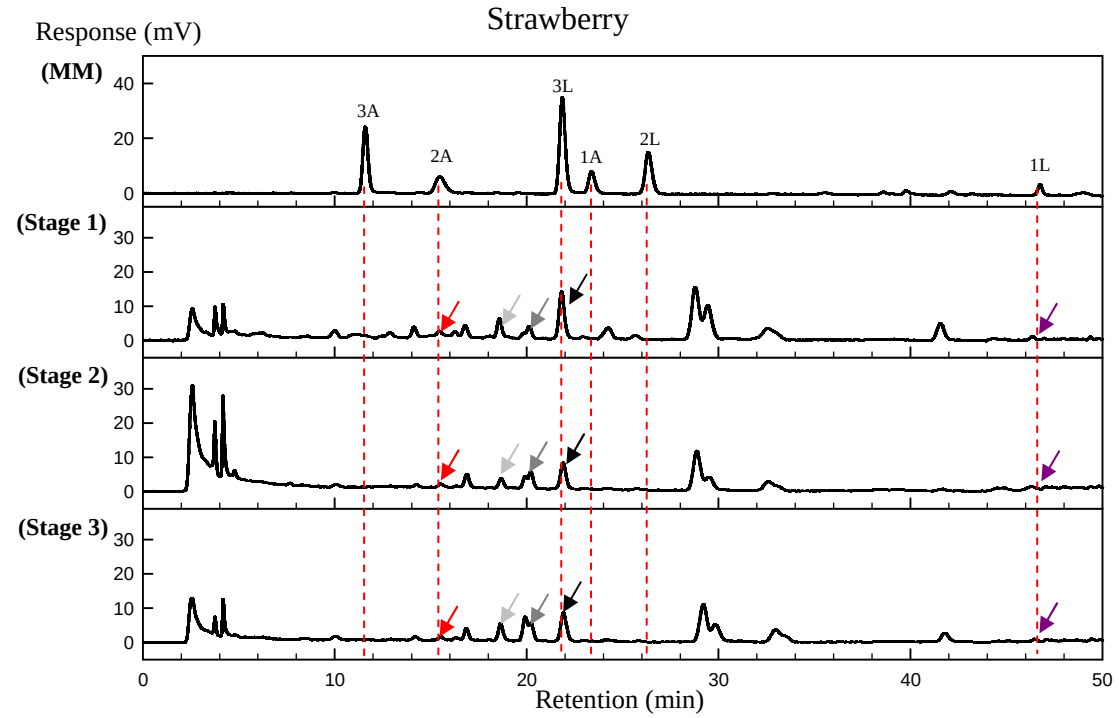

Figure 3.5.3 Continued.

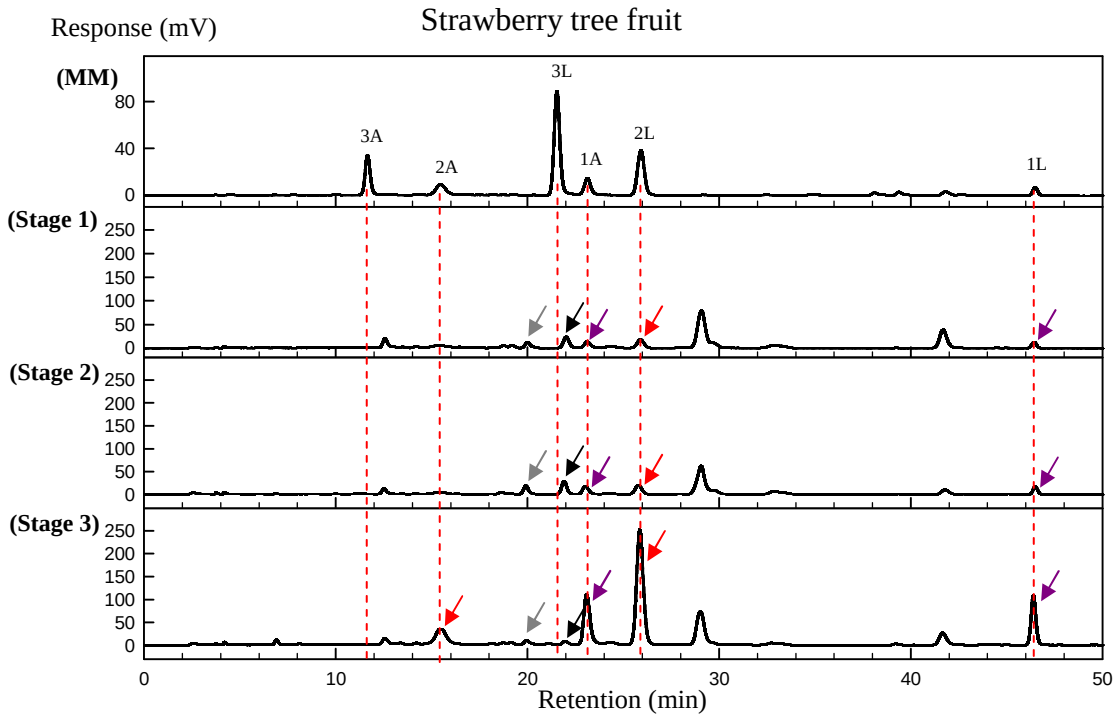

Figure 3.5.3 Continued.

3.6 $NaBH_4$ treatment of fruit AIR for detecting PL and EPG 'fingerprint' compounds

AIR from the seven fruits at each stage of softening was chemically treated with $NaBH_4$ to reduce the AIR polymers (producing $NaBH_4$-AIR). Treatment with $NaBH_4$ would reduce any D-GalA reducing termini to GalO residues. The $NaBH_4$-AIR was delactonised and submitted to Driselase digestion for 14 days. A portion of the digestion products was analysed by HPLC on a PA100 column (Table 3.6.1; Figure 3.6.1).

Based on peaks resolved on the HPLC analysis in Figure 3.6.1, GalA-GalO was detected in all samples at all stages of softening. This was as expected as the production of GalA-GalO could correspond to the D-GalA reducing termini that were produced during fruit ripening by the actions of $^{\bullet}OH$, EPG and/or PL attack. In the quantitative part, the ratio of GalA-GalO to free GalA residues increased during ripening in pear, mango and strawberry tree fruit. Apple, avocado and strawberry also showed an increase at least when stage 1 was compared to stage 3. The ratio remained almost constant in banana throughout all three stages (Table 3.6.1). The production of GalA-GalO is suggested to show a positive correlation with compound $1A^F$ that was produced from pAMAC•AIR (Section 3.4.3). This is because both compounds were from the reducing termini of pectin. Both are suggested to result from $^{\bullet}OH$, EPG and/or PL attack.

In this experiment, one more fingerprint compound was expected to be found in digested $NaBH_4$-AIR, i.e. ΔUA-GalA, the fingerprint for PL attack. Surprisingly, no sample showed the production of this fingerprint compound. This may suggest

that fruit softening in all fruit AIR used in this experiment was not associated with PL attack.

Table 3.6.1 Quantitative analysis of the interesting compounds among Driselase digestion products of $NaBH_4$-AIR

Fruit source	Compounds of interest	Relative area reading of peaks of interest (%)		
		Stage 1	Stage 2	Stage 3
Pear	**GalA-GalO**	0.43	1.16	1.37
	Ratio GalA-GalO:GalA	1:33	1:20	1:12
Mango	**GalA-GalO**	0.59	0.46	1.12
	Ratio GalA-GalO:GalA	1:49	1:95	1:28
Banana	**GalA-GalO**	1.75	2.43	2.31
	Ratio GalA-GalO:GalA	1:8	1:10	1:10
Apple	**GalA-GalO**	0.30	0.61	0.94
	Ratio GalA-GalO:GalA	1:98	1:27	1:34
Avocado	**GalA-GalO**	1.42	12.6	6.41
	Ratio GalA-GalO:GalA	1:30	1:3	1:4
Strawberry	**GalA-GalO**	1.16	1.74	1.55
	Ratio GalA-GalO:GalA	1:26	1:20	1:18
Strawberry tree fruit	**GalA-GalO**	0.77	0.61	1.08
	Ratio GalA-GalO:GalA	1:36	1:42	1:26

A portion of Driselase digestion products of $NaBH_4$-treated AIR representing 20 mg fresh weight fruit was analysed by HPLC on a C_{18} column. Data were extracted from HPLC graphs shown in Figure 3.6.1 where peaks of GalA-GalO and ΔUA-GalA (if any) were quantified by a relative area reading and relative ratio of GalA-GalO:GalA.

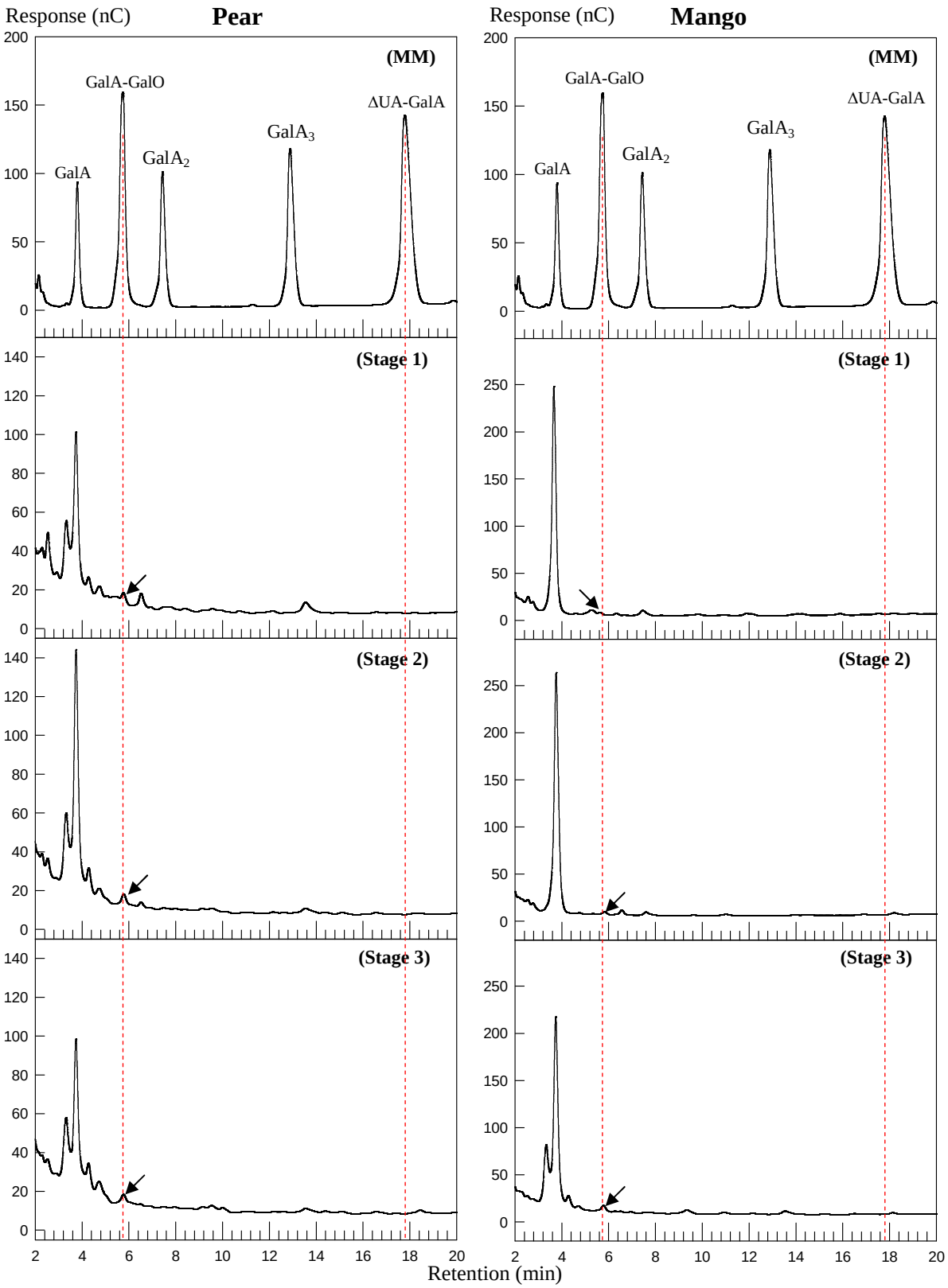

Figure 3.6.1 HPLC-resolution of a Driselase-digested $NaBH_4$-AIR on a PA100 column

Digested products of $NaBH_4$-AIR sample: pear, mango, banana, apple, avocado, strawberry and strawberry tree fruit were resolved by HPLC. MM is a marker mixture that was run in between samples for reference. PAD was used for this HPLC system. Chromatograms continued overleaf.

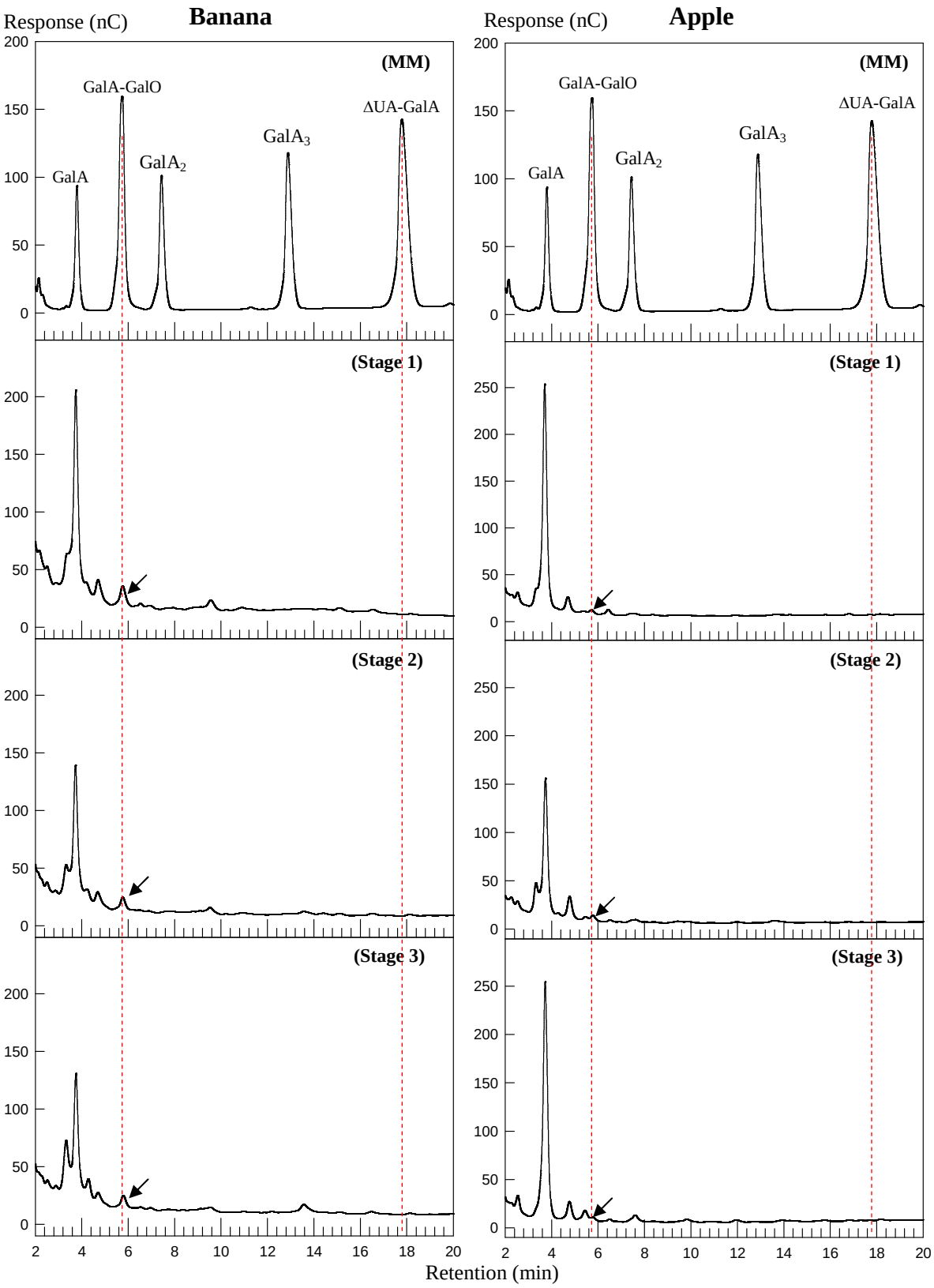

Figure 3.6.1 Continued

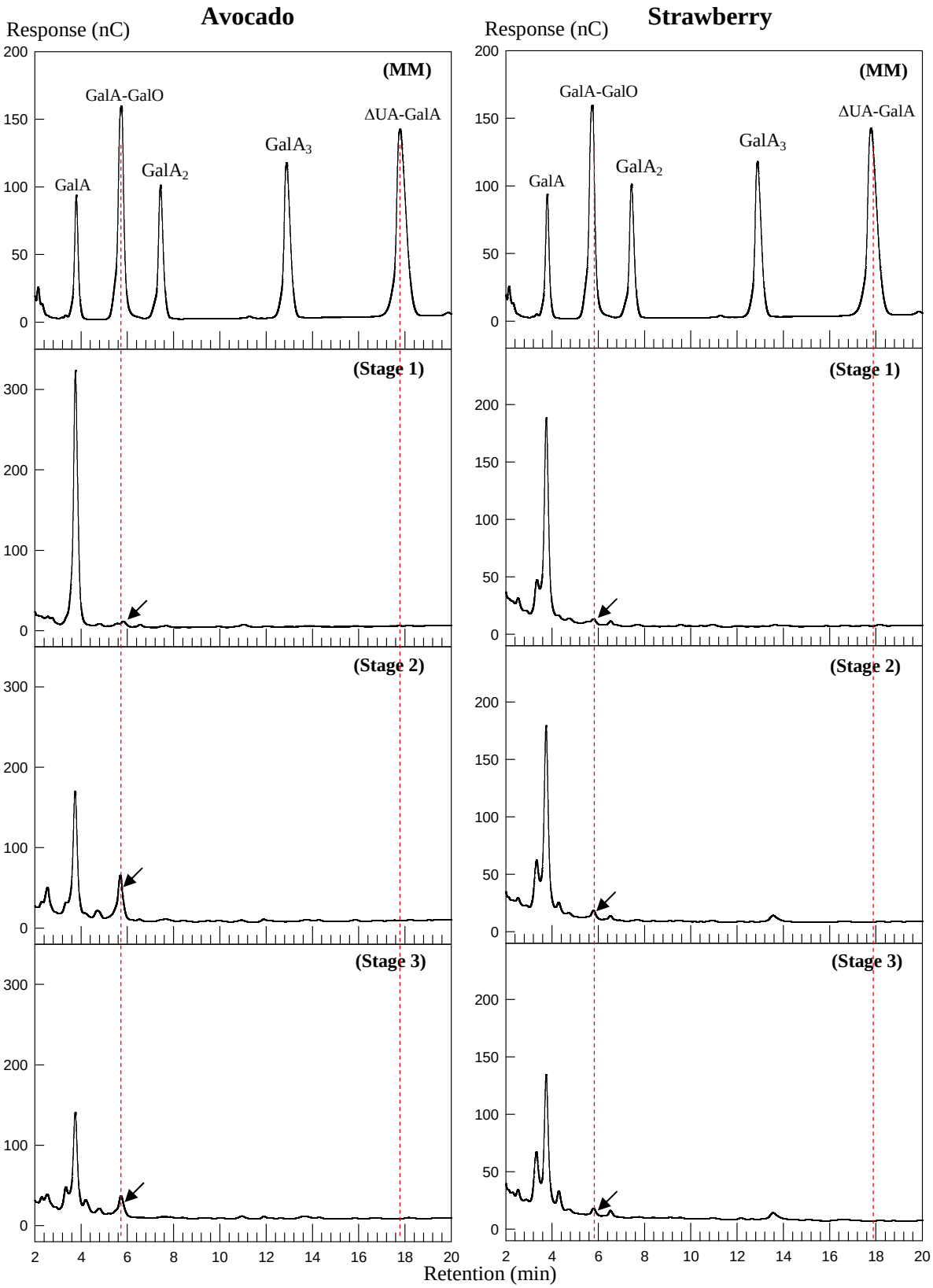

Figure 3.6.1 Continued

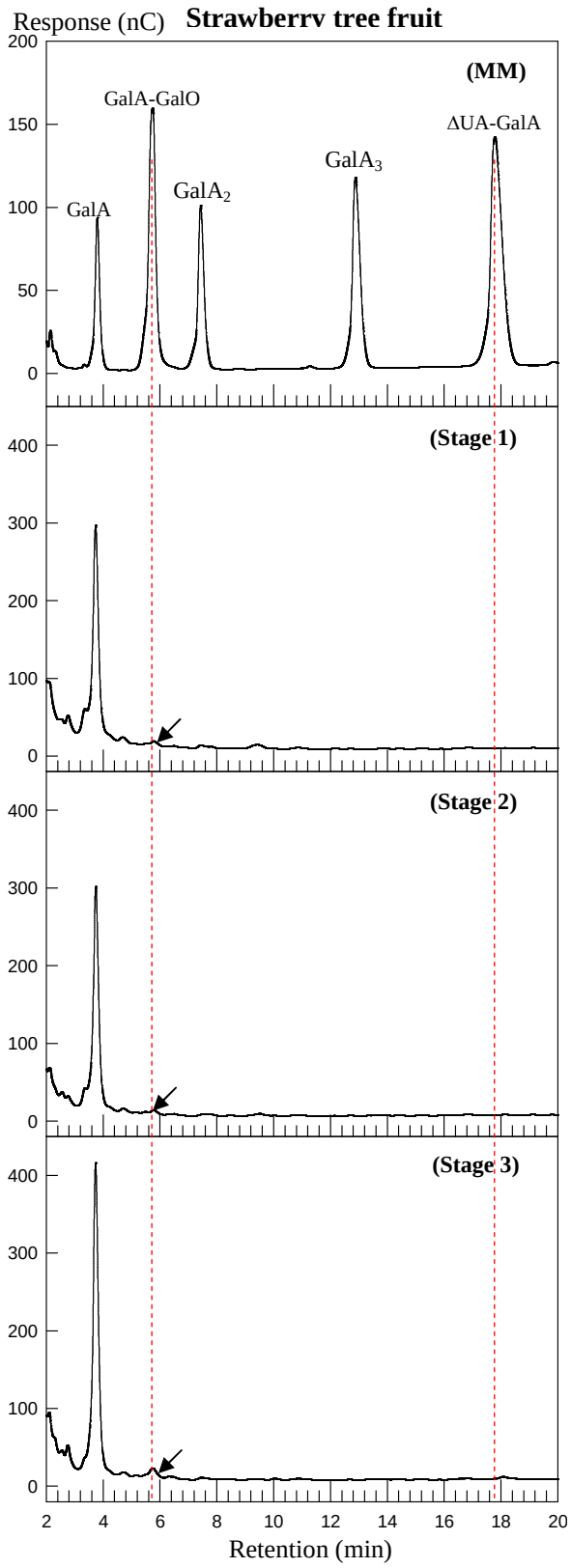

Figure 3.6.1 Continued

3.7 Driselase digestion of untreated fruit AIR in an attempt to detect PL 'fingerprint' compound

An equal portion of AIR from the seven fruits at each stage of softening as has been used in Section 3.6 was directly submitted to Driselase digestion for 14 days (referred to as non-$NaBH_4$-AIR). A portion of the digestion products was analysed by HPLC on a PA100 column

In this experiment, free GalA residues and ΔUA-GalA (if any, which indicates PL action) were expected as the products of digestion but not GalA-GalO. Based on the HPLC result (Table 3.7.1 and Figure 3.7.1), all samples produced free GalA, indicating successful Driselase digestion. Also, most of the samples showed a production of a compound co-eluting with ΔUA-GalA. This observation contradicts the result observed in Section 3.6. Similar yield of ΔUA-GalA were expected from these two treatments.

On the other hand, all samples yielded GalA-GalO. Again, this was not as expected because GalA-GalO is expected only after treatment with $NaBH_4$. Nevertheless, the proportion of GalA-GalO:GalA in this non-$NaBH_4$-AIR (Table 3.7.1) was lower than in $NaBH_4$-AIR (Table 3.6.1). This may suggests that possibly GalO residues naturally existed in fruit AIR, leading to the formation of GalA-GalO after Driselase digestion, and additional GalA-GalO was produced if the fruit AIR was treated with $NaBH_4$.

Table 3.7.1 Quantitative analysis of the interesting compounds among Driselase digestion products of non-$NaBH_4$-AIR

Fruit source	Compounds of interest	Relative area reading of peaks of interest (%)		
		Stage 1	Stage 2	Stage 3
Pear	ΔUA-GalA	0.45	0.59	0.00
	GalA-GalO	1.3	0.79	0.92
	Ratio ΔUA-GalA:GalA	1:146	1:99	-
	Ratio GalA-GalO:GalA	1:51	1:74	1:44
Mango	ΔUA-GalA	0.31	0.36	0.82
	GalA-GalO	0.43	0.54	0.69
	Ratio ΔUA-GalA:GalA	1:122	1:127	1:85
	Ratio GalA-GalO:GalA	1:88	1:85	1:101
Banana	ΔUA-GalA	0.00	0.87	0.81
	GalA-GalO	0.66	1.04	1.1
	Ratio ΔUA-GalA:GalA	-	1:50	1:64
	Ratio GalA-GalO:GalA	1:16	1:41	1:47
Apple	ΔUA-GalA	0.35	0.29	0.35
	GalA-GalO	0.66	0.47	1.11
	Ratio ΔUA-GalA:GalA	1:136	1:163	1:138
	Ratio GalA-GalO:GalA	1:72	1:100	1:43
Avocado	ΔUA-GalA	0.53	0.00	0.00
	GalA-GalO	1.09	3.82	1.43
	Ratio ΔUA-GalA:GalA	1:117	-	-
	Ratio GalA-GalO:GalA	1:57	1:14	1:40
Strawberry	ΔUA-GalA	0.00	0.00	0.00
	GalA-GalO	0.83	1.20	1.71
	Ratio ΔUA-GalA:GalA	-	-	-
	Ratio GalA-GalO:GalA	1:66	1:54	1:37
Strawberry tree fruit	ΔUA-GalA	0.00	0.42	0.92
	GalA-GalO	0.62	0.65	0.63
	Ratio ΔUA-GalA:GalA	-	1:88	1:40
	Ratio GalA-GalO:GalA	1:59	1:57	1:58

A portion of Driselase digestion products of non-AMAC-labelled, non-$NaBH_4$-treated AIR representing 20 mg fresh weight fruit were analysed by HPLC on a C_{18} column. Data were extracted from HPLC graphs shown in Figure 3.7.1 where peaks of GalA-GalO and ΔUA-GalA (if any) were quantified by a relative area reading and ratio of GalA-GalO:GalA and ΔUA-GalA:GalA.

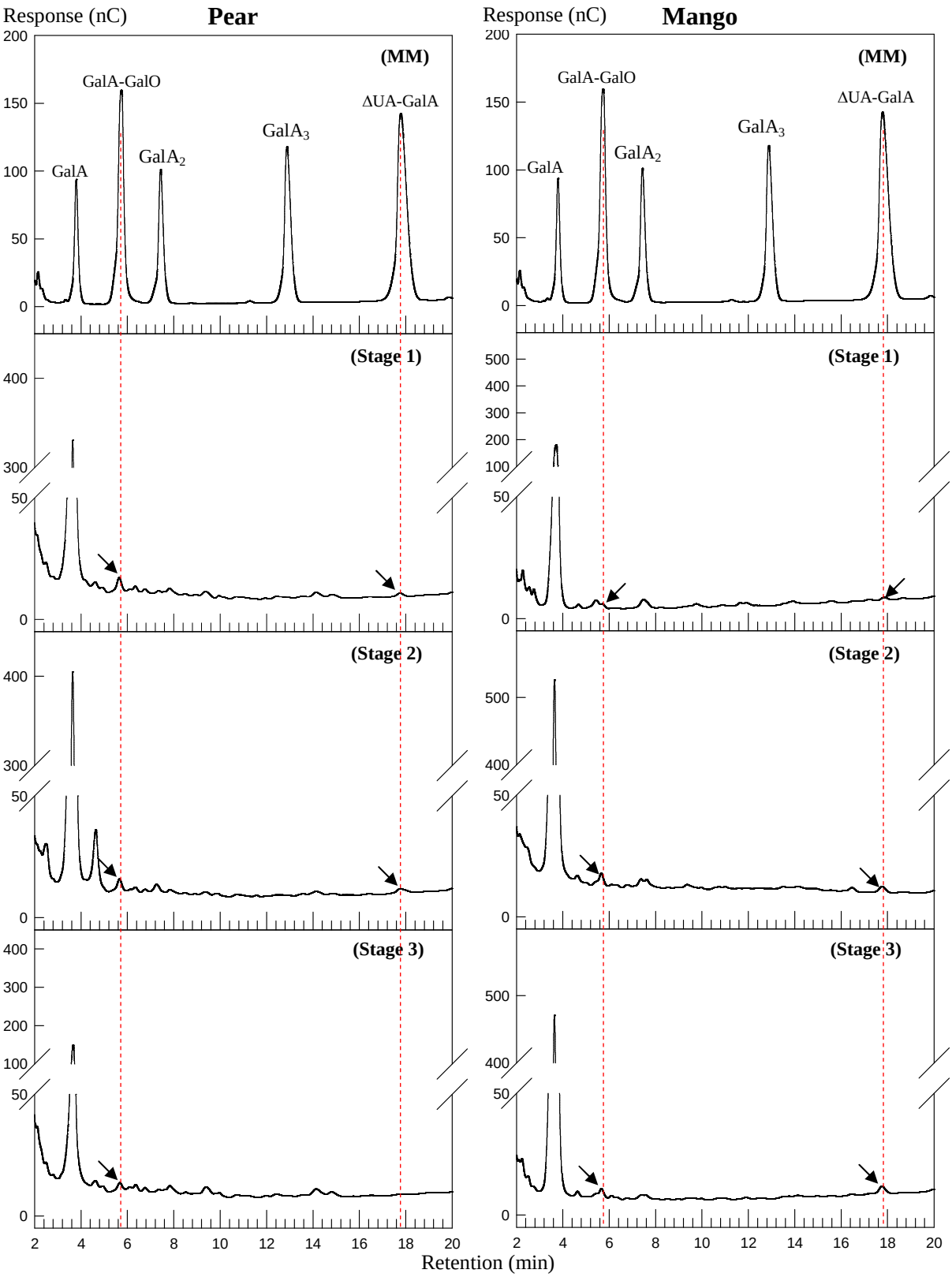

Figure 3.7.1 HPLC-resolution of a Driselase-digested non-$NaBH_4$-AIR on a PA100 column

Digested products of non-$NaBH_4$-AIR sample: pear, mango, banana, apple, avocado, strawberry and strawberry tree fruit were analysed by HPLC. MM is a marker mixture that was run in between samples for reference. PAD was used for this HPLC system. Chromatograms continued overleaf.

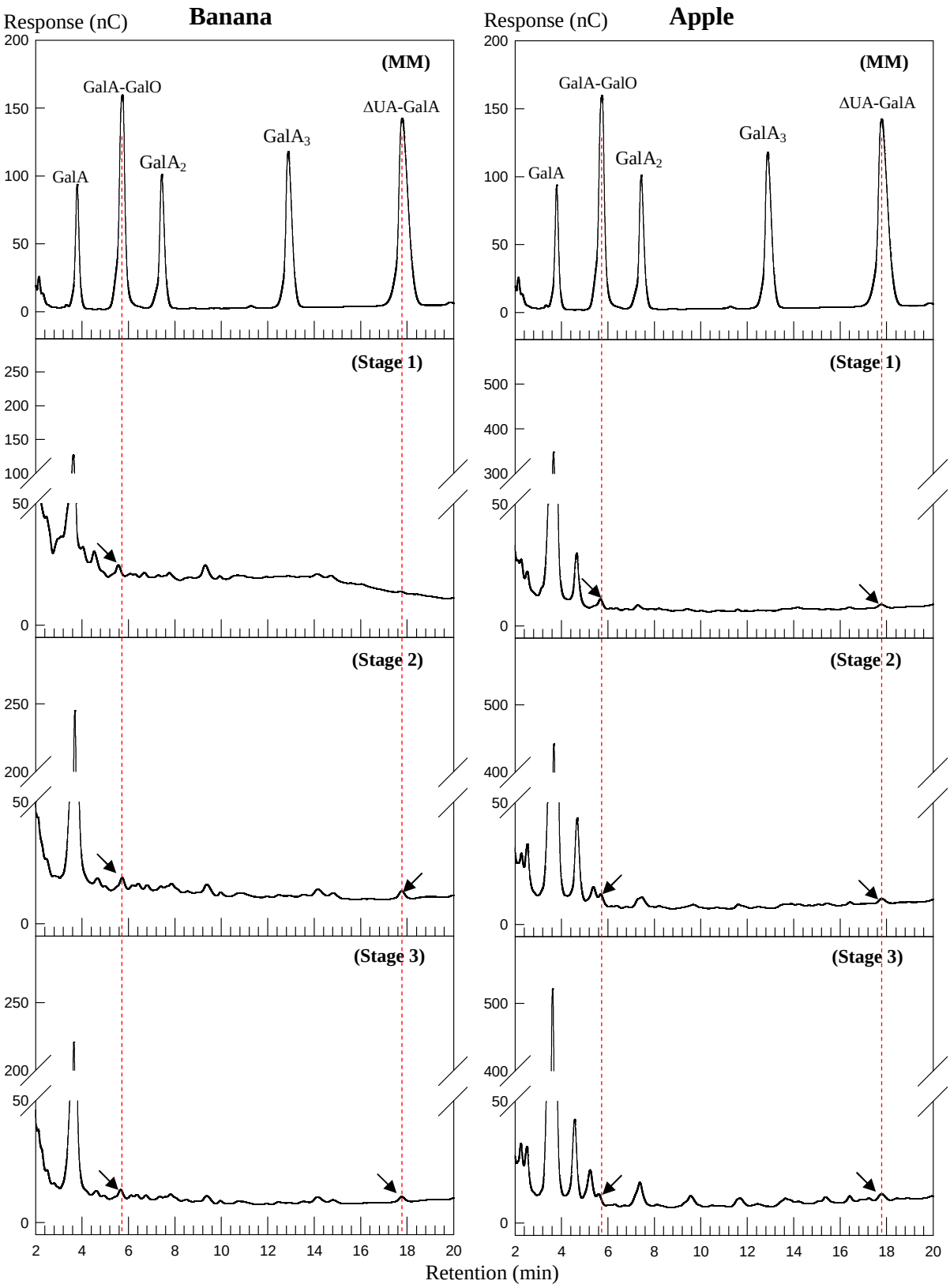

Figure 3.7.1 Continued

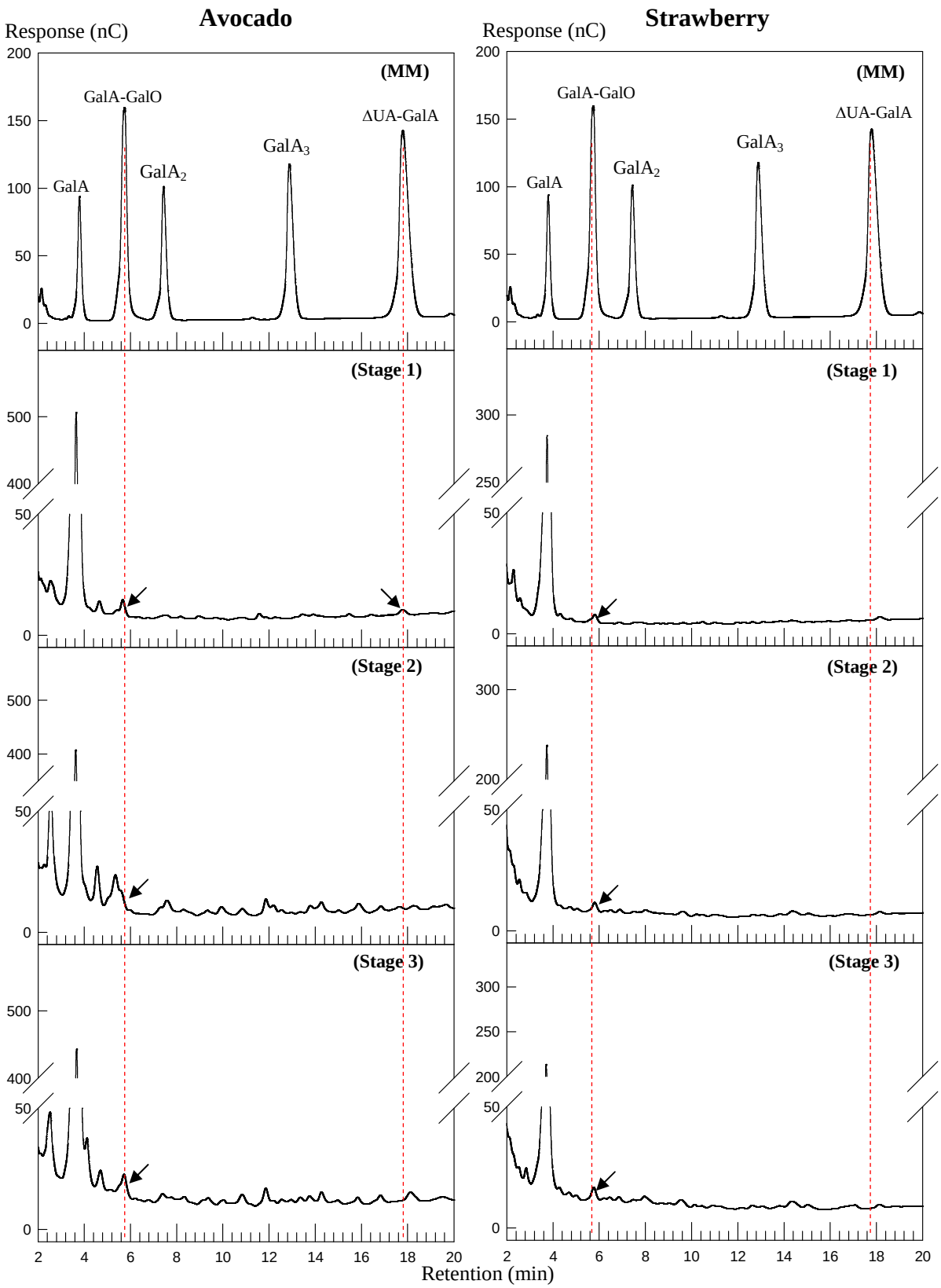

Figure 3.7.1 Continued

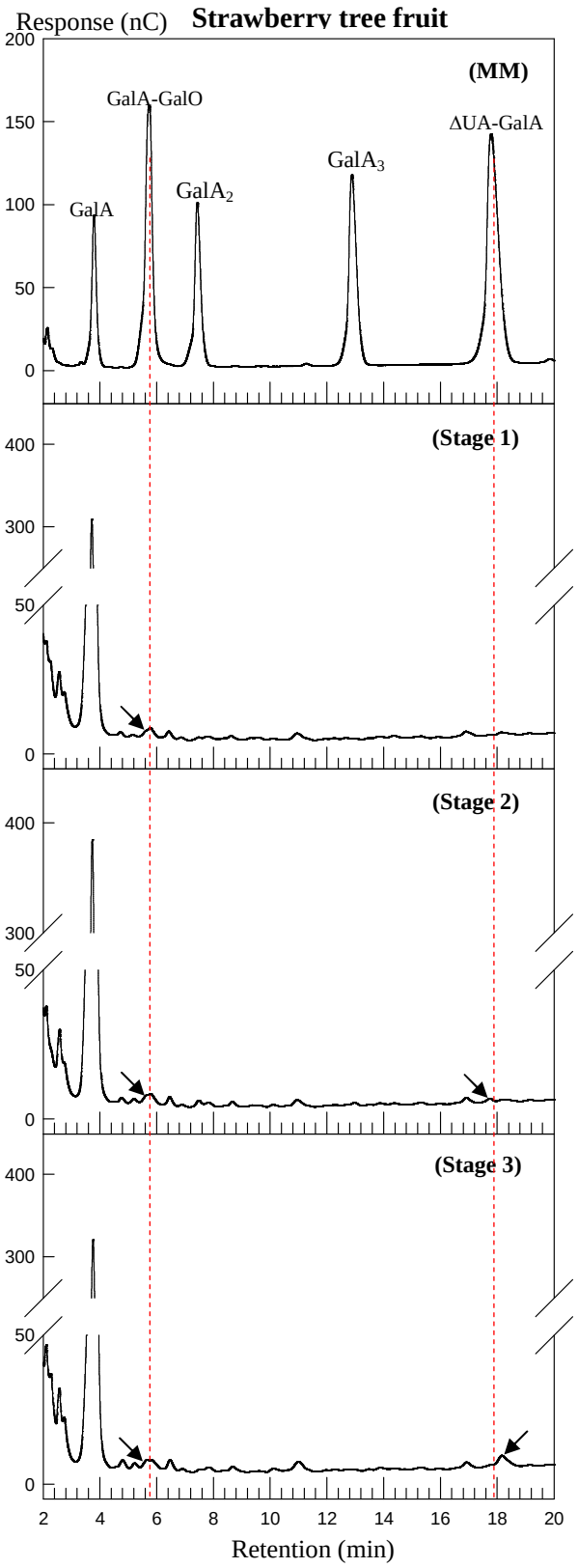

Figure 3.7.1 Continued

3.8 Total non-cellulosic sugar residues in fruit AIR samples

3.8.1 TFA hydrolysate from the pellet of 14 days digestion of pAMAC•AIR, $NABH_4$-AIR and non-$NaBH_4$-AIR analysed by paper chromatography

The remaining residues after 14 days' Driselase digestion of pAMAC•AIR, $NaBH_4$-AIR and non-$NaBH_4$-AIR were hydrolysed with TFA and an equal portion from each was paper chromatographed and stained (Figure 3.8.1, 3.8.2 and 3.8.3) to reveal Driselase-undigested and sugar residues in the fruit AIR samples.

In general, all AIR samples from all treatments showed a similar pattern of sugars, with galacturonic acid, glucose, mannose, arabinose and xylose as the common sugars found in all fruit AIR samples, although some of these sugars were not visible on the chromatogram of pAMAC•AIR, but were detected by HPLC (Section 3.8.2). Glucose that was found in the hydrolysate was possibly from hemicelluloses. Banana sample from each treatment at stage 1 (unripe banana) showed a very high amount of glucose compared with others. This glucose was suggested not only from cell wall components but mostly from starch that is rich in green bananas. The suggestion was supported by the production of two compounds that migrated slower than GalA in the banana stage 1 sample (believed to be maltose and glucose trisaccharides).

Galacturonic acid was probably from the remaining undigested pectic polysaccharides (most probably from the RG-I/RG-II domain), while mannose and xylose were probably from hemicelluloses. Arabinose can arise either from hemicelluloses or from the RG-I/RG-II of pectic polysaccharides. Galactose was found in all samples except banana and it might be a hydrolysis product of hemicelluloses or from the RG-I of pectic polysaccharide. Rhamnose and fucose

were also found in most samples as minor compounds (clearly visible in Figure 3.8.3), possibly from RG-I/RG-II. In addition, fucose could also be from hemicelluloses.

Hemicelluloses were the major components of the AIR that were undigested by Driselase. Therefore, when the pellet was treated with TFA, galactose, glucose, mannose, arabinose and xylose, which are the main constituent of hemicelluloses, were released as free sugars. Although there was still small amount of GalA was left undigested by Driselase, which was assumed from RG-I/RG-II domains, but most of the GalA (mainly represent the homogalacturonan domain of pectic polysaccharide), was successfully digested by Driselase to be analysed in previous sections.

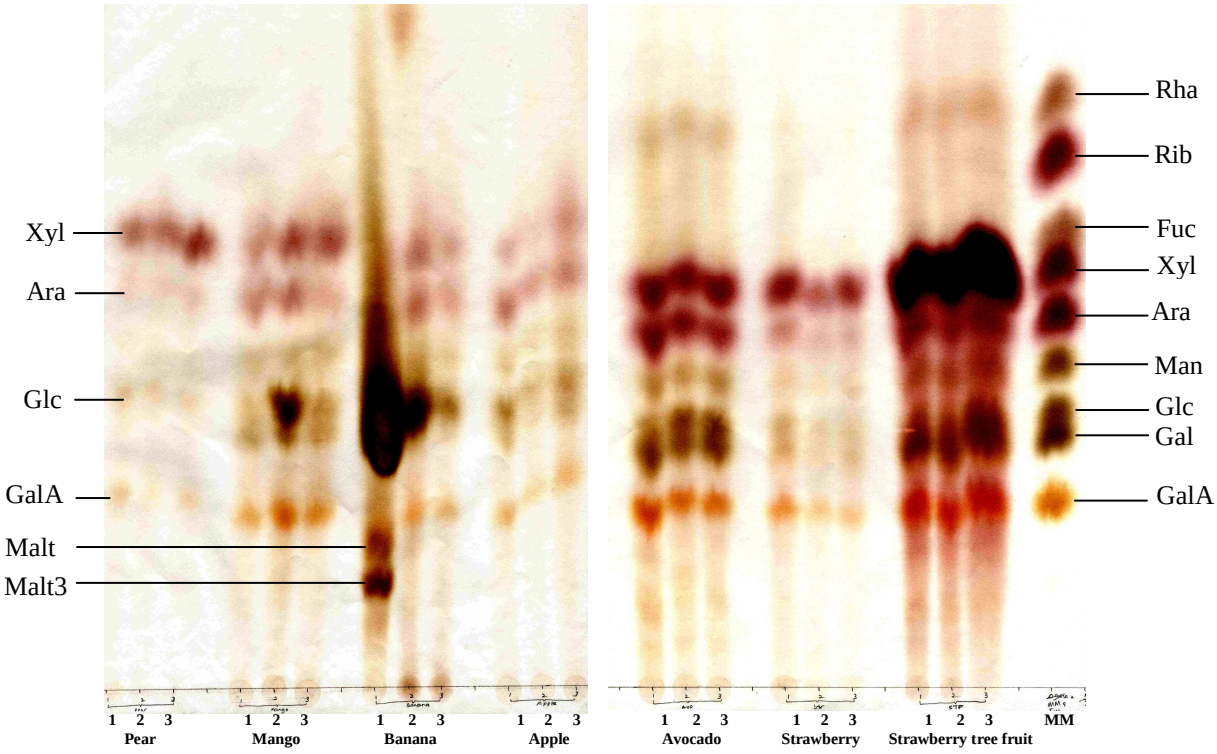

Figure 3.8.1 TFA hydrolysis products of Driselase-resistant pAMAC•AIR separated by paper chromatography

The remaining residues after 14 days' Driselase digestion of pAMAC•AIR were hydrolysed with TFA (2 M, 120°C, 1 h). A portion (40 µl) of the hydrolysates from each sample, corresponding to 160 mg fresh weight fruit of initial AIR, was loaded onto Whatman 1CHR together with monosaccharide marker mixture (MM), and run for 16 hours in B/A/W (12/3/5), followed by another 16 hours in E/P/W (8/2/1). Products were stained with aniline hydrogen-phthalate.

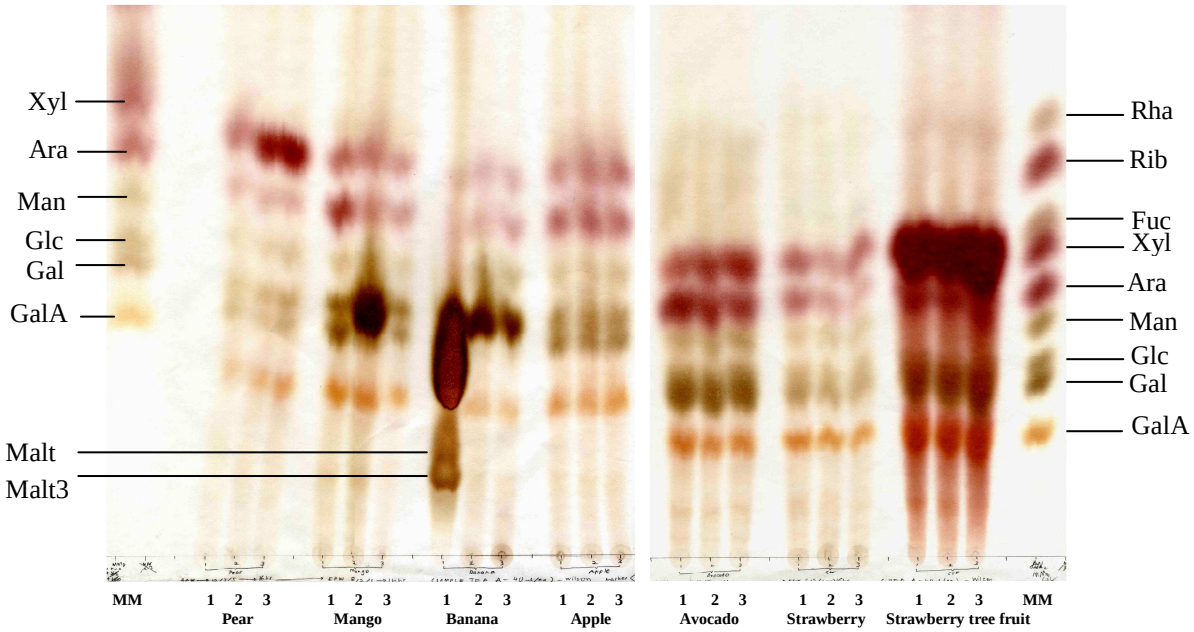

Figure 3.8.2 TFA hydrolysis products of Driselase-resistant $NaBH_4$-treated AIR separated by paper chromatography

Details as for Figure 3.8.1 except sample was from the residue remaining after 14 days Driselase digestion of $NaBH_4$-AIR.

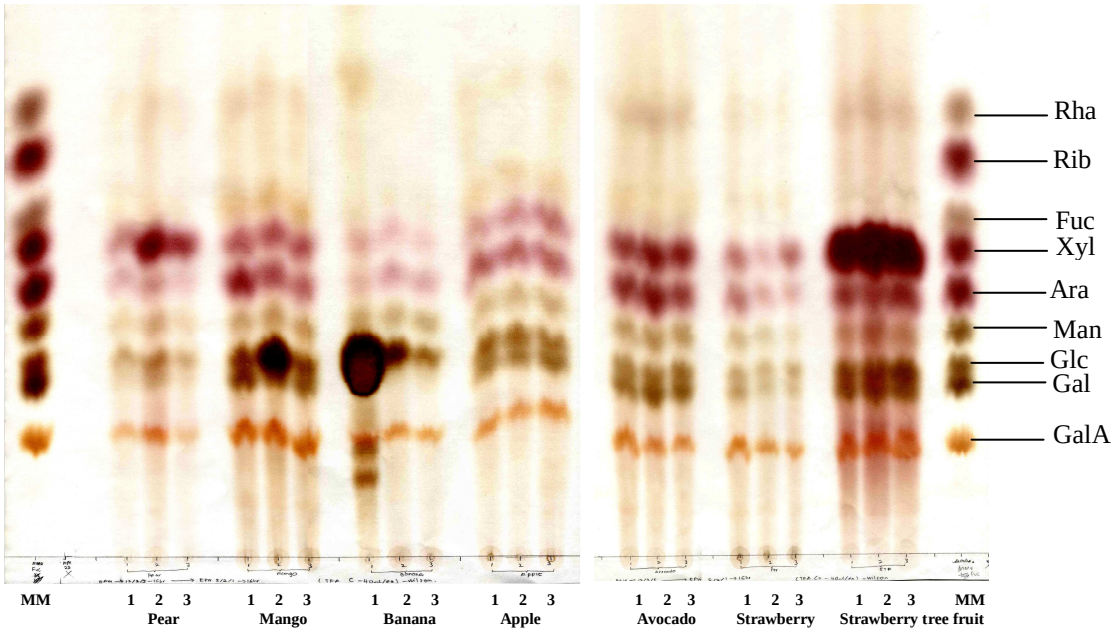

Figure 3.8.3 TFA hydrolysis products of Driselase-resistant Non-$NaBH_4$-treated AIR separated by paper chromatography

Details as for Figure 3.8.1 except sample was from the residue remaining after 14 days Driselase digestion of non-$NaBH_4$-AIR.

3.8.2 HPLC of the TFA hydrolysate of the Driselase-resistant pAMAC•AIR

A portion of pAMAC•AIR TFA-hydrolysate from each AIR fruit sample at three stages of softening was analysed by HPLC on a PA1 column (Figure 3.8.4). However, samples used in this analysis were not from the same source as used in the pAMAC•AIR experiments discussed in previous sections. Therefore, the quantitative values from this experiment could not be directly related to the qualitative values of any compound on the chromatogram in Figure 3.8.1. This particular analysis by HPLC was to get an idea of the quantitative value of the sugar content in the AIR fruit samples.

Table 3.8.1 shows the quantitative values extracted from the chromatograms shown in Figure 3.8.4 and other similar ones (not shown). Glucose was the major sugar detected in pear, mango, banana and avocado whereas in strawberry and strawberry tree fruit, xylose was the main sugar produced after the TFA hydrolysis. Glucose and xylose are two main sugar residues that make up hemicelluloses. Therefore, this suggests that the residue remaining after 14 days Driselase digestion rich in Driselase-resistant hemicelluloses. On the other hand, fucose, rhamnose, GalA and glucuronic acid, the main constituents of pectin, are amongst sugar residues produced with low amount after TFA hydrolysis in all fruit species. This indicates that most of the pectin component had been successfully digest by Driselase to be analysed in previous experiments.

Table 3.8.1 Quantitative analysis of the sugar content of TFA hydrolysis products of Driselase-resistant pAMAC•AIR

Compounds of interest	µg sugar per 20 mg of initial AIR (fresh weight)																	
	Pear			Mango			Banana			Avocado			Strawberry			Strawberry tree fruit		
	Stage 1	Stage 2	Stage 3	Stage 1	Stage 2	Stage 3	Stage 1	Stage 2	Stage 3	Stage 1	Stage 2	Stage 3	Stage 1	Stage 2	Stage 3	Stage 1	Stage 2	Stage 3
Fucose	0.16	0.10	0.00	0.20	0.12	0.57	0.62	0.33	0.00	0.13	0.11	0.20	0.00	0.00	0.00	0.07	0.12	0.08
Rhamnose	0.43	0.16	0.16	0.20	0.06	0.34	0.00	0.00	0.11	0.15	0.14	0.25	0.24	0.32	0.32	0.41	0.30	0.26
Arabinose	2.52	1.06	0.92	1.05	0.72	1.14	0.18	0.51	0.45	0.87	0.69	0.85	0.72	0.79	0.66	0.84	1.35	0.94
Galactose	1.02	0.38	0.37	0.73	0.28	1.86	0.00	0.24	0.20	0.56	0.39	0.68	0.47	0.58	0.48	1.36	1.48	1.17
Glucose	3.57	2.03	2.20	2.95	8.78	11.0	114	34.5	3.45	2.07	2.45	4.13	1.54	1.87	1.99	1.76	2.22	2.76
Xylose	7.49	0.87	0.97	0.32	0.33	1.00	0.00	0.00	0.09	0.63	0.30	0.63	2.40	3.98	3.74	14.1	9.07	5.43
Mannose	0.71	0.37	0.00	0.41	0.15	1.39	0.00	0.54	0.53	0.38	0.25	0.53	0.00	0.00	0.00	0.00	0.00	0.51
Isoprimeverose	0.53	0.52	0.41	0.67	0.38	1.95	0.35	0.98	1.14	0.37	0.39	0.54	0.38	0.32	0.49	0.24	0.41	0.37
Xylobiose	0.00	0.00	0.00	0.00	0.00	1.66	4.33	1.00	0.00	0.00	0.00	0.00	0.00	0.69	0.82	1.35	1.25	0.95
Maltose	0.00	0.00	0.00	0.00	0.00	0.00	0.24	0.00	0.00	0.00	0.00	0.00	0.00	0.00	0.00	0.20	0.00	0.00
Galacturonic acid	1.67	0.41	0.29	0.83	0.61	2.69	2.18	0.69	0.41	0.98	0.25	0.47	1.16	1.14	0.96	1.89	2.48	1.75
Glucuronic acid	0.25	0.00	0.00	0.00	0.00	0.00	0.44	0.00	0.00	0.00	0.00	0.00	0.00	0.28	0.21	0.00	0.00	0.00

A portion of TFA hydrolysate products of Driselase-resistant pAMAC•AIR, represent 20 mg fresh weight of initial AIR were analysed by HPLC on a PA1 column. Data were extracted from HPLC graphs shown in Figure 3.8.4 in which peaks of monosaccharides and disaccharides were quantified.

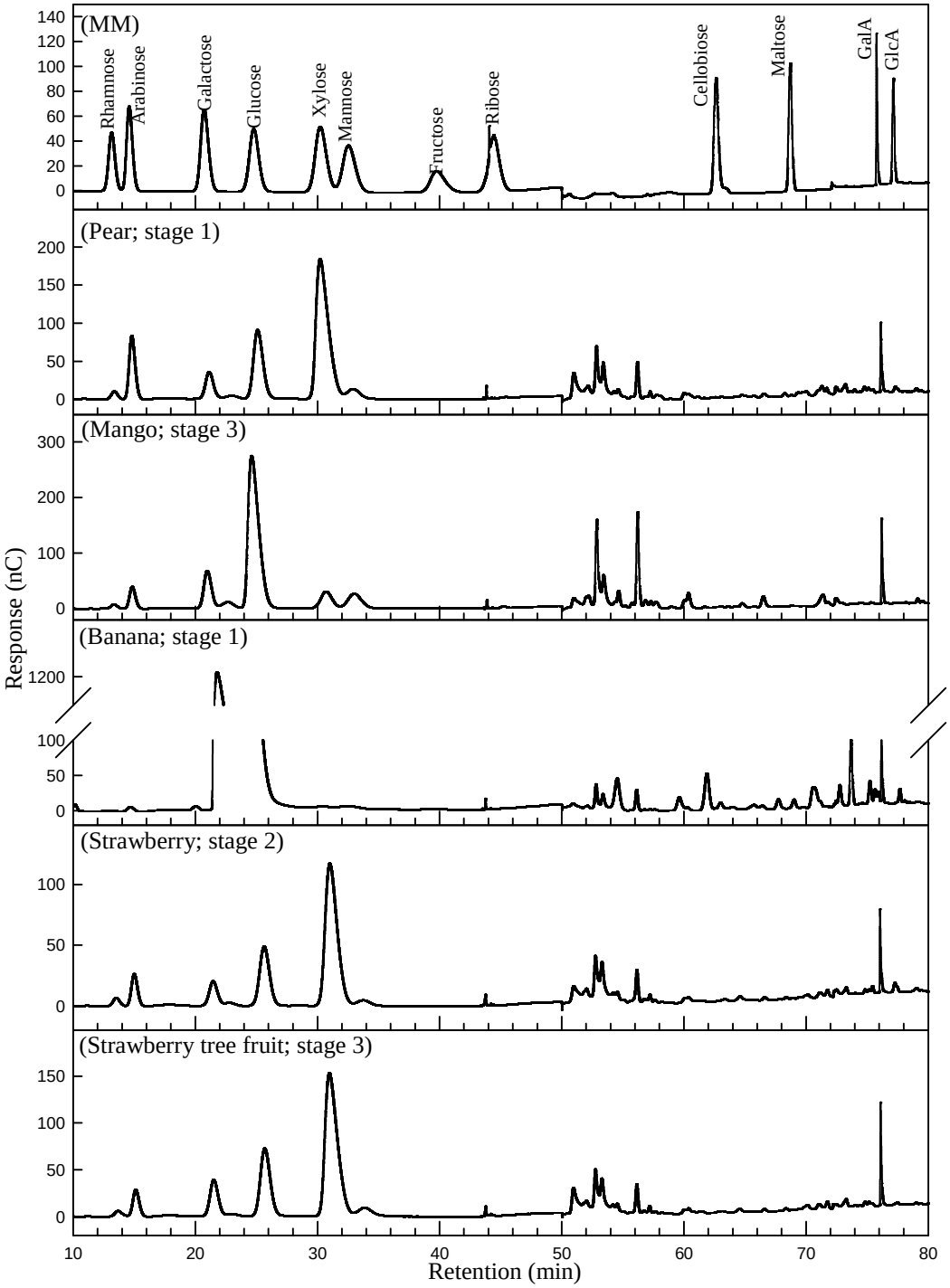

Figure 3.8.4 HPLC-resolution of TFA hydrolysate products of Driselase-resistant pAMAC•AIR on a PA100 column

A portion of TFA hydrolysate products of Driselase-resistant pAMAC•AIR: pear (stage 1), mango (stage 3), banana (stage 1), strawberry (stage 2) and Strawberry tree fruit (stage 3), represent 20 mg fresh weight of initial AIR were analysed by HPLC on a PA1 column. MM is a marker mixture that was run in between samples for reference. PAD was used for this HPLC system.

4. Discussion

4.1 Development of novel fluorescent labelling method to study pectic polysaccharide degradation

The novel method that was developed in this research is useful to investigate one of the major processes in plant development: fruit softening during the ripening process. This novel fluorescent labelling method with 2-AMAC has previously been explored in the Edinburgh Cell Wall Group research (R. A. M. Vreeburg & S. C. Fry, unpublished), mainly to study the ˙OH attack on pectic polysaccharides by recognising and measuring the unique diagnostic compounds (chemical fingerprint) of homogalacturonan molecules left after ˙OH attack. It is an alternative approach which will improve existing fingerprinting approach such as radiolabelling method (*Fry et al*., 2001; Müller *et al*., 2009) on monitoring ˙OH attack during fruit ripening. In my study, it was also found that this developed fluorescent labelling method has the potential not only to reveal ˙OH attack but also to reveal EPG and PL attack.

In general, this developed labelling method has been successfully used in this study to monitor the action of ˙OH *in vitro* and *in vivo*. In *in-vitro* application, ˙OH-treated pectin was successfully labelled with pAMAC which resulted in a clear fluorescent spot on a TLC plate compared with the untreated pectin. The Driselase digested ˙OH-treated pectin produced at least three fingerprint compounds (1A*, 2A*, X*) which provides clear evidence of ˙OH attack and these fingerprint compounds were used as reference for the *in-vivo* experiment. The application of this fluorescent labelling method to seven selected fruits (pear, mango, banana, apple,

avocado, strawberry and strawberry tree fruit) at three stages of softening provides useful information on ˙OH attack *in vivo* which to some degree agreed with the result observed in *in-vitro*. At least two fingerprint compounds ($1A^F$ and $2A^F$) were produced. $2A^F$ was suggested to be exclusive evidence for ˙OH attack while $1A^F$ was suggested to be a useful evidence not only to reveal ˙OH attack but also to reveal EPG and PL attack. X^F was also found in a few samples in *in-vivo* experiments, showed electrophoretic mobility similar to X*; however, the retention time of this compound on HPLC did not agree with that of X* suggesting it is a different compound to X* and remain unidentified. Although several of the fluorescent fingerprint compounds especially X*/X^F were not fully identified and deserve further analysis and the relative contributions of ˙OH, EPG and PL during fruit softening remains unclear, but, this novel fluorescent labelling method will give useful information and lead to the opportunity to use this approach as comparison to other approach for a better knowledge and understanding about ˙OH, EPG and PL action in cell walls.

In addition to the fluorescent labelling method, two set experiments of non-fluorescent labelling methods (see Section 3.6 and 3.7) were also developed particularly to monitor EPG and PL action *in vivo*. The results gave many uncertainties in which one set of experiment opposed another and contradicted earlier reports (see Section 4.4). However, a successful detection of GalA-GalO (fingerprint for EPG action) and ΔUA-GalA (fingerprint for PL action) by HPLC indicates a potential fingerprint method to reveal EPG and PL action during fruit softening *in vivo*. As this is the first study in attempt to monitor the *in-vivo* action of EPG and PL, it will open the way for future study on EPG and PL action in cell walls.

Research in this thesis was started by producing several fluorescent markers that were used for recognizing the chemical fingerprints of $^{\bullet}OH$ attack. By using the labelling method described in Section 1.4.1, several authentic monosaccharides and oligosaccharides were fluorescently labelled with pAMAC. These labelled sugars were used throughout this research as authentic markers. Labelling of these reducing sugars with pAMAC is expected to occur at carbon-1 of the reducing terminus sugar moiety. Figure 3.1.1 shows the authentic markers of Glc-pAMAC, Gal-pAMAC, GalA-pAMAC, $GalA_2$-pAMAC, $GalA_3$-pAMAC and their lactones on an electrophoretogram at pH 6.5.

The 2-AMAC group is generally an uncharged molecule when analysed by electrophoresis at pH 10 (Song *et al.*, 2002) or at pH 8.2 (Goubet *et al.*, 2002) and acquires a positive charge at lower pH such as pH 3 (Lamari *et al.*, 1999). In this study, Glc-pAMAC and Gal-pAMAC were approximately neutral. This observation indicates that the tertiary amino group of Glc-pAMAC and Gal-pAMAC carries an appreciable positive charge at pH 6.5. The net charge of Glc-pAMAC and Gal-pAMAC was estimated to be +0.15 (R. A. M. Vreeburg & S. C. Fry, unpublished) based on their electrophoretic mobility value. In the case of labelled acidic sugars, GalA-pAMAC, $GalA_2$-pAMAC and $GalA_3$-pAMAC gave fluorescent anionic spots with GalA-pAMAC as the slowest and $GalA_3$-pAMAC as the fastest-migrating. At pH 6.5, the —COOH group of GalA-pAMAC possesses a full negative charge and this acidic sugar group strongly promotes the ionisation of the amino group; the net charge of these zwitterions were estimated to be –0.11 (R. A. M. Vreeburg & S. C. Fry, unpublished). However, net charge estimation for $GalA_2$-pAMAC and $GalA_3$-

pAMAC based on their electrophoretic mobility value is less reliable because the two or three —COOH groups will not be fully ionised at pH6.5 (Takeda *et al.*, 2008).

All pAMAC-labelled uronic acid products were prone to form lactones and therefore each pAMAC-labelled sugar migrated as a number of fluorescent spots (Figure 3.1.1 (ii)). However, the lactones could be easily converted to their acidic forms by delactonisation with NaOH. It might be expected that $GalA_2$-lactone-pAMAC would migrate slower than GalA-pAMAC since both have a single ionisable —COOH group whereas $GalA_2$-lactone-pAMAC would have the smaller charge:mass ratio because it is larger than GalA-pAMAC. However, the opposite was observed. A similar pattern was observed in $GalA_3$-lactone-pAMAC and $GalA_2$-pAMAC. This showed that the presence of the ionisable —COOH of the sugar residue near to the tertiary amino group in pAMAC helps the amino group to acquire a more effective positive charge (R. A. M. Vreeburg & S. C. Fry, unpublished).

GalA-pAMAC, $GalA_2$-pAMAC and $GalA_3$-pAMAC were further analysed by HPLC on a C_{18} column (Section 3.1.1.2 and 3.1.1.3). Figure 3.1.2 shows the resolution profile of those pAMAC-markers which is useful as a reference during analysis of the proposed fingerprint compounds after *in-vitro* and *in-vivo* pAMAC-labelling.

4.2 Application of the developed novel fluorescent labelling method for detecting ˙OH attack *in vitro*

The treatment of commercial citrus pectin with Fenton reagent (Section 3.2) to mimic the ˙OH attack that may occur in a plant cell wall aimed to introduce new oxo groups to the mid-chain of the homogalacturonan domain (to produce pAMAC•pectin). Fry *et al.* (2001) reported about 85% of the NaB^3H_4-reacting groups (presumably similar to those reacting with pAMAC) in pectin were destroyed by pre-treatment with NaOH and $NaBH_4$. This explains why the ˙OH-untreated pectin (Figure 3.2.1; sample (c)) did not react with pAMAC and therefore did not show any fluorescent properties when viewed under a 254-nm UV lamp.

Experiments by Fry *et al.* (2001) with Driselase-digested ^{3}H-labelled ˙OH-treated pectin showed several anionic compounds on an electrophoretogram at pH 3.5 with two particularly interesting compounds: Compound 3 was proposed to be a disaccharide which contained a lactone or ester group; and Compound 8 was suggested to be a monosaccharide and showed the greatest increase in ^{3}H-labelling after ˙OH-treatment. Compound 8 was proposed to be a fingerprint useful to show whether pectin has been attacked by ˙OH. The Driselase digestion that was applied to the pAMAC•pectin in my study also generated several anionic fluorescent compounds visible after electrophoresis at pH 6.5 (Figure 3.3.1), with two compounds suggested to have similarities with Compound 3 and Compound 8 as reported in Fry *et al.* (2001). They were a fluorescently labelled dimer and its lactone (labelled 2A* and 2L* in Figure 3.3.1) and a fluorescently labelled monomer (labelled 1A* in Figure 3.3.1). However, in this research, 2A*, the dimer, was the

compound proposed as the most informative fingerprint compound for revealing $^{\bullet}$OH attack on pectic polysaccharides because 2A* was the main compound when pectin was treated with $^{\bullet}$OH.

1A* (GalA•pAMAC) was suggested to have been formed from pAMAC labelling of the newly introduced reducing terminus generated when $^{\bullet}$OH attacks at carbon-4 of pectin. Driselase was proven to be able to release GalA-GalA•pAMAC as free GalA plus GalA•pAMAC (Section 3.1.1.4) which would account for 1A*. 2A* and 2L* were suggested to have been formed from any $^{\bullet}$OH-generated oxo groups at position 2, 3 and/or 4 of the pectic GalA residues (producing pAMAC•UA-GalA). Even though Driselase possess α-galacturonidase activity, Driselase may not recognise the glycosidic bond of pAMAC•GalA-GalA because the attachment of a large pAMAC molecule to the GalA moiety via tertiary amine bond significantly modifies this sugar residue. pAMAC-labelling at position 2, 3 and/or 4 would also yield the 2-, 3- and/or 4-epimers of pAMAC•GalA-GalA (i.e., pAMAC•TalA-GalA, pAMAC•GulA-GalA and pAMAC•GlcA-GalA respectively). It is more unlikely that Driselase would digest the glycosidic bond between these epimers as Driselase probably lacks the activities of α-taluronidase, α-guluronidase and α-glucuronidase, and the products thus show up as a mixture of fluorescent disaccharides (pAMAC•UA-GalA) and their lactones, all approximately co-migrating with the dimer marker of $GalA_2$-pAMAC and its lactone. All these pAMAC•UA-GalA compounds are predicted to have similar ionic properties on the pH 6.5 electrophoretogram. As reported by Fry *et al.* (2001), Driselase may release [^{3}H]GalA-GalA (formed from $^{\bullet}$OH-generated oxo groups at position 2 and/or 3 of the pectin sugar residues) as free monosaccharides because [^{3}H]GalA-GalA could be

recognised by Driselase as a normal cell-wall-related disaccharide, but this is not the case with pAMAC•GalA-GalA. This shows that the pAMAC labelling fingerprint method developed in this study has its own advantage which will eliminated monomer formation when ˙OH attacks the polysaccharides at position 2, 3 and/or 4, by the formation of dimers as the most informative fingerprint compounds for ˙OH attack.

In the development of the novel method *in vitro*, there were two more fluorescent compounds that remain unknown (called X* and 2B* in Section 3.3). The greenish-fluorescing spot of X* surprisingly gave a distinctive migration on the electrophoretogram (Figure 3.3.1). It is difficult to deduce the structure of X* at this stage but it is definitely not a lactone because its abundance was only increased after delactonisation. X* was also proposed not to be a monomeric pAMAC-sugar derivative as it has a very low retention time on HPLC compared to all pAMAC-monomer markers (Figure 3.3.3). X* is proposed to be another kind of fingerprint compound for ˙OH attack on pectic polysaccharides. Further studies are required to identify this compound.

Spot 2B* was not of main interest because it was believed to contain lactone derivative(s), most probably formed by condensation within the pAMAC moiety, not within the sugar moiety. This suggestion is based on its blue-fluorescence colour and its low detectability on HPLC (the HPLC detector had been optimised for greenish-fluorescing compounds). At least half of 2B* was also resistant to delactonisation.

4.3 Application of the developed novel method for detecting ˙OH attack *in vivo*

The application of the developed labelling method to seven selected fruits (pear, mango, banana, apple, avocado, strawberry and strawberry tree fruit) at three stages of softening provides useful information on ˙OH attack *in vivo* which to some degree agreed with the result observed in *in-vitro* experiment. Figure 3.4.1 (ii) shows the Driselase-digestion of pAMAC•AIR of all the fruit samples after delactonisation. There were two particularly interesting compounds, labelled $1A^F$ and $2A^F$, which were suggested to have similarity to compounds 1A* and 2A* from the *in-vitro* experiment.

The fluorescent spot $1A^F$ was probably a GalA•pAMAC (pAMAC attached at the newly ˙OH-introduced reducing terminus of a D-GalA group) because it has a similar electrophoretic mobility as spot 1A* from the *in-vitro* experiment. As judged semi-quantitatively, it increased in intensity from stage 1 to stage 2 and/or 3 of softening in pear, mango, banana, avocado and strawberry tree fruit. A related observation in pear (increase in ^{3}H-labelled monomers released by Driselase digestion) was reported by Fry *et al.* (2001) and in banana (increase in pAMAC-labelled monomer) by R. A. M. Vreeburg & S. C. Fry (unpublished). A ^{3}H-labelled monomeric compound was proposed by Fry *et al.* (2001) as a fingerprint of ˙OH attack. However, a monomeric compound such as $1A^F$ could also possibly be (or include) GalA-pAMAC derived from the increasing number of D-GalA reducing termini formed during fruit ripening by the actions of EPG and/or PL. This is supported by several studies that reported significant increases of EPG activity in

pear (Pressey & Avants, 1976; Hiwasa *et al.*, 2003), banana (Ali *et al.*, 2004) and avocado (Huber & O'Donoghue, 1993) and PL mRNA accumulation in banana (Dominguez-Puigjaner *et al.*, 1997, Payasi & Sanwal, 2003; Marín-Rodríguez *et al.*, 2003) and mango (Chourasia *et al.*, 2006) when fruit softening progressed. Therefore, spot $1A^F$ obtained from AIR was not exclusive evidence of ˙OH attack. It would be interesting for further studies to investigate whether $1A^F$ will increase when treated with EPG and/or PL *in vitro*. This would give a better indication of the production of this compound as the fingerprint for EPG and/or PL attack.

On the other hand, $2A^F$ is concluded to be a limit digestion product, i.e. the suggested "fingerprint" indicating the *in-vivo* action of ˙OH attack; like 2A*, it could possibly include some or all of pAMAC•GalA-GalA, pAMAC•TalA-GalA, pAMAC•GulA-GalA and pAMAC•GlcA-GalA. This putative fingerprint spot, $2A^F$, significantly increased in intensity when hard fruit (stage 1) matured into soft fruit (stage 2 and 3) in mango, banana, avocado and strawberry tree fruit. It was always either absent or very faint at stage 1 (Figure 3.4.1). A similar observation of increasing pAMAC-labelled dimer was reported in banana by R. A. M. Vreeburg & S. C. Fry (unpublished). My observation in banana is also supported by the reported increase in endogenous ˙OH production during the ripening process of banana (Cheng *et al.*, 2008; Yang *et al.*, 2008). Cheng *et al.* (2008) measured the fluorescence intensity of the adduct formed when malondialdehyde reacts with thiobarbituric acid as described by Schopfer *et al.*, 2001 (malondialdehyde is a breakdown product resulted from *in-vivo* ˙OH oxidative cleavage of deoxyribose; in this experiment, deoxyribose were added to banana AIR (three different stages of softening) *in vitro* and incubated for 12 hours). As banana fruit ripened, the relative

yield of the fluorescent adduct increased suggesting that fruit ripening was associated with enhanced $^{\bullet}$OH production in banana. Yang *et al*. (2008) used a similar approach to measure $^{\bullet}$OH production in banana fruit. However, in both these groups' reported experiments, the banana pulp was frozen at several time points followed by a 'rough' treatment including homogenisation and lengthy incubation in deoxyribose and thiobarbituric acid before the adduct was measured. This kind of treatment to the pulp tissue might raise serious concerns as $^{\bullet}$OH is known as a short biological half-life compound and to detect its presence and action directly within the cell walls of living plant tissues is challenging. Therefore, the $^{\bullet}$OH production reported by Cheng *et al.* (2008) and Yang *et al*. (2008) might be due to (or include) the post-harvest and collateral damage resulting from the treatment. This gave an advantage to the alternative method developed in my study by which evidence for $^{\bullet}$OH action in plant cell walls is obtained from a chemical fingerprint left in the wall polysaccharides after the attack and several precautions were taken into account during processing the fruit sample including short handling time and the use of ice-cold ethanol and pre-cooled $Na_2S_2O_3$ to prevent any post-harvest oxidative damage. After taking these precautions, I observed the $2A^F$ spot only in pear at stage 2 of softening, and thus did not obtain clear evidence for sustained $^{\bullet}$OH attack when ripening progressed as reported in Fry *et al.* (2001). There was no evidence of $2A^F$ at any stage in apple and strawberry, indicating that fruit softening in apple and strawberry was probably not associated with $^{\bullet}$OH attack.

In an attempt to quantify the two most interesting compounds, $1A^F$ and $2A^F$, the pAMAC-labelled AIR of seven fruits, each at three stages of softening, were analysed quantitatively by HPLC on a C_{18} column (Section 3.5.3; Table 3.5.2).

Overall, both 1^F and 2^F showed a significant increase from stage 1 to stage 3 of softening in mango, banana, avocado and strawberry tree fruit but not in pear, apple and strawberry. Pear, apple and strawberry are temperate climate species amongst all seven species used in this study and this might influence their ripening mechanism. Ripening mechanism also probably depends on the species as different species of fruits have different patterns of growth and ripening. Thus, those differences in fruit species are expected to influence biochemical modifications of the cell wall and their regulation (Goulao & Oliveira, 2008).

In addition to these two most interesting compounds, there was also a blue-fluorescing spot (known as $2B^F$) in the *in-vivo* labelling experiment with a similar migration pattern to 2B* of the *in-vitro* experiment. However, $2B^F$ was a lactone and could easily be delactonised to its anionic form. There was also an unidentified spot with a unique migration on paper (greenish-fluorescing spot labelled as "X^F"), as observed in banana and strawberry tree fruit, before delactonisation. This spot remained in the banana sample (stage 1) after delactonisation. It was suggested to be similar to X* found in the *in-vitro* experiment based on its migration on an electrophoretogram. However, HPLC analysis of this compound did not agree with the X* in *in-vitro* experiment. Whether X^F is a similar compound to X* and could serve as another kind of fingerprint compound for $^{\bullet}OH$ attack will be interesting and therefore require further investigation.

4.4 EPG and PL action *in vivo* on fruit-pulp cell walls at different stages of softening

In addition to non-enzymic scission by ˙OH, two other mechanisms have been proposed by which the homogalacturonan chains could be attacked and which might therefore contribute to fruit softening during the ripening process: enzymic hydrolysis by EPG and enzymic elimination by PL. Each EPG action creates one new reducing terminus and one new saturated non-reducing terminus whereas each PL action creates one new reducing terminus and one new unsaturated non-reducing terminus. Based on the unique products left by each mechanism after the attack, two more authentic markers were prepared which would help to analyse EPG and PL action *in vivo* i.e. ΔUA-GalA (Section 3.1.2) and GalA-GalO (section 3.1.3).

ΔUA-GalA is an authentic marker to analyse PL action. The preparation of this marker was based on previous research in this lab by R. A. M. Vreeburg & S. C. Fry (unpublished). In addition, amongst many cell wall degrading enzymes, PL is the only enzyme known to produce an unsaturated uronic acid residue. Therefore, ΔUA-GalA would be a useful marker to detect any PL action *in vivo* when AIR from the seven fruits at each stage of softening was digested with Driselase. GalA-GalO is an authentic marker used to analyse EPG action. The preparation of this marker was based on the finding that Driselase failed to cleave the glycosidic bond between GalA and GalO (Fry *et al.*, 2001).

EPG generates the same number of new reducing termini as PL, but unaccompanied by the ΔUA residue at the non-reducing termini. Comparison of

increases occurring in reducing termini (both EPG plus PL actions) relative to an increase in ΔUA non-reducing termini (from PL action only) will indicate the occurrence EPG action. However, we found that $^{\bullet}$OH attack on homogalacturonan also produced a significant number of new reducing termini (by the production of compound 1A*; Section 3.3) and in fact if $^{\bullet}$OH attacks position 1 or 4 of the GalA moiety, the reactions will lead to homogalacturonan cleavage and produce new reducing termini (Figure 1.3.2). The determination of EPG action by this fingerprint method is possible to achieve by comparing the production of ΔUA-GalA (from PL action) and also compound $2A^F$ (from $^{\bullet}$OH action).

Section 3.6 shows an experiment to analyse the reducing termini produced by any or all of EPG, PL and/or $^{\bullet}$OH action *in vivo*. The experiment was conducted by the $NaBH_4$-reduction of AIR from the seven fruits at three stages of softening. This treatment reduced any reducing terminal GalA moieties to GalO, and subsequent Driselase digestion would leave GalA-GalO as a fingerprint for EPG, PL and/or $^{\bullet}$OH action. Figure 3.6.1 and Table 3.6.1 show the HPLC result of this experiment: GalA-GalO was detected in all samples at all stages of softening. This was as expected as the production of GalA-GalO could correspond to the D-GalA reducing termini that were produced during fruit ripening by the actions of EPG, PL and/or $^{\bullet}$OH attack. All samples showed increasing GalA-GalO at least when stage 1 was compared to stage 3, except in banana where it remained steady throughout all three stages.

On the other hand, Section 3.7 was an experiment conducted to detect ΔUA-GalA (indicating any PL action) *in vivo* on fruit-pulp cell walls at three different stages of softening. In this case, GalA-GalO was expected not to be present

in the Driselase digestion products of the AIR because the samples had not been reduced with $NaBH_4$. However, the opposite was observed. All samples showed a production of GalA-GalO. This may suggests that possibly GalO residues are naturally exist in fruit AIR leading to the formation of GalA-GalO after Driselase digestion, and this GalA-GalO was highly produced when the fruit AIR was treated with $NaBH_4$. In addition, most of the samples also showed the production of ΔUA-GalA which did not agree with the result observed in Section 3.6 in which no ΔUA-GalA was observed in any samples. At this stage, analysis of EPG and PL action *in vivo* by chemical fingerprints left after the attack was not conclusive and therefore further studies are required to complete the analysis. This includes a model experiment *in-vitro* of EPG and PL attack on pectin which would give a useful reference of the breakdown product after each attack.

GalA-GalO (when compared to free GalA after AIR was digested with Driselase) was produced at high level in the $NaBH_4$-AIR experiment during fruit softening in banana and avocado. This observation was supported by the detection of EPG activity at high level in banana by Ali *et al.* (2004) and avocado by Huber & O'Donoghue (1993) and may indicate a successful detection of EPG action *in vivo*. This research is not able to distinguish the relation between the two sets of experiments ($NaBH_4$-AIR and non-$NaBH_4$-AIR) in detecting the fingerprint of PL action. However, successful detection of ΔUA-GalA in banana and apple (in the non-$NaBH_4$-AIR experiment) may support several PL activities reported in banana by Payasi and Sanwal (2003) and in apple by Goulao *et al.* (2007).

On the other hand, no evidence for PL action was observed in strawberry in either set of experiments. This seems to contradict the report of high level expression of *PL* genes in strawberry during the ripening stages (Benitez-Burraco *et al.*, 2003), and also the report that expression of an antisense *PL* gene in strawberry was able to decrease post-harvest softening (Jimenez-Bermudez *et al.*, 2002). One possible explanation of this observation might be that the breakdown product of PL attack is processed further to other compound(s); possibly the ΔUA residue at the non-reducing terminus is either reduced to lose the double bond or cleaved off from the polymer and solubilised. Although the results gave many uncertainties in which one set of experiment opposed another and contradicted earlier reports, a successful detection of GalA-GalO and ΔUA-GalA by HPLC in this study indicates a potential fingerprint method to reveal EPG and PL action during fruit softening *in vivo*. As this is the first study in attempt to monitor the *in-vivo* action of EPG and PL, it will leave an exciting opportunity to fill a gap in our knowledge about EPG and PL action in cell walls and open the way for further investigation.

4.5 Summary

Several cell wall-modifying enzymes have been widely reported to be responsible for fruit softening including endo-polygalacturonase (Section 1.3.1) and pectate lyase (Section 1.3.2). More recently, a non-enzymic mechanism by $^{\bullet}OH$ that may contribute in cell wall polysaccharide degradation were also reported in many studies (Section 1.3.3). A chemical fingerprint method to detect the reaction products of $^{\bullet}OH$ attack *in vitro* and *in vivo* had been developed using NaB^3H_4 (Fry *et al.*, 2001). As an

alternative to the radiolabelling method of Fry *et al.* (2001), this research developed a novel fluorescent labelling method that has been successfully used in this study to monitor the action of $^{\bullet}OH$ *in vivo,* particularly during fruit softening. Production of at least three fingerprint compounds in *in-vitro* experiments (1A*, 2A*, X*) and at least two in *in-vivo* experiments ($1A^F$ and $2A^F$) provides good evidence for $^{\bullet}OH$ attack on pectic polysaccharides. $2A^F$ was suggested to be exclusive evidence for $^{\bullet}OH$ attack as it is known to be formed only from $^{\bullet}OH$ cleavage but not from EPG or PL attack. On the other hand, $1A^F$ was suggested to be useful evidence to reveal attack on pectic polysaccharides during fruit softening by any of the three mechanisms (EPG, PL or $^{\bullet}OH$). Therefore, this novel method has the potential to be used to analyse three major mechanisms during fruit softening in one analysis, though the disadvantage of not distinguishing them.

Although several of the pAMAC fluorescent fingerprint compounds, especially X^*/X^F, were not fully identified and deserve further investigation, their distinctive electrophoretic mobilities and elution pattern on HPLC together with the ^3H-labelled fingerprint products reported in Fry *et al.* (2001) offer a valuable diagnostic tool and serve as the basis for further research to study pectic polysaccharide degradation especially in fruit sciences.

References

Ali Z. M., Chin L. H. & Lazan H. (2004) A comparative study on wall degrading enzymes, pectin modifications and softening during ripening of selected tropical fruits. *Plant Science*. 167: 317–327.

Almeida D. P. F. & Huber D. J. (1999) Apoplastic pH and inorganic ion levels in tomato fruit: a potential means for regulation of cell wall metabolism during ripening. *Physiologia Plantarum*. 105: 506–512.

Asif M. H. & Nath P. (2005) Expression of multiple forms of polygalacturonase gene during ripening in banana fruit. *Plant Physiology and Biochemistry*. 43: 177–184.

Atfield G. N. & Morris C. J. O. R. (1961) Analytical separations by high-voltage paper electrophoresis. Amino acids in protein hydrolysates. *Biochemistry Journal*. 81: 606–614.

Bapat V. A , Trivedi P. K., Ghosh A., Sane V. A., Ganapathi T. R. & Nath P. (2010) Ripening of fleshy fruit: Molecular insight and the role of ethylene. *Biotechnology Advance*. 28: 94–107.

Bartley I. M. (1978) Exo-polygalacturonase of apple. *Phytochemistry*. 17: 213–216.

Baydoun E. A. -H. & Fry S. C. (1985) The immobility of pectic substances in injured tomato leaves and its bearing on the identity of the wound hormone. *Planta.* 165: 269–276.

Belfield E. J., Ruperti B., Roberts J. A. & McQueen-Mason S. (2005) Changes in expansin activity and gene expression during ethylene-promoted leaflet abscission in Sambucus nigra. *Journal of Experimental Botany*. 56: 817–823.

Ben-Arie R., Kislev N. & Frenkel, C. (1979) Ultrastructural changes in the cell walls of ripening apple and pear fruit. *Plant Physiology*. 64: 197–202.

Benítez-Burraco A., Blanco-Portales R., Redondo-Nevado J., Bellido M. L., Moyano E. & Caballero J. L. (2003). Cloning and characterisation of two ripening-related strawberry (*Fragaria* x *ananassa* cv. Chandler) pectate lyase genes. *Journal of Experimental Botany*. 54: 633–645.

Brisson L. F., Tenhaken R. & Lamb C. (1994) Function of oxidative cross-linking of cell wall structural proteins in plant-disease resistance. *Plant Cell*. 6: 1703–1712.

Blumer J. M., Clay R. P., Bergmann C. W., Albersheim P. & Darvill, A.G. (2000) Characterization of changes in pectin methylesterase expression and pectin esterification during tomato fruit ripening. *Canadian Journal of Botany*. 78: 607–618.

Brummell D. A. & Harpster M. H. (2001) Cell wall metabolism in fruit softening and quality and its manipulation in transgenic plants. *Plant Molecular Biology*. 47: 311–339.

Brummell D. A. & Labavitch J. M. (1997) Effect of antisense suppression of endopolygalacturonase activity on polyuronide molecular weight in ripening tomato fruit and in fruit homogenates. *Plant Physiology*. 115: 717–725.

Carpita, N. C. and Gibeaut, D. M. (1993) Structural models of primary cell walls in flowering plants: consistency of molecular structure with the physical properties of the walls during growth. *Plant Journal*. 3: 1–30.

Charlwood J., Tolson D., Dwek M. & Camilleri P. (1999) A detailed analysis of neutral and acidic carbohydrates in human milk. *Analytical Biochemistry*. 273: 261–277.

Chen S. X. & Schopfer P. (1999) Hydroxyl-radical production in physiological reactions- a novel function of peroxidase. *European Journal of Biochemistry*. 260: 726–-735.

Cheng G. P., Duan X. W., Shi J., Lu W. J., Luo Y. B. & Jiang W. B. (2008) Effects of reactive oxygen species on cellular wall disassembly of banana fruit during ripening. *Food Chemistry*. 109: 319–324.

Chourasia A., Sane V. A. & Nath P. (2006) Differential expression of pectate lyase during ethylene-induced postharvest softening of mango (*Mangifera indica* var. Dashehari). *Plant Physiology*. 128: 546–555.

Chun J. P. & Huber D. J. (1998) Polygalacturonase-mediated solubilization and depolymerization of pectic polymers in tomato fruit cell walls. Regulation by pH and ionic conditions. *Plant Physiology*. 117: 1293–1299.

Cosgrove D. J. (1999). Enzymes and other agents that enhance cell wall extensibility. *Annual Review of Plant Physiology and Plant Molecular Biology*. 50: 391–417.

Cosgrove D. J. (2005) Growth of the plant cell wall. *Nature*. 6: 850–861.

Crookes P. R. & Grierson D. (1983) Ultrastructure of tomato fruit ripening and the role of polygalacturonase isoenzymes in cell wall degradation. *Plant Physiology*. 72: 1088–1093.

Delmer and Amor (1995) Cellulose biosynthesis. *The Plant Cell*. 7: 987–1000.

Dominguez-Puigjaner E., Llop I., Vendrell M., & Prat S. (1997) A cDNA clone highly expressed in ripe banana fruit shows homology to pectate lyases. *Plant Physiology*. 114: 1071–1076.

Duan X. W., Cheng G. P., Yang E., Yi C., Ruenroengklin N., Lu W. J., Luo Y. B. & Jiang Y. M. (2008) Modification of pectin polysaccharides during ripening of postharvest banana fruit. *Food Chemistry*. 111:144–149.

Eriksson E. M., Bovy A., Manning K., Harrison L., Andrews J., De Silva J., Tucker G. A. & Seymour G. B. (2004) Effect of the colorless non-ripening mutation on cell wall biochemistry and gene expression during tomato fruit development and ripening. *Plant Physiology*. 136: 4184–4197.

Fabi J. P., Cordenunsi B. R., Seymour G. B., Lajolo F. M. & Nascimento J. R. O. (2009) Molecular cloning and characterization of a ripening-induced polygalacturonase related to papaya fruit softening. *Plant Physiology and Biochemistry*. 47: 1075–1081.

Fischer R. L. & Bennett A. B. (1991) Role of cell wall hydrolases in fruit ripening. *Annual Review of Plant Physiology and Plant Molecular Biology*. 42: 675–703.

Fonseca S., Hackler Jr. L., Zvara A., Ferreira S., Baldé A. & Dudits D. (2004) Monitoring gene expression along pear fruit development, ripening and senescence using cDNA microarrays. *Plant Science.* 167: 457–469.

Fray R. G. & Grierson D. (1993) Molecular genetics of tomato fruit ripening. *Trends in Genetics.* 9: 438-443.

Fry S. C. (1998) Oxidative scission of plant cell wall polysaccharides by ascorbate-induced hydroxyl radicals. *Biochemical Journal*. 332:507–515.

Fry S. C. (2000) "The Growing Plant Cell Wall: Chemical and Metabolic Analysis". Reprint Edition. The Blackburn Press, Caldwell, New Jersey.

Fry S. C. (2003) Ripening. In 'Encyclopedia of Applied Plant Sciences'. Academic Press. 794–807.

Fry S. C. (2011) High-voltage paper electrophoresis (HVPE) of cell-wall building blocks and their metabolic precursors. In 'The Plant Cell Wall Methods and Protocols' edited by Popper Z. A. Springer New York. 55–80.

Fry S. C., Dumville J. C., & Miller J. G. (2001) Fingerprinting of polysaccharides attacked by hydroxyl radicals in vitro and in the cell walls of ripening pear fruit. *Biochemical Journal*. 357: 729–737

Fry S. C., Miller J. G. & Dumville J. C. (2002) A proposed role for copper ions in cell wall loosening. *Plant and Soil*. 247: 57–67.

García-Romera I. & Fry S. C. (1994) Absence of transglycosylation of oligogalacturonides in plant apoplasts. *Phytochemistry*. 35: 67–72.

Gardner S. L., Burrell M. M. & Fry S. C. (2002) Screening of Arabidopsis thaliana stems for variation in cell wall polysaccharides. *Phytochemistry*. 60: 241–254.

Gardiner, J. C., Taylor N. G. & Turner S. R. (2003) Control of cellulose synthase complex localization in developing xylem. *Plant Cell*. 15: 1740–1748.

Giovannoni J. J., Della Penna D., Bennett A. B. & Fischer R.L. (1989) Expression of a chimeric polygalacturonase gene in transgenic rin (ripening inhibitor) tomato fruit results in polyuronide degradation but not fruit softening. *Plant Cell*. 1: 53–63.

Goubet F., Morriswood B. & Dupree P. (2003) Analysis of methylated and unmethylated polygalacturonic acid structure by polysaccharide analysis using carbohydrate gel electrophoresis. *Analytical Biochemistry*. 321: 174–182.

Goulao L. F., Santos J., de Sousa I. & Oliveira C. M. (2007) Patterns of enzymatic activity of cell wall-modifying enzymes during growth and ripening of apples. *Postharvest Biology and Technology*. 43: 307–318.

Goulao L. F. & Oliveira C. M. (2008) Cell wall modifications during fruit ripening: when a fruit is not the fruit. *Trends in Food Science and Technology*. 19: 4–25.

Green M. A & Fry S. C. (2005) Vitamin C degradation in plant cells via enzymatic hydrolysis of 4-O-oxalyl-L-threonate. *Nature*. 433: 83–87.

Gross K. C. & Sams C. E. (1984) Changes in cell wall neutral sugar composition during fruit ripening: a species survey. *Phytochemistry.* 23: 2457–2461.

Guerriero G., Fugelstad J. & Bulone V. (2010) What do we really know about cellulose biosynthesis in higher plant? *Journal of Integrative Plant Biology*. 52: 161–175.

Hadfield K. A. & Bennett A. B. (1998) Polygalacturonases: many genes in search of a function. *Plant Physiology*. 117: 337–343.

Hatfield R. & Nevins D.J. (1986) Characterisation of the hydrolytic activity of avocado cellulase. *Plant Cell Physiol*ogy. 27: 541–552.

Hiwasa K., Rose J. K., Nakano R., Inaba A., & Kubo Y. (2003). Differential expression of seven alpha-expansin genes during growth and ripening of pear fruit. *Physiologia Plantarum*. 117: 564–572.

Huber D. J. (1984) Strawberry (*Fragaria ananassa*) fruit softening, the potential roles of polyuronides and hemicelluloses. *Journal of Food Science*. 49: 1310–1315.

Huber D. J. & O'Donoghue E. M. (1993). Polyuronides in avocado (*Persea americana*) and tomato (*Lycopersicon esculentum*) fruits exhibit markedly different patterns of molecular weight downshifts during ripening. *Plant Physiology*. 102: 473–480.

Iiyama K., Lam T. & Thomas J. R. (1994) Covalent cross-links in the cell wall. *Plant Physiology*. 104: 315–320

Ishii T. (1997) *O*-Acetylated oligosaccharides from pectins of potato tuber cell walls. *Plant Physiology*. 113: 1265–1271.

Jackson P. (1993) Fluorophore-assisted carbohydrate electrophoresis- A new technology for the analysis of glycans. *Biochemical Society Transactions*. 21: 121-125

Jackson P. (1996) The analysis of fluorophore-labelled carbohydrates by polyacrylamide gel electrophoresis. Molecular Biotechnology. 5: 101-123

Jarvis M. C. (1984) Structure and properties of pectin gels in plant cell walls. *Plant, Cell & Environment*. 7: 153–164.

Jimenez-Bermudez S., Redondo-Nevado J., Munoz-Blanco J., Caballero J., Lopez-Aranda J. M., Valpuesta V., Pliego-Alfaro F., Quesada M. A. & Mercado J. A. (2002) Manipulation of strawberry fruit softening by antisense expression of a pectate lyase gene. *Plant Physiology.* 128: 751–759.

Kärkönen A. & Fry S. C. (2006) Effect of ascorbate and its oxidation-products on H_2O_2 production in cell-suspension cultures of *Picea abies* and in the absence of cells. *Journal of Experimental Botany*. 57: 1633–1644.

Lamari F., Theocharis A., Hjerpe A. & Karamanos N. K. (1999) Ultrasensitive capillary electrophoresis of sulfated disaccharides in chondroitin dermatan sulfates by laser-induced fluorescence after derivatization with 2-aminoacridone. *Journal of Chromatography*. 730: 129–133.

Lindsay S. E. & Fry S. C. (2007) Redox and wall-restructuring. In 'The Expanding Cell' edited by Verbelen J-P. & Vissenberg K. Springer, Berlin. 159–190.

Lorences E. P. & Fry S. C. (1993) Xyloglucan oligosaccharides with at least two α-D-xylose residues act as acceptor substrates for xyloglucan endotranglycosylase and promote the depolymerisation of xyloglucan. *Physiologia Plantarum.* 88: 105–112.

Lozanov V., Ivanov I. P., Benkova B. & Mitev V. (2009) Peptide substrate for caspase-3 with 2-aminoacridone as reporting group. *Amino Acids.* 36: 581–587.

Maeda E., Kataoka M., Hino M., Kajimoto K., Kaji N., Tokeshi M. & Kido J. (2007) Determination of human blood glucose levels using microchip electrophoresis. Electrophoresis. 28: 2927–2933.

Marín-Rodríguez M. C., Orchard J. & Seymour G. B. (2002) Pectate lyases, cell wall degradation and fruit softening. *Journal of Experimental Botany*. 53: 2115-2119.

Marín-Rodriguez M. C., Smith D. L. Manning K., Orchard J. & Seymour G.B. (2003) Pectate lyase gene expression and enzyme activity in ripening banana fruit. *Plant Molecular Biology*. 51: 851-857.

Martin N. H. & Franglen G. T. (1954) The use and limitations of filter-paper electrophoresis. *Journal of Clinical Pathology*. 7: 87–105.

McNeil M., Darvill A. G., Fry S. C. & Albersheim P. (1984) Structure and function of the primary cell wall of plants. *Annual Review of Biochemistry*. 53: 625-663.

Miller A. R. (1986) Oxidation of cell wall polysaccharides by hydrogen peroxide: a potential mechanism for cell wall breakdown in plants. *Biochemical and Biophysical Research Communications*. 141: 238–244.

Müller K., Tintelnot S., & Leubner-Metzger G. (2006) Endosperm-limited Brassicaceae seed germination: Abscisic acid inhibits embryo-induced endosperm weakening of *Lepidium sativum* (cress) and endosperm rupture of cress and *Arabidopsis thaliana*. *Plant and Cell Physiology*. 47: 864–877.

Müller K., Linkies A., Vreeburg R. A. M., Fry S. C., Krieger-Liszkay A. & Leubner-Metzger G. (2009) *In vivo* cell wall loosening by hydroxyl radicals during cress seed germination and elongation growth. *Plant Physiol*ogy. 150: 1855–1865.

Nogata Y., Ohta H. & Voragen A. G. J. (1993) Polygalacturonase in strawberry fruit. *Phytochemistry*. 34: 617–620.

Payasi A. & Sanwal G. G. (2003) Pectate lyase activity during ripening of banana fruit. *Phytochemistry*. 63: 243-248.

Payasi A., Misra P. C. & Sanwal G. G. (2006) Purification and characterization of pectate lyase from banana (*Musa acuminate*) fruits. *Phytochemistry*. 67: 861–869.

Payasi A., Mishra N. N., Chaves A. L. & Singh R. (2009) Biochemistry of fruit softening: an overview. *Physiology and Molecular Biology of Plants*. 15: 103-113.

Payasi A. & Sanwal G. G. (2010) Ripening of climacteric fruits and their control. *Journal of Food Biochemistry*. 34: 679–710.

Perrone P., Hewage C. M., Thomson A. R., Bailey K., Sadler I. H. & Fry S. C. (2002) Patterns of methyl and O-acetyl esterification in spinach pectins: new complexity. *Phytochemistry*. 60: 67–77.

Pitt D. (1988) Pectin lyase from *Phoma medicaginis* var pinodella. In: 'Methods in Enzymology' edited by Wood W. A., Kellogg S. T. Academic Press, San Diego. 161: 350–354.

Popper Z. A. & Fry S. C. (2003) Primary cell wall composition of bryophytes and charophytes. *Annals of Botany*. 91: 1–12.

Popper Z. A. & Fry S. C. (2005) Widespread occurrence of a covalent linkage between xyloglucan and acidic polysaccharides in suspension-cultured angiosperm cells. *Annals of Botany*. 96: 91–99.

Prasanna V., Prabha T. N. & Tharanathan R. N. (2007) Fruit ripening phenomena: an overview. *Critical Reviews in Food Science and Nutrition*. 47: 1–19.

Pressey R. & Avants J. K. (1976) Pear polygalacturonases. *Phytochemistry*. 15: 1349–1351.

Quesada M. A., Blanco-Portales R., Pose S., Garcia-Gago J. A., Jimenez-Bermudez S., Caballero J. L., Pliego-Alfaro F., Mercado J. A. & Munoz-Blanco J. (2009) Antisense down-regulation of the FaPG1 gene reveals an unexpected central role for polygalacturonase in strawberry fruit softening. *Plant Physiology*. 150: 1022–1032.

Redgwell R. J., Fischer M., Kendal E. & MacRae E. A. (1997) Galactose loss and fruit ripening: high-molecular-weight arabinogalactans in the pectic polysaccharides of fruit cell walls. *Planta*. 203: 174–181.

Redondo-Nevado J., Moyano E., Medina-Escobar N., Caballero J. L. Munoz-Blanco J. (2001). A fruit-specific and developmentally regulated endopolygalacturonase gene from strawberry (*Fragaria x ananassa* cv. Chandler). *Journal of Experimental Botany*. 52: 1941–1945.

Richmond P. A. (1991) Occurrence and functions of native cellulose. In: 'Biosynthesis and Biodegradation of cellulose' edited by. Haigler C. H. & Weimer P. J. Dekker. New York, USA. 5–23.

Rop O., Sochor J., Jurikova T., Zitka O., Skutkova H., Mlcek J., Salas P., Krska B., Babula P., Adam V., Kramarova D., Beklova M., Provaznik I. & Kizek R. (2011) Effect of five different stages of ripening on chemical compounds in medlar (*Mespilus germanica L.*). *Molecules*. 16: 74–91.

Rose J. K. C., Hadfield K. A., Labavitch J. M. & Bennett A. B. (1998) Temporal sequence of cell wall disassembly in rapidly ripening melon fruit. *Plant Physiology*. 117: 345–361.

Roy S., Vian B. & Roland J. -C. (1992) Immunocytochemical study of the deesterification patterns during cell wall autolysis in the ripening of cherry tomato. *Plant Physiology and Biochemistry*. 30:139–146.

Sharples S. C. & Fry S. C. (2007) Radio-isotope ratios discriminate between competing pathways of cell wall polysaccharide and RNA biosynthesis in living plant cells. *Plant Journal*. 52: 252–262.

Schellera H. V., Jensena J. K., Sørensena S. O., Harholta J. & Geshi N. (2007) Biosynthesis of pectin. *Physiologia plantarum*. 129: 283–295.

Schols H. A., Bakx E. J., Schipper D., Voragen A. G. J. (1995) A xylogalacturonan subunit present in the modified hairy regions of apple pectin. *Carbohydrate Research*. 279: 265–279.

Schols H. A. & Voragen A. G. J. (2002) The chemical structure of pectins. In 'Pectins and Their Manipulation' edited by Seymour G. B. & Knox J. P. Blackwell/CRC Press. 150–173.

Schopfer P. (2001) Hydroxyl radical-induced cell-wall loosening *in vitro* and *in vivo*: implications for the control of elongation growth. *The Plant Journal*. 28: 679–688.

Schopfer P., Plachy C. & Frahry G. (2001) Release of reactive oxygen intermediates (superoxide radicals, hydrogen peroxide, and hydroxyl radicals) and peroxidase in germinating radish seeds controlled by light, gibberellin, and abscisic acid. *Plant Physiology*. 125:1591–1602.

Schuchmann M. N. & Von Sonntag C. (1977) Radiation chemistry of carbohydrates. Part 14. Hydroxyl radical induced oxidation of D-glucose in oxygenated aqueous solution. *Journal of the Chemical Society*. Perkin Trans II: 1958-1963.

Schweikert C., Liszkay A. & Schopfer P. (2002) Polysaccharide degradation by Fenton reaction- or peroxidase-generated hydroxyl radicals in isolated plant cell walls. *Phytochemistry*. 61: 31–35.

Shekhawat N. S. & Galston A. W. (1983) Isolation, culture and regeneration of moth bean vigna-aconitifolia leaf protoplasts. *Plant Science Letters*. 32: 43–51.

Song J. F., Weng M. Q., Wu S. M. & Xia Q. C. (2002) Analysis of neutral saccharides in human milk derivatized with 2-aminoacridone by capillary electrophoresis with laser-induced fluorescence detection. *Analytical Biochemistry*. 304: 126–129.

Stratilová E., Markovic O., Dzurová M., Maloviková A., Capek P. & Omelková J. (1998) The pectolytic enzymes of carrots. *Biologia*. 53: 731–738.

Suntornwat O., Lertwikoon N., Bungaruang L., Chaimanee P. & Speirs J. (2000) Cloning and characterization of a putative endo-polygalacturonase cDNA from ripening mango (*Mangifera indica* Linn cv. Nam Dok Mai) *Acta Horticulturae*. 509: 153–158.

Takeda T. & Fry S.C. (2004) Control of xyloglucan endotransglucosylase activity by salts and anionic polymers. *Planta*. 219: 722–732.

Takeda T., Miller J. G. & Fry S. C. (2008) Anionic derivatives of xyloglucan function as acceptor but not donor substrate for xyloglucan endotransglucosylase activity. *Planta*. 227: 893–905.

Thompson J. E. & Fry S. C. (2000) Evidence for covalent linkage between xyloglucan and acidic pectins in suspension-cultured rose cells. *Planta*. 211: 275–286.

Toole G. A., Smith A. C. & Waldron K. W. (2002) The effect of physical and chemical treatment on the mechanical properties of the cell wall of the alga *Chara corallina*. *Planta*. 214: 468–475.

Tucker G. A. & Grierson D. (1987). Fruit ripening. In 'The Biochemistry of Plants' edited by Davies D. D. Academic Press, New York. 12: 265–318.

Tucker G. A. & Seymour G. B. (2002) Modification and degradation of pectins. In 'Pectins and Their Manipulation' edited by Seymour G. B. & Knox J. P. Blackwell/CRC Press. 150–173.

Uchiyama H., Dobashi Y., Ohkouchi K. & Nagasawa K. (1990) Chemical change involved in the oxidative reductive depolymerization of hyaluronic acid. *Journal of Biological Chemistry*. 265: 7753–7759.

Von Sonntag C. (1987) The Chemical Basis of Radiation Biology. London: Taylor & Francis.

Vreeburg R. A. M. & Fry S. C. (2005) Reactive oxygen species in cell walls. In: 'Antioxidants and Reactive Oxygen Species in Plants' edited by Smirnoff N. Blackwell, Oxford. 215–249.

Wakasa Y., Kudo H., Ishikawa R., Akada S., Senda M., Niizeki M. & Harada T. (2006) Low expression of an endopolygalacturonase gene in apple fruit with long-term storage potential. *Postharvest Biology and Technology*. 39: 193–198.

Willats W. G. T, Orfila C., Limberg G., Buchholt H. C., van Alebeek G. J. W. M., Voragen A. G. J., Marcus S. E., Christensen T. M. I. E., Mikkelsen J. D., Murray B. S & Knox J. P. (2001) Modulation of the degree and pattern of methyl-esterification of pectic homogalacturonan in plant cell walls — Implications for pectin methyl esterase action, matrix properties, and cell adhesion. *Journal of Biological Chemistry*. 276: 19404–19413.

Wright K. & Northcote D. H. (1975) Acidic oligosaccharide from maize slime. *Phytochemistry*. 14: 1793–1798.

Wu Q., Szakacs-Dobozi M., Hemmat M. & Hrazdina G. (1993) Endopolygalacturonase in apples (*Malus domestica*) and its expression during fruit ripening. *Plant Physiology*. 102: 219–225.

Yang S. Y., Su X. G., Prasad K. N., Yang B., Cheng G. P. & Chen Y. L. (2008) Oxidation and peroxidation of postharvest banana fruit during softening. *The Pakistan Journal of Botany*. 40: 2023–2029.

Zegota H. (2002) Some quantitative aspects of hydroxyl radical induced reactions in gamma-irradiated aqueous solutions of pectins. *Food Hydrocolloids*. 16: 353–361.

Zeiger E. & Hepler P. K. (1976) Production of guard cell protoplasts from onion and tobacco. *Plant Physiology*. 58: 492–498.

Zhao X., She X., Du Y. & Liang X. (2007) Induction of antiviral resistance and stimulatory effect by oligochitosan in tobacco. *Pesticide Biochemistry and Physiology*. 87: 78–84.